LAPPEENRANTA UNIVERSITY OF TECHNOLOGY
School of Energy Systems
Department of Environmental Technology
Sustainability Science and Solutions
Master's thesis 2019

Eppu Väänänen

MODELING AND DYNAMIC SIMULATION OF MBR PROCESS IN METSÄ-SAIRILA WWTP

Examiners: Professor Risto Soukka
Associate professor Eveliina Repo
Supervisor: D. Sc. Anna Mikola

TIIVISTELMÄ

Lappeenrannan teknillinen yliopisto
LUT School of Energy Systems
Ympäristötekniikan koulutusohjelma
Sustainability Science and Solutions

Eppu Väänänen

MBR prosessin mallintaminen ja dynaaminen simulointi Metsä-Sairilan jätevedenpuhdistamolla

Diplomityö

2019

89 sivua, 49 kuvaa ja 11 taulukkoa

Työn tarkastajat: Professori Risto Soukka
Apulaisprofessori Eveliina Repo

Työn ohjaaja: TkT Anna Mikola

Hakusanat: kalvobioreaktori, jätevedenpuhdistamo, prosessimallinnus, dynaaminen simulointi, kalvojen tukkeutuminen, solun ulkopuoliset polymeerit, mikrobien liukoiset tuotteet

Uusi kalvosuodatustekniikkaan perustuva 63,000 henkilön asukasvastineluvun jätevedenpuhdistamo valmistuu käyttöön vuonna 2020 Mikkeliin. Tämän työn tarkoituksena on tutkia kalvosuodatuksen tukkeutumiseen vaikuttavia tekijöitä ja simuloida erilaisia prosessiolosuhteita tukkeutumisen minimoimiseksi.

Tässä diplomityössä luotiin kaksi uutta prosessimallia käyttäen apuna olemassa olevia malleja. Biologista mallia laajennettiin ja siihen lisättiin solun ulkopuolisten polymeerien ja mikrobien liukoisten tuotteiden malli. Mekaaninen tukkeumamalli lisättiin bioreaktorimalliin. Mallit kalibroitiin stressitilanteessa ajetulta pilottilaitokselta saadulla datalla. Tämän työn tulokset osoittavat, että stressaavat olosuhteet lisäävät tukkeutumista ja niitä voidaan minimoida oikealla laitoksen ajamisella. Tukkeutuminen voitiin linkittää biologiseen aktiivisuuteen.

ABSTRACT

Lappeenranta University of Technology
LUT School of Energy Systems
Degree Programme in Environmental Technology
Sustainability Science and Solutions

Eppu Väänänen

Modeling and dynamic simulation of MBR process in Metsä-Sairila WWTP

Master's thesis

2019

89 pages, 49 figures and 11 tables

Examiners: Professor Risto Soukka
Associate professor Eveliina Repo
Supervisor: D. Sc. (Tech) Anna Mikola

Keywords: membrane bioreactor, wastewater treatment plant, process modeling, dynamic simulation, membrane fouling, extracellular polymeric substances, soluble microbial products

A new membrane bioreactor will be in operation in Mikkeli in 2020 with a population equivalent of around 63,000. The aim of this study is to determine parameters that cause fouling in Membrane Bioreactors, study the dynamics of fouling behavior and to simulate different process conditions that could minimize fouling behavior.

Two different process models were created in this Master's thesis with the help from existing models. A biological model was extended with extracellular polymeric substances and soluble microbial products. A mechanistic membrane fouling behavior was added to bioreactor model. The models were calibrated with the data available from pilot plant operated in stressful conditions. The results of this work show that stressful conditions enhance fouling and could be minimized with correct operation of the treatment plant. The fouling could be linked to biological activity.

ACKNOWLEDGEMENTS

I would like to give huge thank you to my supervisor Anna Mikola for all the help and assistance during the many hours of work. This work would have not been possible without her expertise and dedication to process modeling.

I would like to thank Water Utility of Mikkeli and the operational stuff for help in measuring, analyses and operation of pilot MBR plant. The staff gave me views that I would not otherwise have noticed. I would like to thank my examiners, Risto Soukka and Eveliina Repo, for pushing me forward during hard times and helping in many different laboratory analyses. I am thankful for Khum Gurung and Maija Sihvonen for helping me with sometimes very weird questions and for finalizing my Thesis. I would give my sincerest thanks to MVTT, RIL ry, Lappeenranta University of Technology and Ramboll Finland Oy for financial support. It greatly helped me to finish this Thesis.

Last, but certainly not least, I would like to thank my family, friends and other supporters.

In Lappeenranta 4.11.2019

Eppu Väänänen

TABLE OF CONTENTS

LIST OF SYMBOLS

J	flux	[L/m^2*h], [m/s]
p	pressure	[bar], [Pa]
Q	flow	[m^3/d], [Nm3/h]
T	temperature	[ºC], [K]
V	volume	[m^3], [L]

Subscrits

c	colloidal
s	soluble
t	total
x	particulate

Abbreviations

ASM	Activated Sludge Model
BOD	Biological oxygen demand
CAS	Conventional activated sludge
CASP	Conventional Activated Sludge Process
CFV	Crossflow Velocity
COD	Chemical oxygen demand
CSTR	Completely stirred tank reactor
DO	Dissolved oxygen concentration
EPS	Extracellular polymeric substances
HRT	Hydraulic retention time
MBR	Membrane Bioreactor
MLSS	Mixed liquor suspended solids
NHx	Ammonia/ammonium
NITO	Nitrifying organisms
NOx	Nitrite and nitrate
OHO	Ordinary heterotrophic organisms

SMP	Soluble microbial products
SRT	Solids retention time
TMP	Transmembrane Pressure
WWTP	Wastewater treatment plant

1 INTRODUCTION

Wastewater treatment plants have gained more publicity lately. In the past, removing harmful or poisonous substances was enough, but modern plants may even be a source of nutrients while removing harmful substances with high efficiency. These new plants require better control and modern technologies to meet the requirements for nutrient recovery and removal of pollutants. One of the possible technologies for higher quality effluent is the membrane bioreactor (MBR). MBR combines the widely-used conventional activated sludge process (CASP) with membrane filtration.

In Europe, there are several plants that have used the MBR process for decades (Skinner 2017) but MBRs are not yet widely used in the Nordic countries. One of the reasons is the high energy consumption compared to CASP. Also, MBR tends to have higher fouling rate in cold temperatures and the interactions of fouling related to physical, chemical and biological interactions are not well known and may be difficult to predict. A lot of effort has been put to create models that could predict membrane fouling and to model the biological behavior that influences fouling. (Janus 2013). Many researchers have linked the extracellular polymeric substances (EPS) and soluble microbial products (SMP) to membrane fouling.

The main goal of this thesis is to create a full plant biokinetic model which can predict EPS and SMP concentrations and to calibrate it with data gathered from a pilot plant. The model includes a full plant mechanistic membrane fouling model that is linked to EPS and SMP concentrations. Secondly, the goal is to analyze different driving strategies to minimize membrane fouling behavior and to illustrate the behavior by simulations how different operational conditions affect membrane fouling. Modeling chemical and biological processes related to phosphorus removal are not in the scope of this thesis.

This thesis shows that modeling fouling behavior is challenging and needs expert knowledge in biochemistry and some understanding of water treatment processes. Some knowledge of those subjects is also needed for understanding the models. This should be considered before starting a project, which includes model creation to ensure that enough measuring and

analyzes are made and there is an adequate amount of data available. Also, the model calibration and validation phase should be stopped when results with enough accuracy are reached.

2 MBR PROCESS

Membrane bioreactor combines two separate processes. One part of the treatment process is the bioreactor, where biological activity of micro-organisms generates sludge floc particles. Micro-organisms also treat the different compounds of influent wastewater. In the second part of the process, biologically treated water is separated from activated sludge using membrane filtration. (Park et al. 2015).

2.1 Biological wastewater treatment

Biological wastewater treatment is based on a wide variety of diverse types of micro-organisms, where environmentally harmful organic compounds and nutrients are converted into non-harmful form using microbial activity.

2.1.1 Influent wastewater

Influent wastewater comes to treatment facilities from municipal sources. The sources can be residential, commercial, industrial or natural, e.g. ground water or surface water. Influent wastewater is a complex mixture of different components, which vary depending on the source. For planning and operating the treatment process, it is important to know different physical, chemical and biological characteristics of raw wastewater. (Tchobanoglous 2003) Especially, if a treatment process is being modeled, it is important to characterize influent wastewater to get reasonable predictions from model (Melcer et al. 2003).

2.1.1.1 Physical characteristics

Total solids (TS) concentration, which consists of floating matter, matter that settles, colloidal matter and matter in soluble state, is the most important physical characteristic of wastewater. It is measured by evaporating and drying a wastewater sample at a temperature of 103°C to 105°C. Total solids concentration is usually analyzed further by various methods to get a better understanding of the solids in wastewater. The most important fractions are total suspended solids (TSS) and volatile suspended solids (VSS). TSS is measured by first filtrating the sample through a 0.45 μm filter, drying at the filter at the same temperature as in TS analysis and weighing the sample afterwards. VSS is measured using a similar

filtration method but the residues in filter are ignited at the temperature of around 500 °C and the filter is weighed afterwards. VSS is supposed to be the organic part of the TS. (Tchobanoglous 2003)

One important physical characteristics is also temperature, which greatly affects the microbial activity. Temperature around 25 - 35 °C is found to be optimum for bacterial activity. Other physical characteristics include turbidity, color, odor, conductivity, particle size distribution and density. (Tchobanoglous 2003)

2.1.1.2 Chemical characteristics

In chemical characterization wastewater is commonly divided in organic and inorganic constituents. Two important inorganic constituents are nitrogen and phosphorus, which are also seen as the main nutrients for biological growth. Even though they are usually inorganic compounds in influent wastewater, they are also construction material for cells. Organic compounds are usually composed of carbon, hydrogen, oxygen and nitrogen. In activated sludge modeling, total chemical oxygen demand (COD_T), which describes the fraction of matter that can be oxidized chemically, and fractioning COD_T to different components, is important as the activated sludge models are usually based on them (Melcer et al. 2003; Rieger et al. 2012).

The test, which is used to determine COD_T is based on oxidizable matter's reaction with dichromate in acidic conditions presented in the following equation:

$$C_nH_aO_bN_c + d * Cr_2O_7^{2-} + (8d + c)H^+ \rightarrow$$
$$nCO_2 + \frac{a+8d-3c}{2}H_2O + cNH_4^+ + 2dCr^{3+} \quad (1)$$

where: $d = \frac{2n}{3} + \frac{a}{6} - \frac{b}{3} - \frac{c}{2}$. (Tchobanoglous 2003).

The first step to fractionate COD_T further is to determine its biodegradability. Biodegradable (COD_B) and unbiodegradable (COD_{UB}) fractions of COD can be divided further into sub-portions. Fractioning of COD_T is presented in Figure 1.

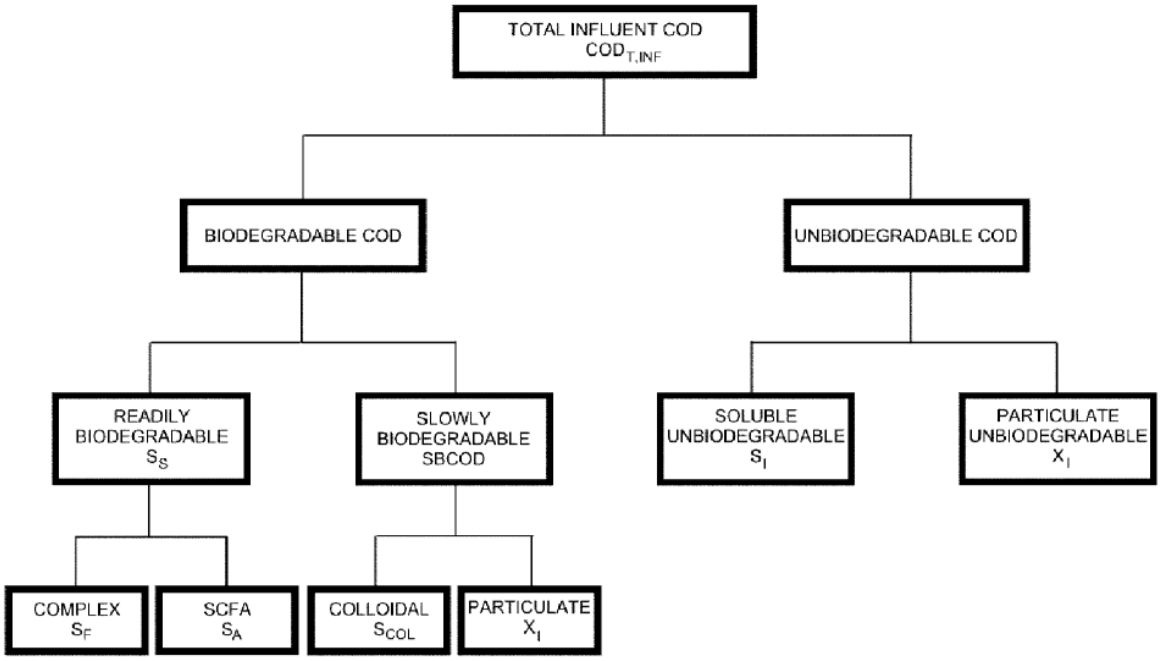

Figure 1. Division of municipal wastewater COD into components (Melcer et al. 2003, p. 67)

Biodegradable portion is the portion of COD_T that microbes can consume when enough oxygen is present within a certain time, usually 5 or 7 days. To determine biodegradable portion, usually a standard BOD test is applied. The test will not give absolute ultimate biochemical oxygen demand (UBOD) value. To estimate the UBOD, usually data from BOD test must be modeled. (Tchobanoglous 2003). Biodegradable portion can be further divided into readily biodegradable COD (S_S) and slowly biodegradable COD (SBCOD). Readily biodegradable material is hypothesized to be material that is absorbed and consumed immediately by micro-organisms and converted to energy and synthesis. Sub-divisions of readily biodegradable material are complex readily biodegradable COD (S_F) and short-chain volatile fatty acids (S_A). Slowly biodegradable material is particulate (X_S), colloidal (S_{COL}) or complex organic molecules that need extracellular enzymatic processing before microbes can consume them. The unbiodegradable portion of COD is unaffected by biological activity. It is divided in to two sub-portions, soluble unbiodegradable (S_I) and particulate unbiodegradable (X_I). (Melcer et al. 2003).

The main sources of nitrogen in wastewater are animal and plant origin and atmospheric nitrogen. Nitrogen and its compounds have several oxidation states and their chemistry is complex. Microbial activity with varying pH and salinity affects oxidation states positively

or negatively. The most important as well as the most common forms in wastewater with oxidation states are ammonia (NH_3, -III), ammonium (NH_4^+, -III), nitrogen gas (N_2, 0), nitrite ion (NO_2^-, +III) and nitrate ion (NO_3^-, +V). Nitrate and nitrite are usually characterized separately as they greatly affect the wastewater system performance. Other forms of nitrogen are usually called total Kjeldahl nitrogen (TKN), which includes ammonia, ammonium and organically bound ammonia. Nitrogen characterization is presented in Figure 2. (Melcer et al. 2003; Tchobanoglous 2003)

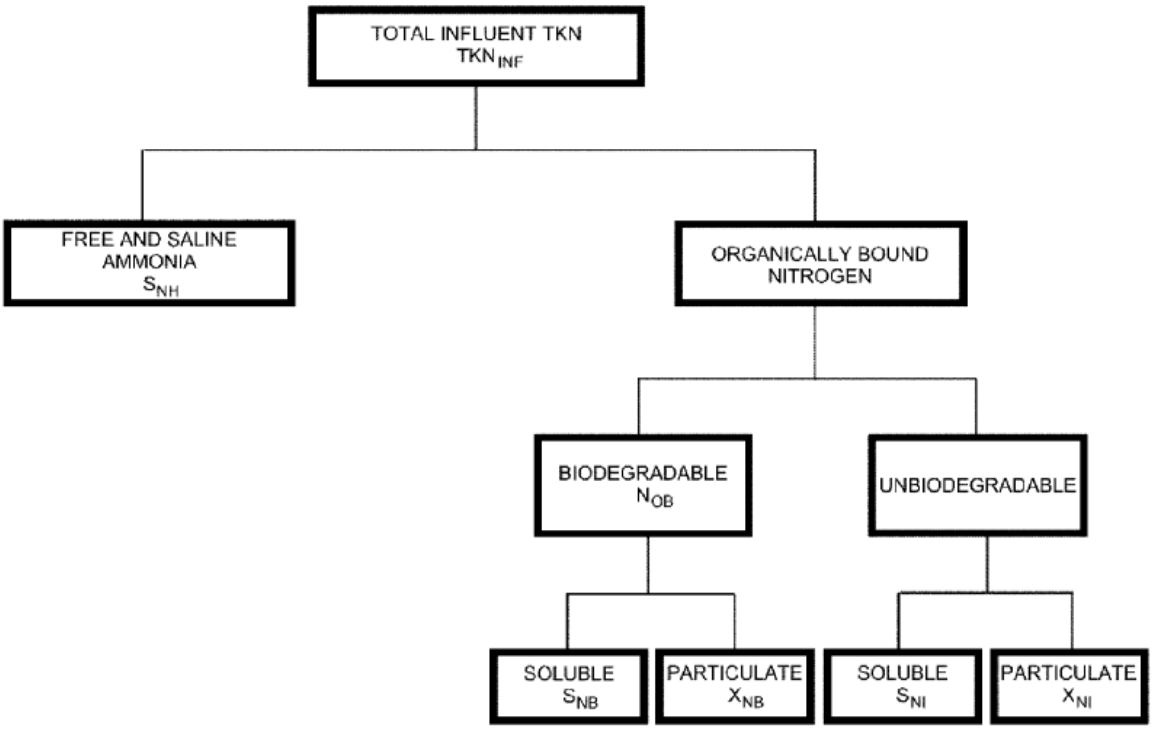

Figure 2. Division of municipal wastewater TKN into components (Melcer et al. 2003 p. 72)

Further fractioning divides biodegradable nitrogen (N_{OB}) into soluble biodegradable nitrogen (S_{NB}) and particulate biodegradable nitrogen (X_{NB}). Unbiodegradable nitrogen is also unaffected by biological activity. It is divided into soluble unbiodegradable nitrogen (S_{NI}) and particulate unbiodegradable nitrogen (X_{NI}). (Melcer et al. 2003).

Phosphorus is also an important nutrient for organisms, and they are found to affect algal blooms and their runoffs are of high interest. Usually, phosphorus in aquatic solutions is orthophosphate, polyphosphate or organic phosphate. Orthophosphates can be consumed directly by micro-organisms. Polyphosphates include at least two phosphorus atoms and they must go through slow hydrolysis before breaking to orthophosphates. (Tchobanoglous 2003)

One important chemical characteristic is pH. It represents the concentration of H^+ ions in aquatic solutions according to following equation:

$$pH = -log_{10}[H^+] \quad (2)$$

The range of suitable pH values for biological life is narrow. Usually, treated effluent should have a pH value of around 6.5 - 8.5. (Tchobanoglous 2003)

Other chemical characteristics include alkalinity, gases and metallic constituents. Alkalinity is the total quantity of hydroxides (OH^-), carbonates (CO_3^{2-}), and bicarbonates (HCO_3^-), which are important for biological treatment and for neutralizing acidic conditions. Gases in wastewater include the most common atmospheric gases and hydrogen sulfide (H_2S), ammonia (NH_3), and methane (CH_4), which are formed during decaying of organic matter. Wastewater includes also many different metals, however typically only in trace quantities. Some of them are necessary for microbes to grow properly. (Tchobanoglous 2003)

2.1.1.3 Biological characteristics

Generally, living single-cell micro-organism can be divided in to prokaryotes and eukaryotes. Prokaryotes in wastewater are smaller in size and much simpler in structure than eukaryotes. Prokaryotes include bacteria, blue-green algae and archaea. Eukaryote micro-organisms in wastewater are much more complex and they include fungi, yeast, algae, protozoa, and rotifers. Viruses are not included in prokaryotes or eukaryotes and they are parasites, which need a host cell to reproduce. Prokaryotes are mainly responsible from the biological activity of treatment process and they are usually characterized further. Especially, bacteria can be divided to autotrophic and heterotrophic bacteria, which are further discussed in chapter 2.1.2. (Tchobanoglous 2003).

2.1.2 Activated sludge

Activated sludge process (ASP) was first applied to use in 1913. The biomass in wastewater was observed to been activated by aeration, mixing and recirculating it back to the beginning of biological treatment process. Activated sludge can then treat influent wastewater by consuming different organic, nitrogen and phosphorus compounds.

The main attribute of the process is the formation of floc particles of around 50-200 µm in size. The floc particles remain together due to extracellular polymeric substrates, which are produced by bacteria. These sludge flocs can be settled down by gravity settling and moved back to beginning of the process while remaining clear liquid from the top part can be discharged as effluent. Activated sludge floc particles consists of wide variety of microbes and protozoa species, which convert different parts of organic compounds and nutrients into less harmful form.

The conversions occurring for treating different compounds are organism and boundary dependent. The most important of them, a conversion called aerobic oxidation, occurs when organic compound is the electron donor and oxygen is the electron acceptor. Two other very important conversions are called nitrification and denitrification. In nitrification, ammonia is converted to nitrite and nitrite further to nitrate, while in denitrification nitrate is converted to nitrogen gas. These reactions need a carbon source as they are also part of the microbe's metabolism. Carbon source, electron donor and electron acceptor form a product. Some examples are presented in Table 1. (Evenblij et al. 2006; Tchobanoglous 2003)

Table 1. Classification of micro-organisms by electron donor, electron acceptor, sources of cell carbon and end products, modified from (Tchobanoglous 2003, p. 563).

Type of bacteria	Reaction name	Carbon source	Electron donor	Electron acceptor	Products
Aerobic heterotophic	Aerobic oxidation	Organic compounds	Organic compounds	O_2	CO_2, H_2O
Aerobic autotrophic	Nitrification	CO_2	NH_3, NO_2	O_2	NO_2, NO_3
Facultative heterotrophic	Anoxic denitrification	Organic compounds	Organic compounds	NO_2, NO_3	N_2, CO_2, H_2O

To grow, bacteria need a carbon source, electron donor and electron acceptor as mentioned in Table 1 above. They also need inorganic nutrients like nitrogen, phosphorus, sulfur, potassium, calcium, and magnesium to produce new cellular material. Also, growth factors, which are also known as organic nutrients, are essential to organisms as they are a part of cell material or as precursors. The major growth factors can be classified to amino acids, nitrogen bases and vitamins. The need for growth factors varies from one organism to another. (Tchobanoglous 2003)

Bacteria reproduce by binary fission or by budding. Binary fission is more common where one bacteria divides in to two separate individuals. As the binary fission may happen in minutes, one bacteria can produce several copies from itself even in short period of time. However, in environment like wastewater, the condition limitations will prevent the exponential growth and the number of bacteria will stay rather constant based on the amount of nutrients and substrates. (Tchobanoglous 2003)

Figure 3 shows the bacteria and substrate concentration in a batch reactor to illustrate the different growth patterns of bacteria. In the beginning, there is an excess of substrates and nutrients with very small quantity of biomass population. The first phase called the lag phase represents the time for bacteria to adapt to environmental conditions before they start to reproduce efficiently. The second phase is the exponential growth phase where bacteria are reproducing at maximum growth rate. This is possible because there is no limiting factor in substrates or nutrients. During this phase, the growth curve is exponential, and growth is mainly limited by temperature. The third phase is the stationary phase where biomass concentration stays rather constant and growth is not exponential as bacteria cells start to die in the lack of substrates and nutrients. The fourth phase is the death phase where all the substrate is used, and no growth occurs. The death rate is often observed to be relatively constant fraction of the remaining biomass. (Tchobanoglous 2003)

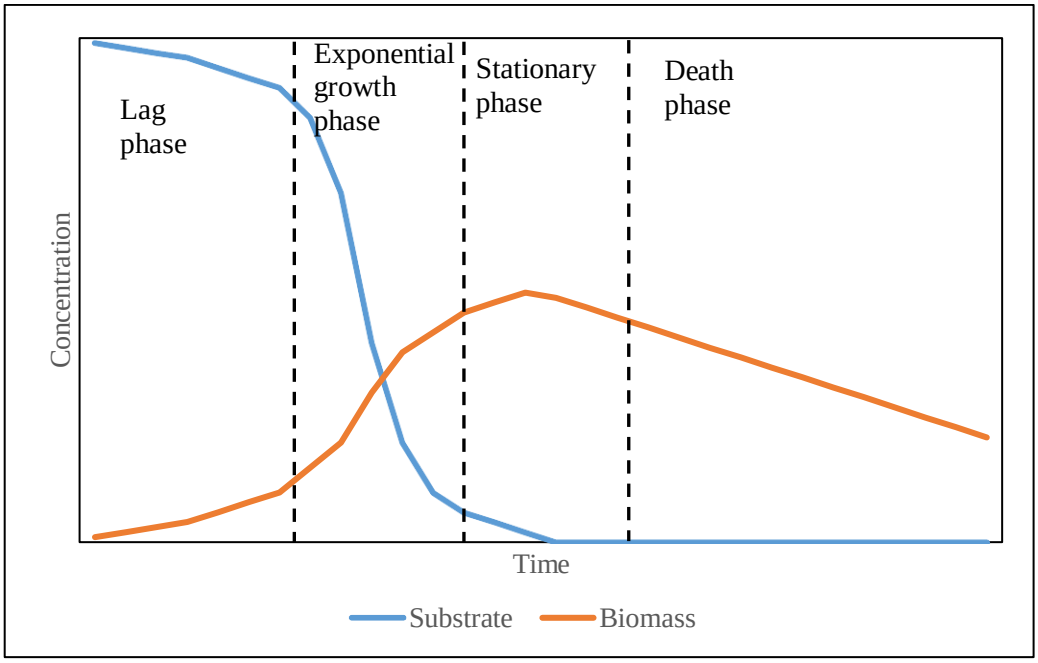

Figure 3. Batch process biomass growth phases with changes in substrate and biomass versus time, modified from (Tchobanoglous 2003, p. 566).

The overall biomass yield can be expressed by the following equation:

$$Biomass\ yield\ Y = \frac{g\ biomass\ produced}{g\ substrate\ utilized} \quad (3)$$

Values for *Y* vary depending of the type of microbes and substrates consumed by the specific microbes. (Tchobanoglous 2003). As different types of bacteria have different optimum growth and decay conditions (e.g. pH), these conditions should be optimized in different parts of the process to enhance optimal growth and substrate utilization for certain types of micro-organisms. Utilization rate of substrates consumed by microbes can also be expressed kinetically. Monod (1949) introduced the following equation for microbial growth kinetics in pure cultures using only one substrate:

$$\mu = \mu_{max} * \frac{S}{K_S + S} \quad (4)$$

where:

μ = specific growth rate, $1*d^{-1}$

μ_{max} = maximum growth rate, $1*d^{-1}$

S = growth limiting substrate concentration, mg/L

K_S = substrate affinity, mg/L.

It should be noted that all parameters in equation 4 are specific to certain microbes and substrate, i.e. they should be measured for different microbe populations independently.

2.1.3 Conventional activated sludge process

The main parts of the conventional activated sludge process (CASP) are pretreatment, biological treatment and clarification. The focus is to maintain effective and healthy activated sludge in the process, which will treat the pollutants biologically. (Evenblij et al. 2006) A typical flow scheme of a CASP is presented in Figure 4.

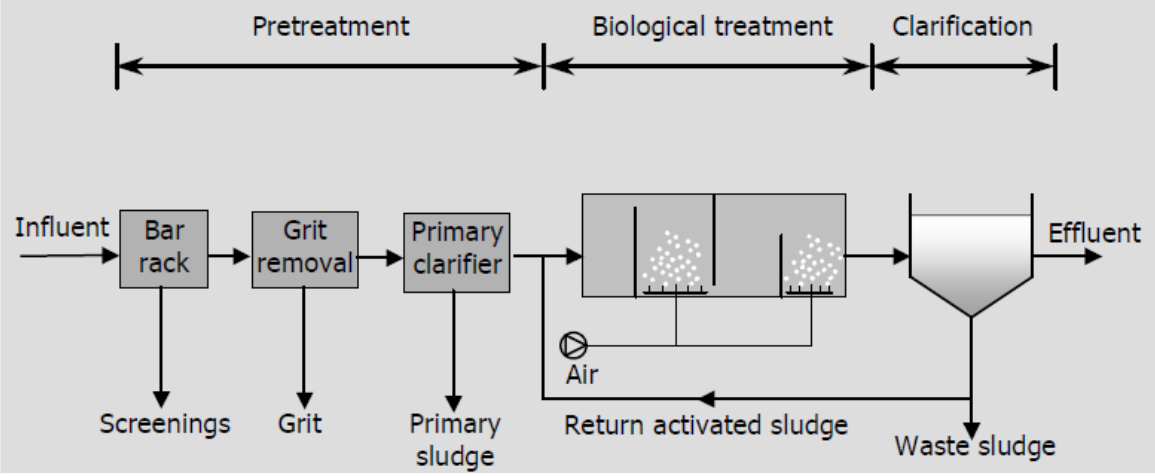

Figure 4. Typical flow scheme of a conventional activated sludge process (Evenblij et al. 2006, p.23)

Pretreatment consists typically of mechanical and chemical process units, which remove coarse material, grit, fat, and grease. Screens are typically located in the beginning of the process and they are used to remove the coarsest material. Depending on the influent quality, screens are followed by grit and grease removal units. Grit and grease removal are followed by primary clarifier. Flocculants are used to remove parts of phosphorus and COD. Typically, primary clarifier removes around 30 - 50% of total BOD_5 and 50 - 80% of TSS. (Tchobanoglous 2003)

2.1.3.1 Biological treatment

Directly after pretreatment, the actual biological treatment takes place. Typically, biological treatment consists of different tanks or otherwise separated sections. As biological treatment is based on microbial activity, the focus is to maintain good growth conditions. Microbes need carbon source, electron donor, and electron acceptor. For BOD removal, which is the most important pollutant to be removed, microbes need oxygen to act as electron acceptor. Typically, oxygen is diffused to mixed liquor by aeration devices and dissolved oxygen levels are carefully controlled.

However, some microbes need NO_2 and NO_3 to act as electron acceptor. These microbes are responsible for denitrification where nitrogen is removed from the process to atmosphere as inert nitrogen gas (N_2). Denitrifying microbes cannot compete against aerobic heterotrophic microbes when dissolved oxygen concentrations are above certain levels. To achieve good nitrogen removal, some of the tanks or sections should be operated without aeration to keep oxygen levels low enough.

Biological treatment needs careful control and should be operated differently during different influent loads. Also, pH and alkalinity should be controlled to maintain proper microbial growth. Efficient mixing maintains a good interaction between sludge flocs and mixed liquor. Especially, in non-aerated parts, mixing is important for maintaining movement.

To keep the floc particles activated, they should be recirculated back to the beginning of the biological treatment process. Usually, this return sludge is withdrawn from the bottom of the secondary clarifier. The old microbes should be removed occasionally to keep the flocs in a good growth phase. Excess sludge can be removed from the return sludge channel or from other parts of the biological treatment process. Excess sludge amount affects solids retention time (SRT), which should be also controlled carefully. (Tchobanoglous 2003)

2.1.3.2 Clarification

The final step in CASP is clarification where sludge flocs are settled to the bottom of the clarifier. The process is based on the gravity where sludge particles settle based on their

settleability. Flocculants are usually applied to enhance the sludge floc settleability by increasing their size and density. Activated sludge is circulated from the bottom or near the bottom of the secondary clarifier to the beginning of biological treatment process. Effluent is discharged from or near the top of the clarifier. (Evenblij et al. 2006; Tchobanoglous 2003)

2.1.4 Extracellular polymeric substances (EPS) and soluble microbial products (SMP)

Extracellular polymeric substances (EPS) and soluble microbial products (SMP) are produced and consumed due to the microbial activity of active cells. EPS are mainly polysaccharides and proteins and they are important part of activated sludge as they help to form the floc particles. They also ease cell interactions with the environment and help to protect the cells by forming protective layer around them. They can also accumulate nutrients from the wastewater. SMP contain much more diverse types of substances than EPS and they are smaller in size. (Evenblij et al. 2006). EPS and SMP are formed when active cells secrete them. They are also formed in cell lysis and hydrolysis. The metabolism and formation of EPS and SMP is presented in Figure 5.

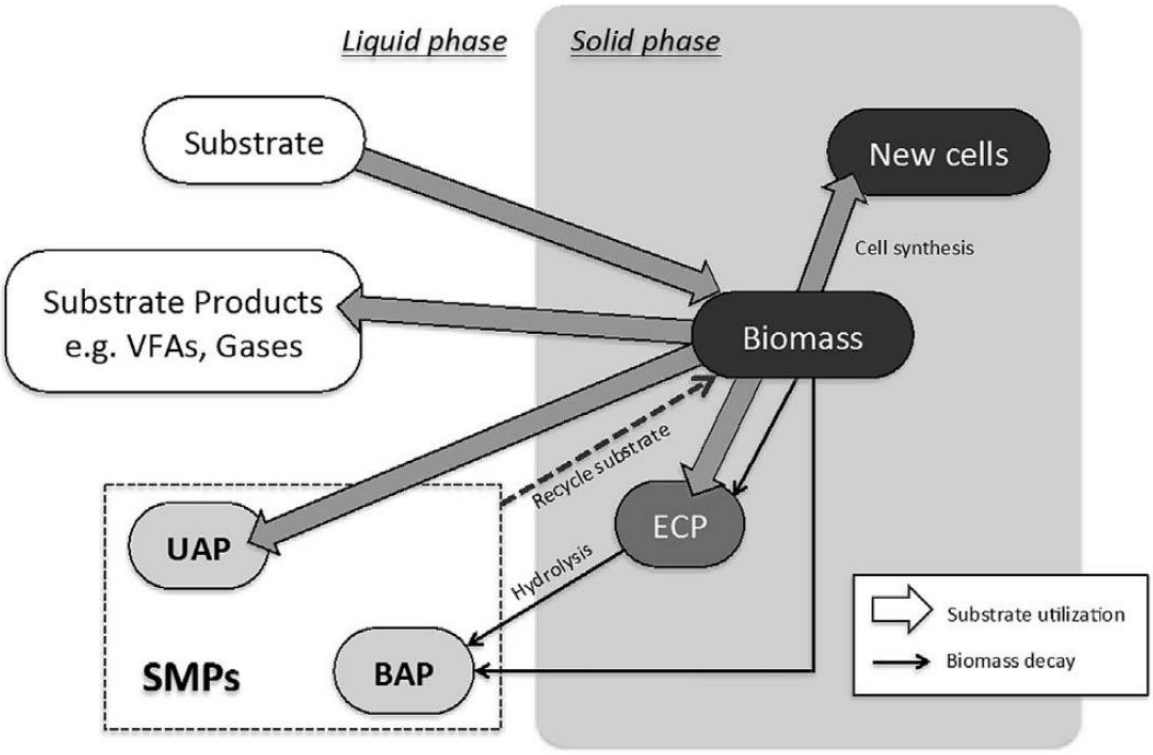

Figure 5. Metabolism of SMP and EPS (ECP in the picture) formation in a heterotrophic biological wastewater treatment system. (Kunacheva et al. 2014)

As shown in Figure 5, EPS are formed when active cells grow or lyse. Further EPS is hydrolysed to biomass-associated products (BAP) which is one part of SMP. BAP are formed also during biomass decay. Utilisation-associated products (UAP) are formed when active cells grow and consume substrates. Active cells can also use SMP as a substrate while growing. (Kunacheva et al. 2014)

EPS are attached to the cell surface and consist mainly of polysaccharides and proteins. They vary in size and composition but look like filaments or strings. One way to characterize EPS is to divide them in to loosely bound EPS (LB-EPS) and tightly bound EPS (TB-EPS). LB-EPS are loosely attached to cell surface and will withdraw from cell surface even in small shear stress. This is also found to be one of the reasons why LB-EPS causes more fouling in MBR systems than TB-EPS. TB-EPS is more tightly attached to cell surface. Another way to characterize EPS is by its composition. Even though EPS are mainly composed of polysaccharides and proteins, EPS are much more complex in structure and include also content from cell decomposition. (Evenblij 2006; Zhang et al. 2012; Kunacheva et al. 2014).

SMP is formed both in hydrolysis of EPS or microbes and when microbes grow and utilize substrates. The amount of SMP in activated sludge systems is found to be influenced by SRT, HRT and different shock conditions. Different shock conditions are found to stress cells and while stressed, they increase SMP production. This has been achieved by decreasing the available substrates or varying temperature rapidly. Also, there seems to be an optimum SRT for minimum SMP production. (Evenblij 2006; Kunacheva et al. 2014). These conditions should be discovered while operating an MBR process to minimize the SMP production.

2.2 Membrane filtration

In MBR, membrane filtration is used for solids removal instead of gravity sedimentation in the secondary clarifier used in CASP. Membrane allows only some constituents to pass through and for optimal effluent quality, usually needs different operational conditions compared to CASP. Otherwise, the process scheme is similar to CASP, as seen in Figure 6.

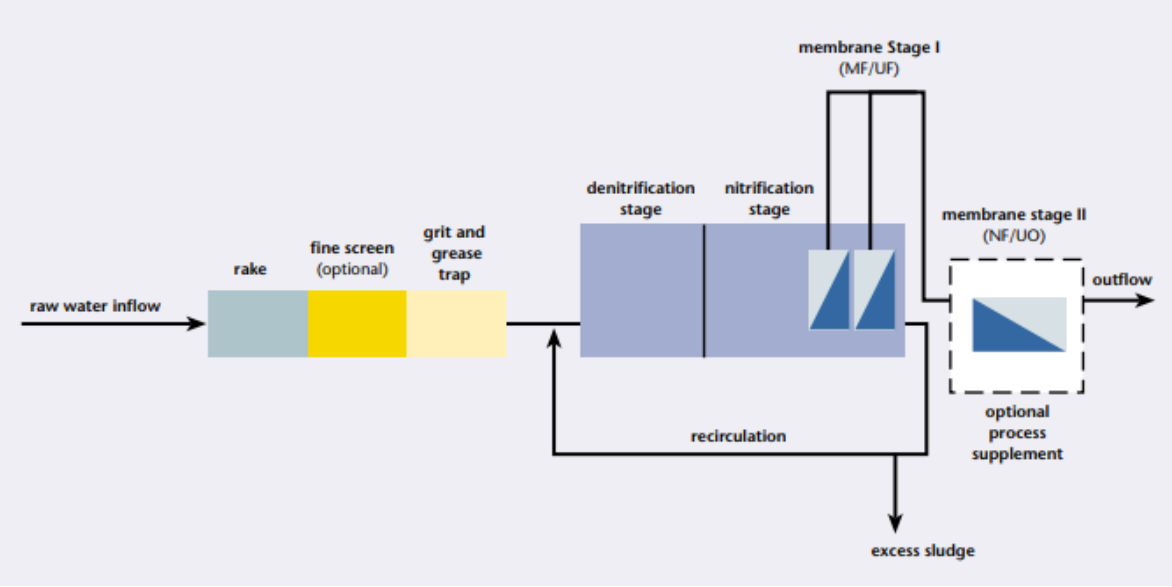

Figure 6. Typical MBR process scheme (Friedrich et al. 2003, p. 65).

Membrane bioreactor's performance is often described with the following equation:

$$J = \frac{Q}{A} \tag{4}$$

where:

J = permeate flux [L/(m^2*h)], or [m/s]

Q = permeate flow [m^3/h]

A = area of membrane [m^2].

Membrane tank is typically scoured by air to circulate the sludge and to scour the membranes clean from different substituents. The amount of air scouring is process-specific and may be much higher than aeration needed for aeration tanks. (Friedrich et al. 2003). Membrane filtration can be classified in to four different processes, which vary based on their pore size. These processes are reverse osmosis (RO), nanofiltration (NF), ultrafiltration (UF) and microfiltration (MF) whose pore sizes are presented with different components in Figure 7. (Evenblij et al. 2006).

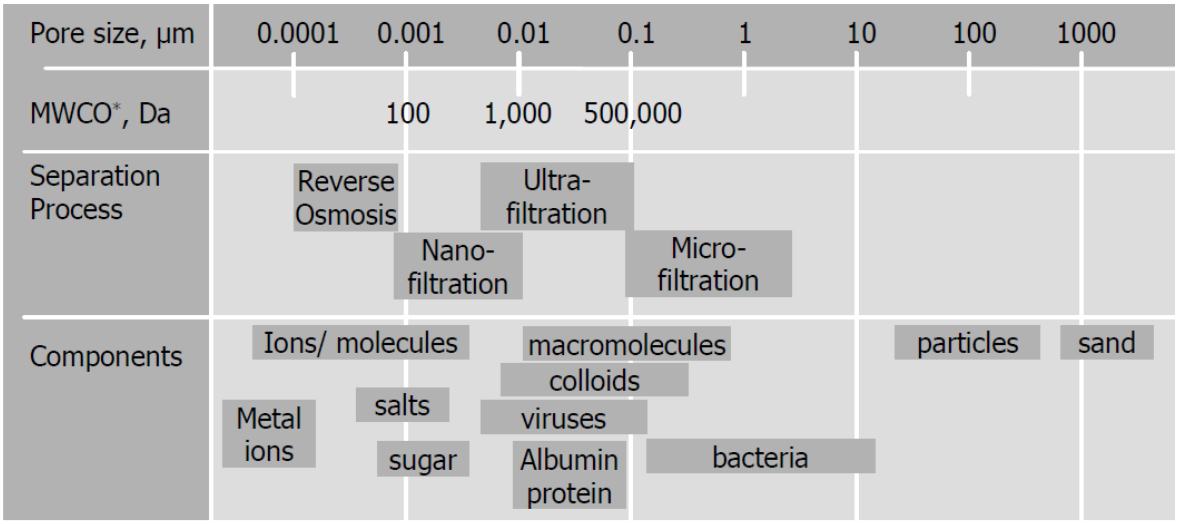

Figure 7. Particle sizes of various components as well pore sizes of separation processes (Evenblij et al. 2006, p. 32)

The most commonly used processes for wastewater treatment are micro and ultrafiltration. Ultrafiltration removes particles in the range between 0.02 - 0.1µm, which include all bacteria and most of the colloids, viruses, and macromolecules. Microfiltration removes particles in the size of around 0.1 - 1 µm which includes all suspended solids and most of the bacteria and biggest colloids and macromolecules. Even though reverse osmosis and nanofiltration would be more effective filtration methods as they could remove much smaller

particle size foulants, they are usually not used in MBR systems as the main particle separator. However, they can be used in tertiary treatment. (Janus 2013).

The pore size of membrane also defines its selectivity, which can also be expressed as molecular weight cut off (MWCO). It equals the molecular weight of a solute, which is rejected with 90 % efficiency. The following equation is applicable for rejection factor:

$$R = 1 - \frac{c_{i,permeate}}{c_{i,feed}} \quad (5)$$

where:

R = rejection factor [-]

$c_{i,permeate}$ = concentration of component i in permeate side [mg/L]

$c_{i,feed}$ = concentration of component i in feed side [mg/L].

(Evenblij et al. 2006)

In MBR process, a trans-membrane pressure (TMP) is usually used as the driving force to push the liquid through a membrane. The MBR can be driven by varying permeate flux (J) while keeping the TMP constant, or by varying TMP while keeping J constant. Under laminar conditions, the following equation applies to a permeate flux for pure solvent:

$$J = \frac{\Delta P}{\eta_p R_t} \quad (6)$$

where:

J = permeate flux [L/m^2*h], or [m/s]

ΔP = trans membrane pressure [Pa], or [bar]

η_p = permeate dynamic viscosity [Pa * s]

R_t = total filtration resistance [m^{-1}].

If foulants are present, the total filtration resistance (R_t) is the sum of the clean membrane resistance (R_m) and fouling resistance (R_f), as presented in equation 7:

$$R_t = R_m + R_f \quad (7)$$

Permeate dynamic viscosity is commonly close to pure water viscosity. The following temperature dependent equation can be applied:

$$\eta_p = \frac{479 * 10^{-3}}{(T+42.5)^{1.5}} \quad (8)$$

where:

η_p = permeate dynamic viscosity [Pa * s]

T = temperature [°C].

(Evenblij et al. 2006).

In MBRs, the membranes are directly in contact with mixed liquor. Physicochemical interactions between the membranes, its pores and mixed liquor lead to membrane fouling, which can be categorized in different ways (Chang et al. 2002).

To classify membrane fouling by its permanency, fouling is divided to reversible, irreversible and irrecoverable fouling. Reversible fouling occurs when suspended solids, colloids and gels in mixed liquor create a cake layer, which accumulates to membranes. Reversible fouling can be minimized or prevented completely with low flux combined with high CFV and/or high air flows. To periodically remove reversible fouling, backwashing and relaxation are performed. Irreversible fouling occurs when dissolved and some colloidal matter are absorbed inside pores. This matter accumulates over time and constricts the pores or blocks them completely. Irreversible fouling cannot be cleaned by mechanical cleaning methods, but chemical cleaning can be done. Irrecoverable fouling generates over long time and cannot be removed by mechanical and chemical cleaning methods. (Janus 2013)

Another way to categorize fouling is by dividing the types of foulants by their biological and chemical features. Biofouling is associated with the activity of bacterial cells or flocs where they are in contact with membrane surface. Depending on the conditions bacterial cells may form dense biofilms, which create more resistance than cake layer, and release SMP and EPS, which further increase fouling. Organic fouling is the deposition of EPS and SMP inside the membrane pores and to the surface. The precipitation of different inorganic compounds, inorganic fouling, can happen chemically if ion concentrations are over saturation concentrations, or biologically when bacterial cells and biopolymers cause the precipitation. The most dominant of these are biofouling and organic fouling while inorganic fouling happens only in certain conditions. (Janus 2013).

Membrane fouling is typically caused by four different types of fouling mechanisms as shown in Figure 8. Number 1 is pore constriction, where particles with small diameter are attached and accumulated inside pore walls. Number 2 shows complete pore blockage where pores are blocked completely by particles bigger than the pore size. In number 3 also the larger particles partly block the pores. Number 4 shows cake formation where a mix of particles with various sizes attach to membrane surface but allow liquid to flow between particles. All four mechanisms reduce membranes performance and their force may be different based on conditions in membrane, mixed liquor and their interactions. (Janus 2013.)

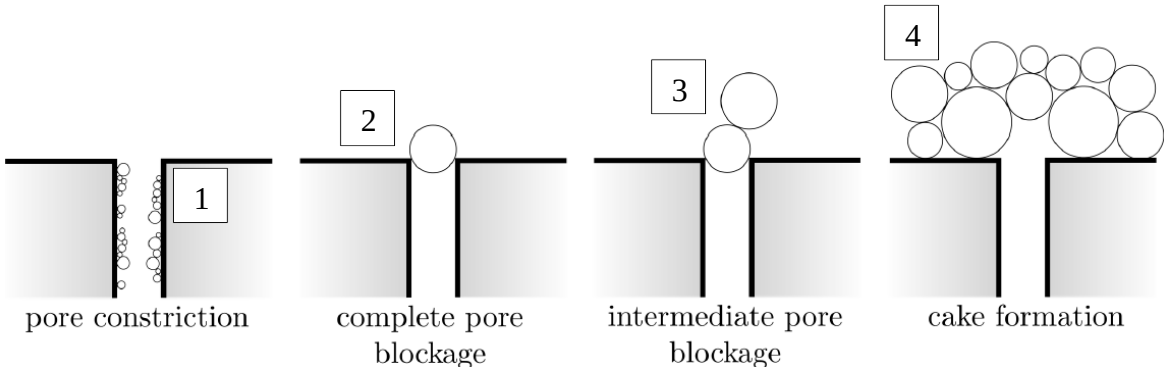

Figure 8. Classical fouling model visualization, modified from (Janus 2013, p. 146).

2.3 Comparing MBR to CASP

As mentioned before, the biggest difference between MBR and CASP is the circulation of solids. CASP is sensitive to floc settleability and parts of the TS can leak to effluent during abnormal process conditions. This means that MBR can be operated with much longer SRT, which is also easier to control as the MLSS concentration is same in all parts of the tanks. A higher circulation sludge flow can be maintained, which leads to a higher overall MLSS concentration and better biosorption. Consequently, the footprint of the plant is smaller. Also, higher MLSS is found to enhance virus removal (Miura et al. 2009) and membranes also reject almost all microbes, which improves effluent quality.

The chemicals for pH control are typically different in the MBR compared to CASP. MBR is controlled by NaOH as CaO_3 or other calcium-based chemicals typically used in CASP

may cause scaling to membranes. (Janus 2013) This leads to better pH control but may be more expensive to control.

One of the major disadvantages for MBR is the need for intensive air scouring of the membranes. This causes higher operational costs and higher energy demand, especially in larger systems. Also, membranes need to be cleaned chemically to prevent fouling. (Friedrich et al. 2003; Janus 2013; Evenblij 2006)

3 MODELING AND SIMULATION OF ACTIVATED SLUDGE AND MEMBRANE FILTRATION

The basis for modeling is the representation of a real-life object, process or situation in a numerical form. These representations use mathematical equations and are called numerical models, which can be simulated using simulators. Usually many datasets are needed for a numerical model to be applicable, and validation is needed for models to behave correctly under various conditions. (Rieger et al. 2012).

Numerical models are used for different purposes, which can be divided into prognostic, diagnostic and educational, as shown in Figure 9. In prognostic applications, models are often used for plant optimization or design mainly to predict the future. In diagnostic applications, models are used for understanding the functioning of different processes. Educational applications can be used for teaching the systems specific behaviour and can be also useful for consulting purposes. (Hug et al 2009).

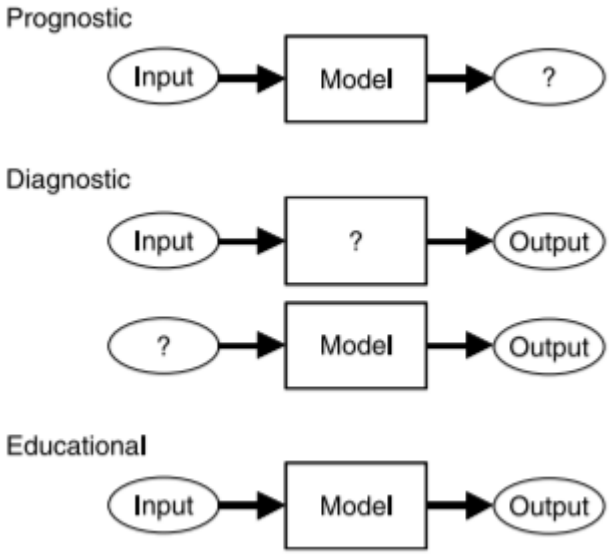

Figure 9 Various purposes for using wastewater process models (Hug et al 2009.)

To create a proper wastewater system model, some key issues should be taken into account. These include reliable measurements, selecting important characteristics and behaviour and

making some simplifying approximations and assumptions. Also, the accuracy of simulation results and the reliability of outputs should be noted.

One of the most important issues in creating a model is determining its boundaries. They might include only the plant or maybe some larger system like the whole city. This is mainly why model inputs rarely are same for different models. Also, the scope of the model affects the inputs needed. The inputs must usually be generated from different observations from real world.

Observations, which are used as inputs should be converted into model input variables to be useful in model simulation. Also, model outputs should be converted so that calculated results can be compared with real world observations. Activated sludge models need variables that represent the input concentrations of different compounds as well as other important components like temperature or flow. Often the modeled system needs sub-models, which describe different processes or operational units (e.g. membrane filtration).

A set of differential equations is used in the activated sludge models. The equations are used to calculate the accumulation of different state variables (C_x) in a time step (dt) and volume (V). Influent (Q_{in}) and effluent (Q_{out}) flow as well as biokinetic conversion (r) should also be considered. Equation 9 shows the basic form of differential equation used in activated sludge modeling.

$$\frac{dM}{dt} = \frac{d(v * C_x)}{dt} = r * V + Q_{in} * C_{x,in} - Q_{out} * C_{x,out} \quad (9)$$

The first term on the right-hand side is the biokinetic model conversion. The other terms on the right-hand side represent the transport model of components inside and outside of the specific model. Hydraulic behaviour can be modeled by linking many separate reactors to represent different systems. Also, other terms like precipitation or transport of gases can be added to the equation. (Rieger et al. 2012).

3.1 The GMP Unified Protocol

To unify projects in wastewater process modeling, a unified protocol is introduced by IWA Task Group. The unified guideline includes 5 steps which are discussed further in the following chapters. All the steps should be agreed and reviewed with all the parties involved in the project called stakeholders, before continuing to the next step. The proposed illustration of the steps and links between them is described in Appendix II. (Rieger et al. 2012)

3.1.1 Project definition

Upon starting a new modeling project, it is important to define its meaning and aim. Stakeholders should pay careful attention to this step as it may greatly affect the budget and schedule. Determining the scope properly gives the whole project group a good understanding of how to proceed. Changing or expanding the scope has a strong impact on all parts of the project.

This step consists of problem statement, objectives, requirements and client agreement. The problems should be solved with the model and objectives are determined to achieve those solutions. Objectives are model boundaries, for example, and required variables for calibration. Requirements determine the needed resources such as staff and budget. Finally, stakeholders should agree on the project definition before continuing to the next step. (Rieger et al. 2012)

3.1.2 Data collection and reconciliation

Data collection and reconciliation are found to be one of the most effort taking phases in wastewater process modeling. All the phases should be implemented with care as it saves time in the following modeling steps. Also, the input data quality strongly affects the calibration step.

3.1.2.1 Understanding the plant

The first phase is understanding the plant, which includes possible site visits, process flow scheme analyses and communication with WWTP workers. The plant should be understood as operated. Process flow scheme analyses together with piping and instrumentation diagram give deeper understanding of treatment steps and operation modes for different situations. Design should be compared with real status of the plant as the actual location of probes may differ from the designed locations (Rieger et al. 2012).

3.1.2.2 Collection of existing data

The second phase is collection of existing data. Figure 10 shows the different data types for wastewater process modeling projects.

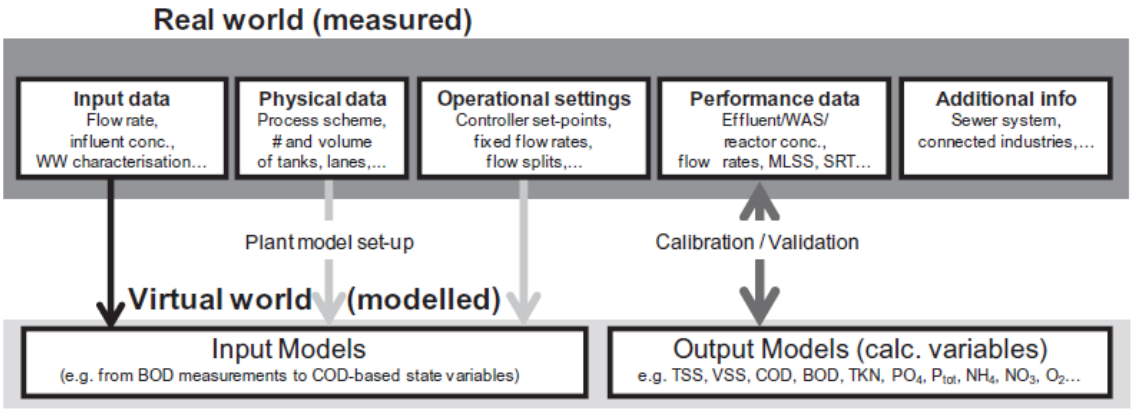

Figure 10. Data types required for simulation studies (Rieger et al. 2012, p.57)

Input data is measured directly from the system. Some of the input data can be further analyzed in laboratory such as different compounds of COD in the influent. An example of physical data is the volume of a certain tank. Operational settings are used to operate a WWTP. These can be set points of dissolved oxygen in aeration tanks, for example. Input data, physical data and operational settings are used to create input models.

Performance data describes the performance of the WWTP. These include effluent concentration, MLSS, SRT and many other variables. Performance data is used as a comparison for output models to calibrate and validate created virtual model parameters. (Rieger et al. 2012)

3.1.2.3 Data analysis and reconciliation

The third phase is data analysis and reconciliation where the quality of the data should be checked. True value is never known but in a closed wastewater treatment system input-output relation with process knowledge gives information about the accuracy of the measurements. Figure 11 shows that systematic errors can be caused by calibration curve errors, offsets or signal drifts. Random errors are caused by errors in measuring equipment, measuring practice or differing environmental conditions. Outliers should be removed while processing data.

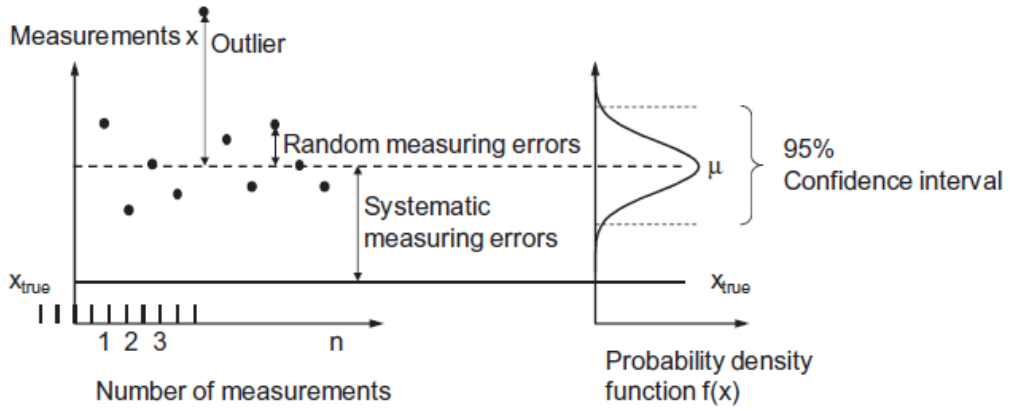

Figure 11. Definition of systematic errors, random errors and outliers (Rieger et al. 2012)

Data reconciliation includes 4 steps: fault detection, fault isolation, fault identification and data reconciliation. In the first step, data is visualized, structured and descriptive statistics is performed. Data visualization gives a good overview of the data and can reveal some serious faults, such as incorrect time stamps of the samples. In data structuring, the data is grouped to represent certain conditions. After structuring, descriptive statistics can be carried out. They give more detailed insight to variety of plants load compared to design load. Then simple and advanced sanity checks are being performed with mass balance analyses. If no faults are detected and data is found to be sufficiently accurate, no other steps are needed. If faults are detected, the second step is performed.

In the fault isolation step, mass balances are combined, expert knowledge and validation experiments are performed until all faults are isolated and validated. Expert knowledge is

used to form hypotheses how to find faults and perform validation experiments. Overlapping mass balances can also help to locate errors. The third step, fault identification, includes quantification experiments and special experiments and is performed until all faults are quantified. Sources of errors can be divided according to their causes. These causes are flow measuring, sampling, analytical methods and online sensors. In the fourth step data is reconciled by resolving the faults. This is performed by re-calibrating devices, repairing or resolving issues and correcting existing data. This step is important as activated sludge models usually have a closed mass balance. Finally, stakeholders agree that data and measuring devices are set with enough accuracy. (Rieger et al. 2012).

3.1.2.4 Additional measurement campaigns

After data reconciliation some critical data may still be missing. Additional measuring should be planned carefully as it needs a lot of effort and may cause additional costs. If intensive additional measurements are needed, client agreement is required. (Rieger et al. 2012).

3.1.3 Plant model set-up

For plant model set-up, a few things should be noted. Setting the boundaries correctly is important as it affects the assumptions, which are made on the model. All process units should be inspected, and it should be decided if some of them need sub-models such as a detailed settling model inside the clarification unit. Also, the assumptions should be planned carefully as they simplify the model. (Rieger et al. 2012).

3.1.4 Calibration and validation

Calibration is iteration to obtain simulation results that are close enough to the measured values by changing the values of the model parameters. The calibration parameters should be chosen carefully. The model is calibrated when the decided tolerances in previous steps are not exceeded. Validation is performed to check whether the measured values match with the calibrated parameter values. General validation is typically included in ASM models as they have been used for several years. Project specific validation needs to be done and typically requires intensive measuring campaigns during different project conditions. (Rieger et al. 2012).

3.1.5 Simulation and result interpretation

Simulation and result interpretation are strongly linked to the project definition step. This step is used to fulfil the project definition step requirements. During this step, the calibrated and validated model is used to simulate the previously decided scenarios. One of the key components include deciding whether to use dynamic or steady-state simulations. Steady-state simulations can be used to estimate the overall mass balance, for example, but dynamic simulations are usually needed for peak flow simulations and for sizing pumps or blowers. The most important part of result interpretation is to show results in a clear and understandable way. (Rieger et al. 2012).

3.2 Literature review

Literature review was performed to acquire information on models related to the MBR process. Both the biological models for biopolymers and mechanistic models for membrane fouling were reviewed. The main goal was to find models that can be used in the scope of this thesis.

3.2.1 Biological models

Biological models include models, which describe the EPS and SMP behaviour in the MBR process. These are found to be the main biopolymers, which are not included in ASM models. Review of the models is presented in Table 2.

Table 2 Review of the biological models including biopolymers.

Author and year	Basic structure	Bio-polymers	New components / processes	Calibrated / validated	Summary of findings
Jiang et al. 2008	ASM2d	S_{UAP}, S_{BAP}	2 / 6	Yes / Yes	SRT is the key operational parameter affecting SMP concentrations. Higher SRT increases UAP concentration and decreases BAP concentration. Contrariwise, lower SRT yields higher BAP and lower UAP.
Laspidou and Rittmann 2001	-	X_{EPS}, S_{BAP}, S_{UAP}	6 / 11	Yes / Yes	EPS correlates with active biomass and accumulates while decay is dominant. BAP correlates with EPS. UAP concentration is the highest of soluble components when substrate utilization is high.

Lu et al. 2001	ASM1	S_{UAP}, S_{BAP}	2 / 4	Yes / No	SMP is divided into two separate biopolymers.
Ahn et al. 2006	ASM1	X_{EPS}, S_{BAP}, S_{UAP}	3 / 5	Yes / No	MBR sludge has different parameter values compared to CASP sludge. SRT affects EPS concentration.
Janus 2013	ASM1	X_{EPS}, S_{BAP}, S_{UAP}	3 / 7	Yes / Yes	SMP correlates with effluent soluble COD. High HRT produces higher amounts of EPS. SMP is more affected by growth than decay.
Janus 2013	ASM3	X_{EPS}, S_{BAP}, S_{UAP}	3 / 6	Yes / Yes	EPS relates to growth more than to decay.

Earliest models assumed that microbes can consume UAP and BAP similarly and biomass growth is directly linked on their concentration. However, during later studies it was found that UAP and BAP are not similar in their composition and Jiang (2008) noted that BAP has larger molecular weight and a different approach is required to model its behavior. Later findings support the view that UAP and BAP are formed separately as shown previously in Figure 5.

Most of the biological models are based on the well-known ASM models. Only the model presented by Laspidou and Rittmann (2001) has its own basic structure for biological behavior. Their model is also the most complex with 6 components and 11 processes for biopolymers. Even with the complex model, they managed to calibrate and validate it sufficiently.

3.2.2 Mechanistic fouling model

Mechanistic fouling models include many different approaches on membrane fouling and how to minimize or prevent it. Some of the parameters of these models are hard to measure or require a lot of effort in calibration. Models for membrane fouling should be carefully chosen. A short review of the main models created for membrane fouling in wastewater treatment is presented in Table 3.

Table 3 Review of fouling models.

Author and year	Calibrated / validated	Model(s)	Summary of findings
Liang et al. 2006	Yes / Yes	Reversible and irreversible fouling, cake transport	MLSS is related to reversible fouling. Soluble matter relates to irreversible fouling.
Broeckmann et al. 2005	Yes / No	Pore blockage and constriction, cake formation, back flushing	Particle adhesion and distribution have a strong impact on the filtration characteristics.
Wu et al. 2012	Yes / Yes	Pore constriction, cake formation	Cake thickness and porosity relate to air scouring, colloids strengthen the cake formation.
Nagaoka et al. 1998	Yes / No	EPS accumulation, detachment and consolidation	Flux is the key parameter influencing fouling especially near critical flux.
Ho and Zydney 2007	Yes / Yes	Back transport phenomenon	Operation below critical flux prevents high fouling.
Janus 2013	Yes / Yes	Back washing, cake compressibility, SMP deposition, cake formation	Cake deposition related to TMP profiles, irreversibly fouling relates more to flux than SMP concentration.

Nagaoka et al. (1998) introduced the shear induction model for cake detachment and attachment. They linked it to shear stresses caused by permeate flow and air scouring intensity. They were able to calibrate the model but failed to validate it properly. However, their findings could be linked to different operational conditions. Ho and Zydney (2007) introduced the back-transport model for cake detachment and related it to forces affecting the cake. They were also able to validate the model. Janus (2013) further improved these models and implemented them to the same model.

Liang et al (2006) divided the resistance to irreversible and reversible fouling. They related the reversible model to MLSS concentration but failed to include shear stresses or particle back-transport. They also noticed the relation to SMP concentration but related the

irreversible fouling only to permeate flow. Wu et al. (2012) further included the pore constriction model. Janus (2013) added both to irreversible fouling model.

4 METHODS

4.1 Wastewater treatment in Mikkeli

Mikkeli is a mid-sized city with a population of approximately 54,000 people. Around 86% of the households are connected to municipal water network and the influent coming to the main treatment plant in Kenkäveronniemi is mainly municipal wastewater. This chapter describes the existing MBR pilot plant in Kenkäveronniemi and the new Metsä-Sairila MBR which is planned to be in operation in 2020.

4.1.1 Pilot MBR in Kenkäveronniemi WWTP

Pilot MBR is in operation since March 2014. The process is shown in Figure 12. Influent is pumped directly from current Kenkäveronniemi WWTP's effluent channel of primary sedimentation. Influent is pumped through basket filter to an anaerobic tank (volume 600 L) where it is mixed properly. The biological part consists of an aerobic reactor (volume 1800 L) and membrane filtration tank (volume 1800 L). Activated sludge is circulated back to the aerobic reactor from the membrane filtration tank. Excess sludge is pumped from membrane filtration tank. Permeate is sucked through membranes with vacuum pumps and discharged to Kenkäveronniemi WWTP's aeration tanks. Maximum capacity of pilot is around 2.7 m^3/d for long term operation.

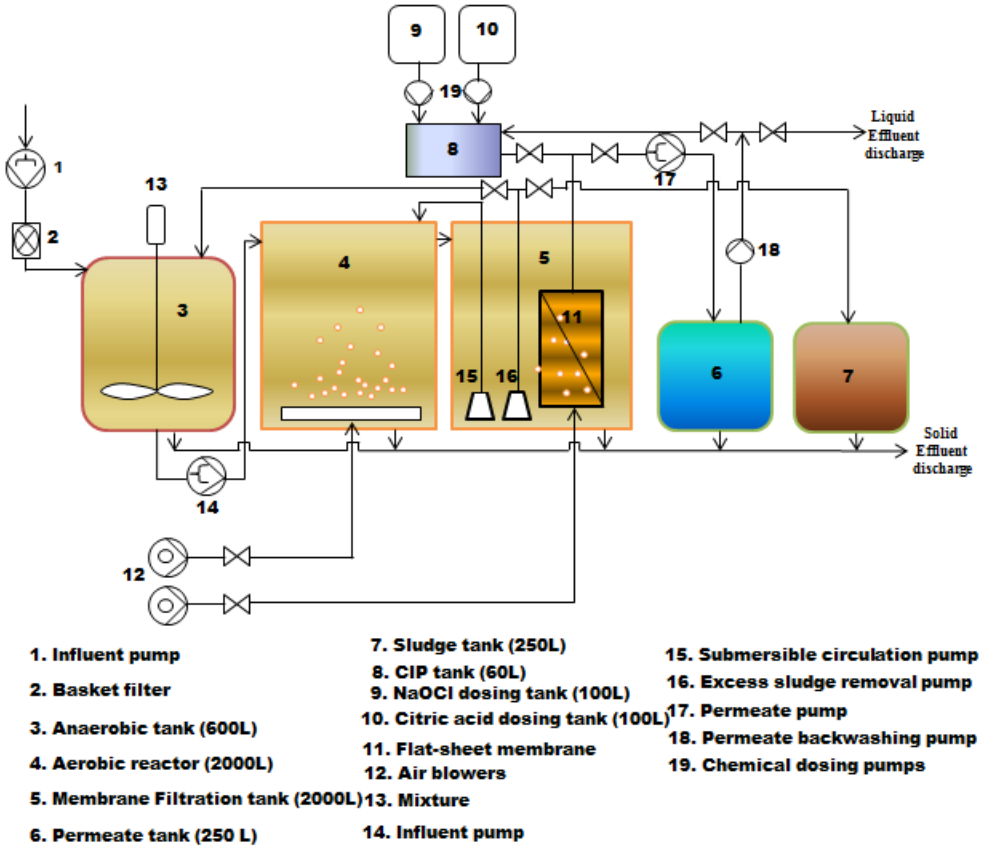

Figure 12. Schematic diagram of the MBR pilot plant (Gurung 2014).

Membranes are flat sheet membranes with nominal pore size of 0.4 µm and a membrane area of 8 m^2. Membrane is cleaned with coarse air bubbles to remove the attached cake, which causes reversible fouling. Citric acid and NaOCl are used for chemical cleaning to remove substances inside membrane pores that cause irreversible fouling. Chemical cleaning is done approximately three times per year.

As there is no denitrification phase, some modifications were made to achieve anoxic conditions in the pilot plant in the beginning of 2017. Cycled aeration was achieved in aeration tank with a time switch and a mixer was added to enable mixing while aeration was not on. To mimic famine stress conditions, influent was turned off occasionally.

4.1.2 Metsä-Sairila new MBR

The new Metsä-Sairila MBR is designed to be in operation in 2020 with a population equivalent of around 63,000. In addition to the households in Mikkeli, it will also treat

wastewater from the surrounding areas. The process is shown in Figure 13. Influent to the new MBR will be pumped from the equalization basin. The first part of the new process includes coarse screening, grit and sand removal, and fine screening. The second part is the primary clarifier, which can be bypassed partially to provide enough carbon for denitrification during low loads. Primary sludge will be pumped to sludge treatment. Aluminum will be used as flocculant and it will be dosed to the beginning of the grit removal. The total volume of the primary clarifier will be 990 m^3.

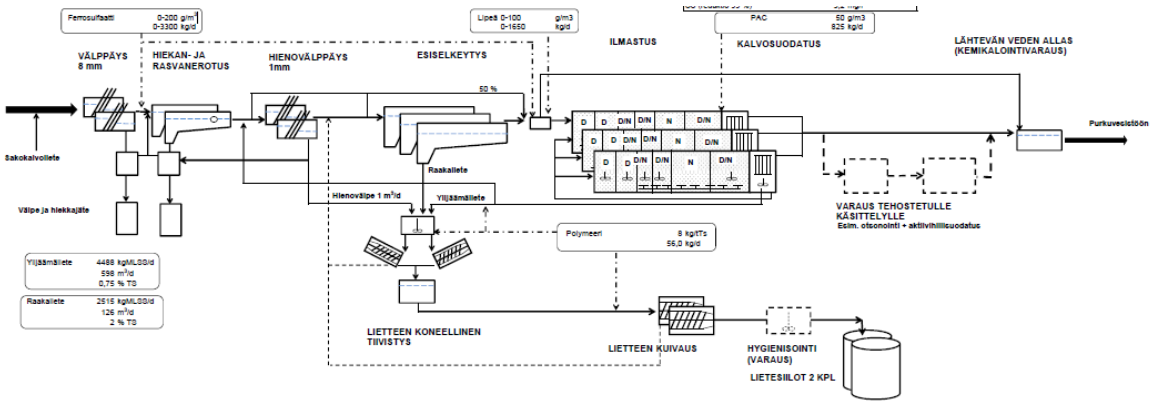

Figure 13. Schematic diagram of Metsä-Sairila new MBR plant.

The next part is the biological treatment, which consists of three parallel trains. Each train consists of six different sections. First two of the sections, with a total volume of 3000 m^3, do not have aeration. This is because return sludge flowing from the last section is high in oxygen concentration because of membrane scouring and it needs to be consumed by micro-organisms to save some of the energy needed for aeration. Influent will be pumped to second section. Aeration in sections three and four, total volume of 3000 m^3, will be controlled based on temperature and effluent NH_4 concentration to ensure complete nitrification but on the other hand enhance nitrogen removal. Last sections five and six, total volume of 3000 m^3, will always be aerated. Activated sludge is pumped from the end of sixth section to membrane filtration tanks, which are also in three parallel lines. Membranes will be submersed flat sheet membranes with a nominal pore size of 0.2 µm, a total area of 60 000 m^2 and total volume of filtration tanks 3000 m^3. Permeate is sucked through membranes with vacuum pumps.

4.2 Measuring and data collection from pilot process

Measuring and analyses with the data collected from online-analysers for pilot process model calibration were carried out between November 2016 and December 2017. The full analytical sheet from influent wastewater to pilot MBR is as Appendix III, the full sheet of MLSS with EPS and SMP analyses is as Appendix IV and Appendix IX. Analyses of different components presented in Table 4 were done according to SFS standards.

Table 4 Components with their respective SFS standard.

Component	Standard
TSS [mg/L]	SFS-EN 872
VSS [mg/L]	SFS-EN 872
COD [mg O_2/L]	SFS 5504
BOD_5 [mg O_2/L]	SFS-EN 1899
TP [mg/L]	SFS 3026
TN [mg/L]	SFS 5505
NO_3-N [mg/L]	SFS 3030
NO_2-N [mg/L]	SFS 3030
NH_4-N [mg/L]	SFS 5505

4.2.1 COD fractioning

As activated sludge models are mainly based on different COD fractions, characterizing COD is important. Wentzel et al. (1995 and 1999) proposed a method to analyze readily biodegradable COD (S_S) from influent wastewater. Laitala (2005) tested the method for seven different Finnish WWTPs and found that the method is applicable for analyzing S_S concentration in influent wastewater. The method is based on microbes consuming S_S while aerating wastewater sample. An oxygen uptake rate (OUR) is measured during the test and plotted out. The following equations can be applied for measuring the concentration of S_S:

$$S_S = \frac{1}{1-Y_{ZH}} * \int_{=0}^{=d} (OUR_{total} - OUR_{SBCOD}) * dt$$
$$= \frac{1}{1-Y_{ZH}} * \int_{=0}^{=d} OUR_{S_S} * dt$$
$$= \frac{\mu_H * Z_{BH(0)}}{Y_{ZH} * slope * 24} * (e^{slope * t_d} - 1) \quad (10)$$

$$\mu_H = slope * 24 - K_{MP} + b_H \quad (11)$$

$$K_{MP} = \frac{OUR_{SBCOD(t=s)} * 24}{\frac{1-Y_{ZH}}{Y_{ZH}} * Z_{BH(0)} e^{slope*(t=s)}} \quad (12)$$

$$Z_{BH(0)} = \frac{e^{intercept} * 24}{\frac{1-Y_{ZH}}{Y_{ZH}} * (slope*24 + b_H)} \quad (13)$$

where:

S_S = readily biodegradable COD, mg COD/L

Y_{ZH} = heterotrophic yield = 0,666 mg COD/mg COD

OUR_{total} = total OUR during the test

OUR_{SBCOD} = OUR due to slowly biodegradable COD

μ_H = heterotrophic maximum specific growth rate on SS, 1/d

$Z_{BH(0)}$ = heterotrophic active biomass concentration, mg COD/L

slope = slope of $\ln OUR_{(t)}$ versus time (h) plot

t_d = time of precipitous drop in OUR(h)

K_{MP} = heterotrophic maximum specific growth rate on SS, 1/d

b_H = heterotrophic specific death rate, 1/d

$OUR_{SBCOD(t=s)}$ = OUR due to SBCOD only, mg O/(L*h)

(t=s) = time immediately following the precipitous drop in OUR(h)

intercept = $\ln OUR_{(t=0)}$ of $\ln OUR_{(t)}$ versus time (h) plot

[26]

Total truly soluble COD can be measured with a method proposed by Park et al. (1997). The test is done by flocculating and stirring the wastewater sample with $Zn(OH)_2$ in alkaline conditions. After flocs have settled to the bottom, supernatant is filtered through a 0.45 µm filter and the COD is measured from filtrate. The procedure removes all colloid and particulate matter so only the soluble fraction of COD remains. (Park et al. 1997).

4.2.2 Protein and carbohydrate analyses

Protein and carbohydrate concentrations were analysed according to methods proposed by Lowry et al (1951) for proteins and Dubois et al (1956) for carbohydrates, respectively.

These methods are commonly used in many scientific articles for total quantification of carbohydrates and proteins concentration in wastewater, activated sludge and their constituents.

The method for proteins is based on the reaction where copper ions react with peptide bonds and form a blue molecule with Folin-Ciocalteu reagent, which can be measured by colorimetric techniques (Lowry et al. 1951). As the Lowry protein assay is based on reactions with peptide bonds and forms a single blue molecule with each of the bonds, this method can overestimate the overall protein concentration if they consist of monopeptides, polypeptides or other organic polymers. Reactions of 80 different compounds with Folin-Ciocalteu reagent were also studied by Everette et al. (2010). Their results showed that many other compounds than proteins in SMP and EPS reacted with the reagent. Thus, the Lowry protein assay may overestimate the total protein concentration (Kunacheva et al. 2014)

The Phenol-Sulfuric Acid method is based on the reaction of carbohydrates and phenol, which forms an orange-yellow colour. The colour is measured by colorimetric methods with the absorbance at 420 nm. (Dubois et al. 1956). Glucose and dextrose can be used for standard curve creation (Kunacheva et al. 2014).

4.2.3 Mixed liquor analyses

The maximum nitrification test was conducted to measure the nitrification capacity of mixed liquor. High F/M batch test was used for estimating maximum nitrification and the test was done according to Methods for Wastewater Characterization in Activated Sludge Modeling (2003).

Analysis of SMP and EPS in mixed liquor can be done in several ways. Kunacheva and Stuckey (2014) reviewed and discussed different ways to extract and analyse SMP and EPS with their constituents. The methods used in this work are presented in Appendix V and they include centrifugation, precipitation, ultrasonication and heat extraction to get the total amount of different components of SMP and EPS with reasonable amount of effort.

4.3 Modeling and simulation software

Dynamita's Sumo© process modeling and simulation software was used for modeling and simulation. One of the key reasons for choosing Sumo was its full modifiability for creating and modifying own and previously created biological models and process units. This was essential as studying MBR fouling needs new parameters and changes to well-known ASM models as they do not yet include biopolymers and can still over or under estimate some values, for example if the MLSS concentration is outside the range of the usual concentration of the CAS process. Also, process units need modifying as there is no MBR unit with fouling feature.

Python 3.7 was used for calibrations and simulations as well with results interpretation. Python can be used for automation of Sumo, for example giving the parameter values as a string for Sumo for sequential simulation runs.

5 MODELING

For modeling the MBR and its fouling behaviour, a calibrated and validated biokinetic model Sumo 1 was modified with new components and processes for biopolymers mainly introduced by Janus (2013). The parameters for biopolymers growth kinetics were partially calibrated to correspond to data gathered from the pilot process. Also, a new process unit, which includes a bioreactor with membrane filtration for effluent was created, tested, and its fouling related parameters were partially calibrated. The model creation and sensitivity analysis are presented in chapter 5.1. Chapter 5.2 describes the modeling of pilot process and its calibration phase.

5.1 Creating extended biokinetic model and MBR process unit

5.1.1 Extended biokinetic model

A well-calibrated and validated Sumo1 biokinetic model by Dynamita was used for base structure for biological activity. Some of the parameters for the Sumo 1 biokinetic model were calibrated as an initial step. Also, the aeration was calibrated to get more correct dissolved oxygen concentration levels for further study. The model used in base structure initialization is presented in Figure 14.

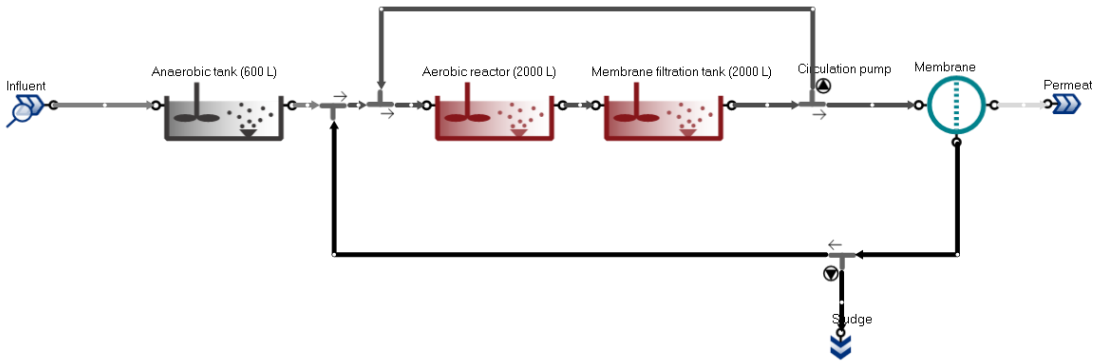

Figure 14. Model used for extended biokinetic model creation and parameter estimation.

The model is a simplified version of pilot process with constant aeration enabling fully aerobic conditions and simple point separator, which rejects all solids and colloids while

letting only the soluble content to pass to permeate. SRT is set to 60 d and influent composition is set to match Sumo1 biokinetic models default values with constant flow.

Extended biokinetic model was mostly adopted from Janus's PhD Thesis (2013). Three new components to Sumo 1 biokinetic model were added for biopolymers: X_{EPS} for EPS, S_{UAP} for utilization associated products fraction of SMP and S_{BAP} for biomass associated products fraction of SMP. Even though many researchers have developed complex models, e.g. modeling protein and carbohydrates contents of biopolymers, the simpler approach for modelling SMP and EPS was chosen mainly because it can be measured without too time-consuming and complex laboratory work. Also, this kind of model's behaviour is well verified with many studies (Janus 2013; Jiang et al. 2008; Laspidou et al. 2001) and the biopolymer fouling can be divided in to two differently formed fractions of SMP. (Laspidou et al. 2001). The illustration of main interactions is presented in Figure 15.

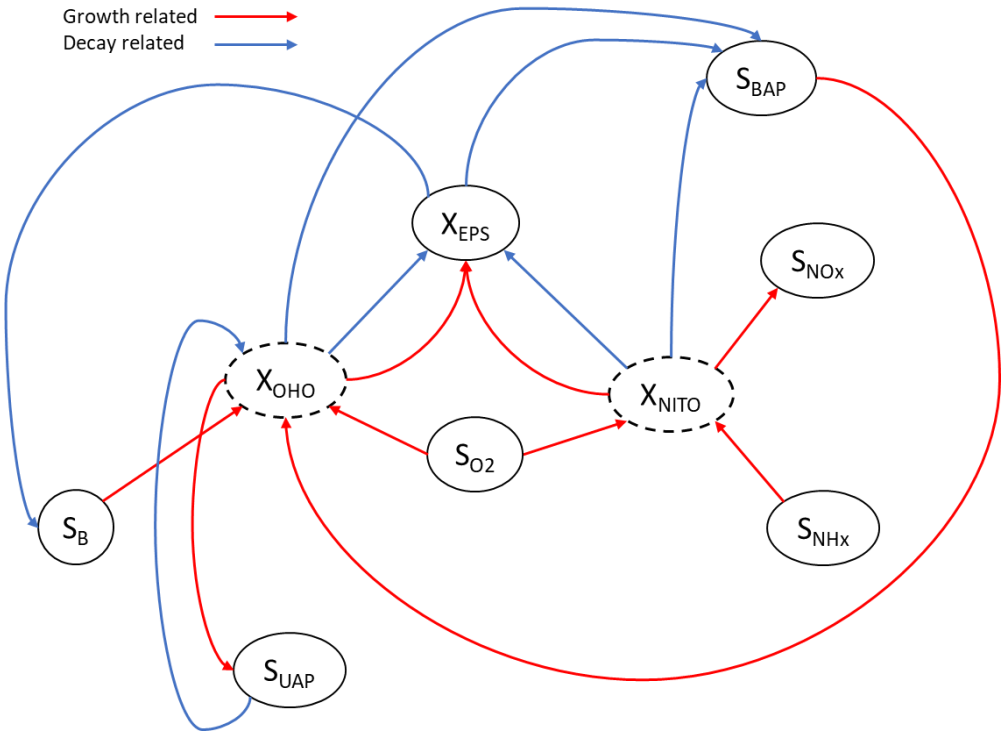

Figure 15. Illustration of some of the biokineticl models' interactions.

Gujer matrix from extended biokinetic model is as Appendix VI and only EPS and SMP related modifications are presented in it. Kinetic and stoichiometric parameters with their estimated default values are presented in

Table 5.

Table 5 Kinetic and stoichiometric parameters with their default values.

Symbol	Name	Default value
Kinetic parameters		
K_{BAP}	Half saturation coefficient for BAP	85
$\mu_{BAP,20}$	Maximum growth rate on BAP in 20 °C	0.15
K_{UAP}	Half saturation coefficient for UAP	100
$\mu_{UAP,20}$	Maximum growth rate on UAP in 20 °C	0.45
$k_{h,EPS,20}$	Hydrolysis of EPS in 20 °C	0.17
Stoichiometric parameters		
$f_{SB,EPS}$	Fraction of SB released during EPS hydrolysis	0.4
$f_{EPS,OHO}$	Fraction of EPS produced on OHO growth	0.1
Y_{SMP}	Yield of SMP	0.45
γ_{OHO}	Fraction of SUAP formed during OHO growth	0.0924
f_{BAP}	BAP produced from OHO decay	0.0215
$f_{EPS,d,OHO}$	EPS produced from OHO decay	0.025

5.1.2 Sensitivity analysis for EPS and SMP model parameters

To see that the extended biokinetic model works correctly and to see how the interactions work, several simulations with varying key parameters were done. The layout of the model used in testing simulations is presented in Figure 14. In the first simulation set, the half saturation coefficient for UAP (K_{UAP}) was varied between 50 and 250. The simulation results with concentrations of different components inside membrane filtration tank are presented in Figure 16a – e.

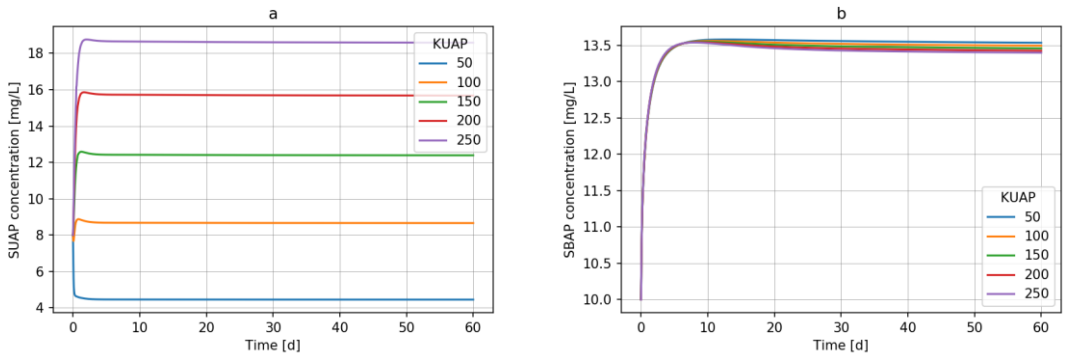

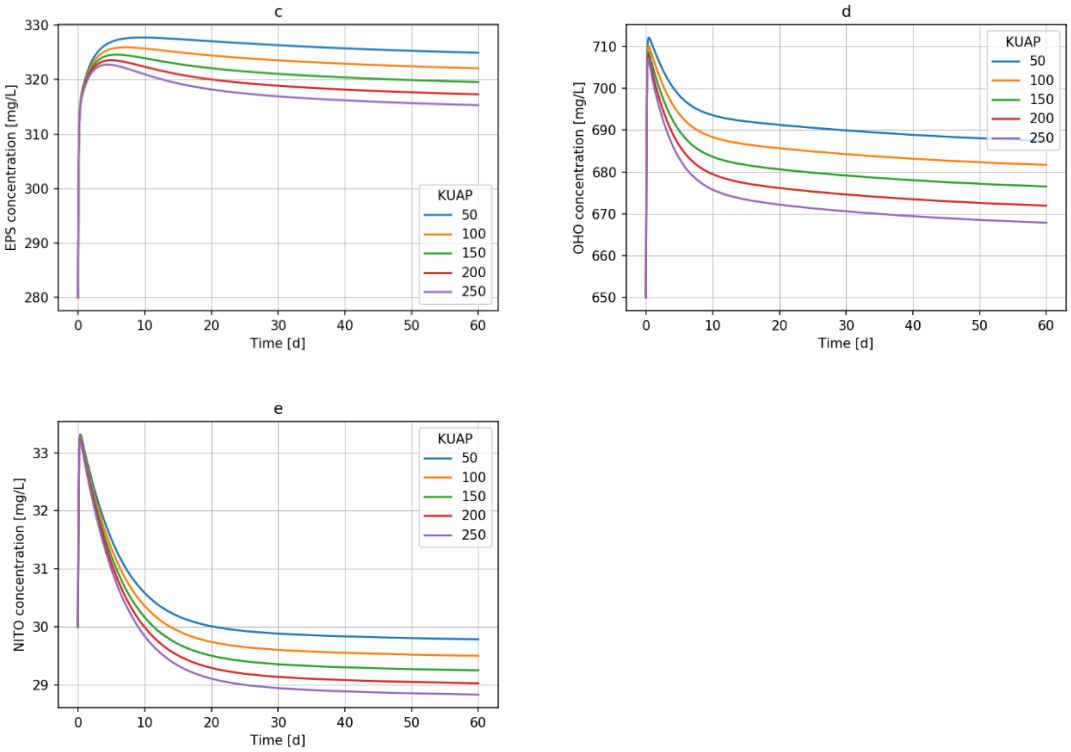

Figure 16. Simulation results with varying K_{UAP}.

Figure 16a shows the simulated S_{UAP} concentration and higher value for K_{UAP} affects increasingly to S_{UAP}. Figure 16b shows the simulated S_{BAP} concentration and changing value for K_{UAP} has very minimal effect to S_{BAP} concentration. Figure 16c – e shows that increasing K_{UAP} decreases the concentrations of EPS, OHO, and NITO.

In the second simulation set, the maximum growth rate on UAP ($\mu_{UAP,20}$) was varied between 0.25 and 0.65. The simulation results with concentrations of different components inside membrane filtration tank are presented Figure 17a - e.

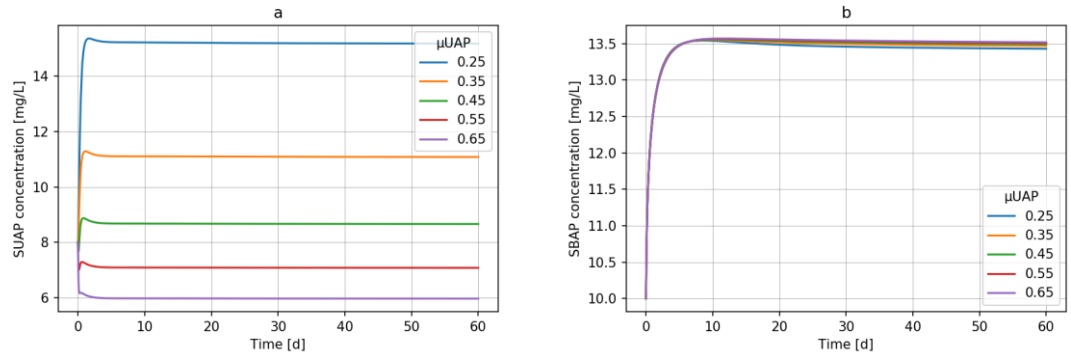

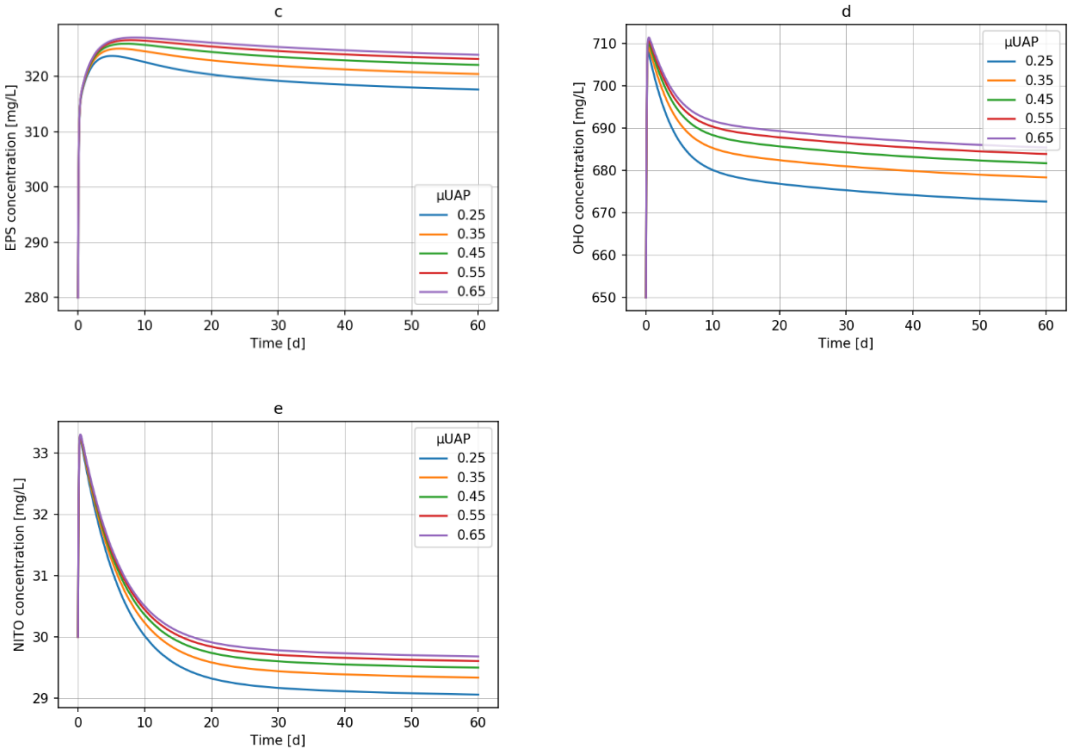

Figure 17. Simulation results with varying $\mu_{UAP,20}$.

Figure 17a shows the simulated S_{UAP} concentration and contrariwise to $K_{UAP,}$ higher values for $\mu_{UAP,20}$ decrease the S_{UAP} concentration. Also, $\mu_{UAP,20}$ has not much effect on S_{BAP} and concentrations are similar as in Figure 16b. Figure 17c – e shows that increasing the $\mu_{UAP,20}$ increase the concentrations of EPS, OHO, and NITO, too.

Next, the half saturation coefficient for BAP (K_{BAP}) were varied between 50 and 250. The simulation results are presented in Figure 18a – e.

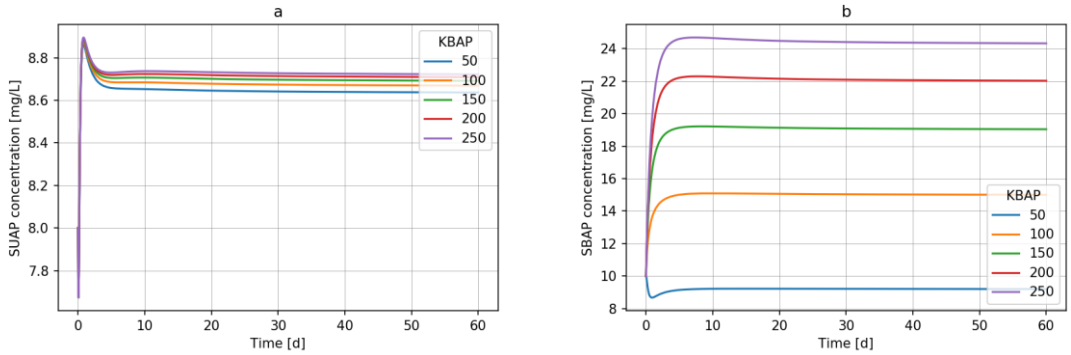

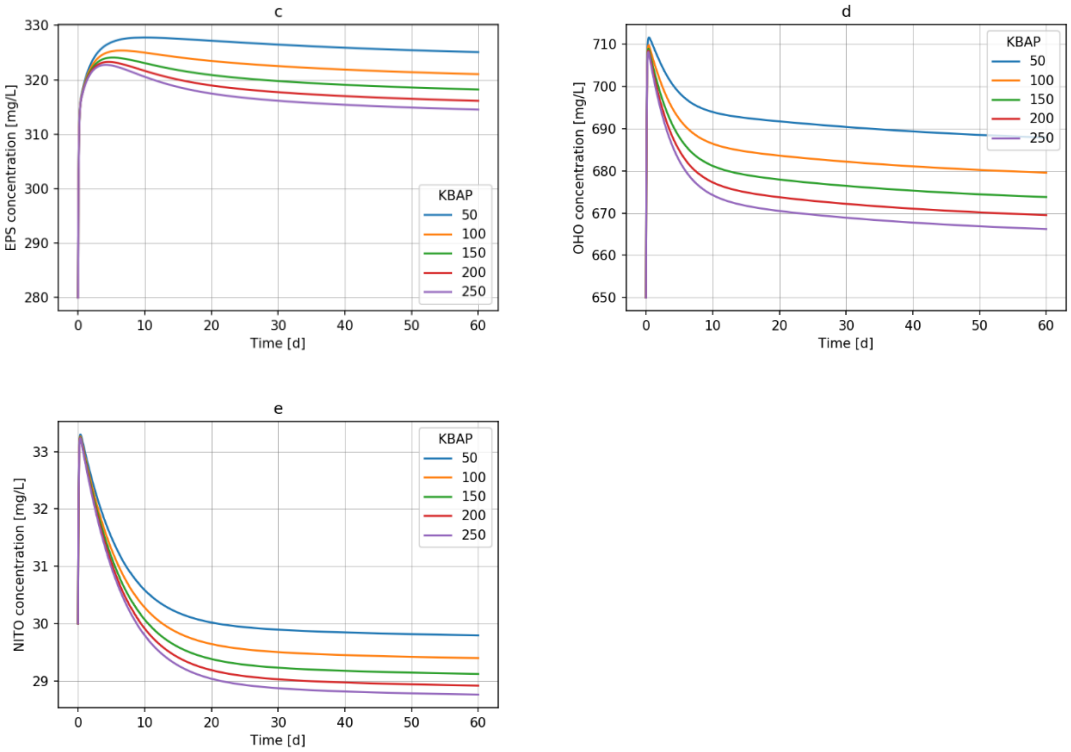

Figure 18. Simulation results with varying K_{BAP}.

Figure 18a shows that K_{BAP} has minimal effect on S_{UAP}. Figure 18b shows that higher value for K_{BAP} increases the SUAP concentration. Figure 18c – e shows that increasing K_{BAP} decreases the concentrations of EPS, OHO, and NITO.

For the next simulation set, the maximum growth rate of BAP ($\mu_{BAP,20}$) was varied between 0.05 and 0.25. The simulation results are presented in Figure 19a – e.

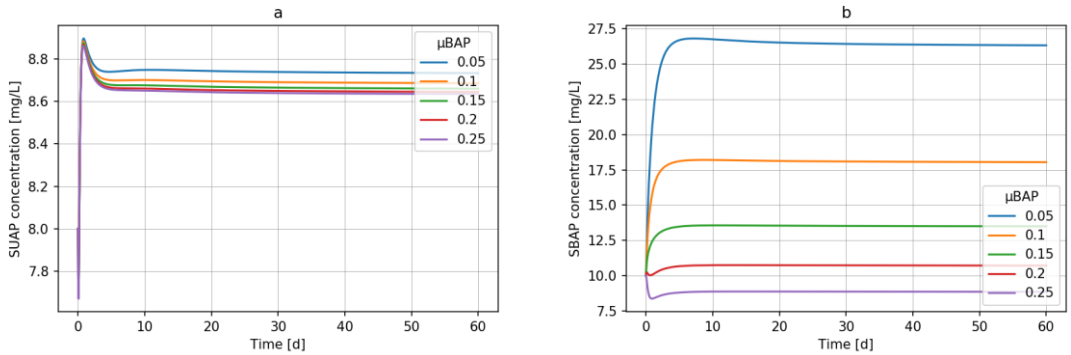

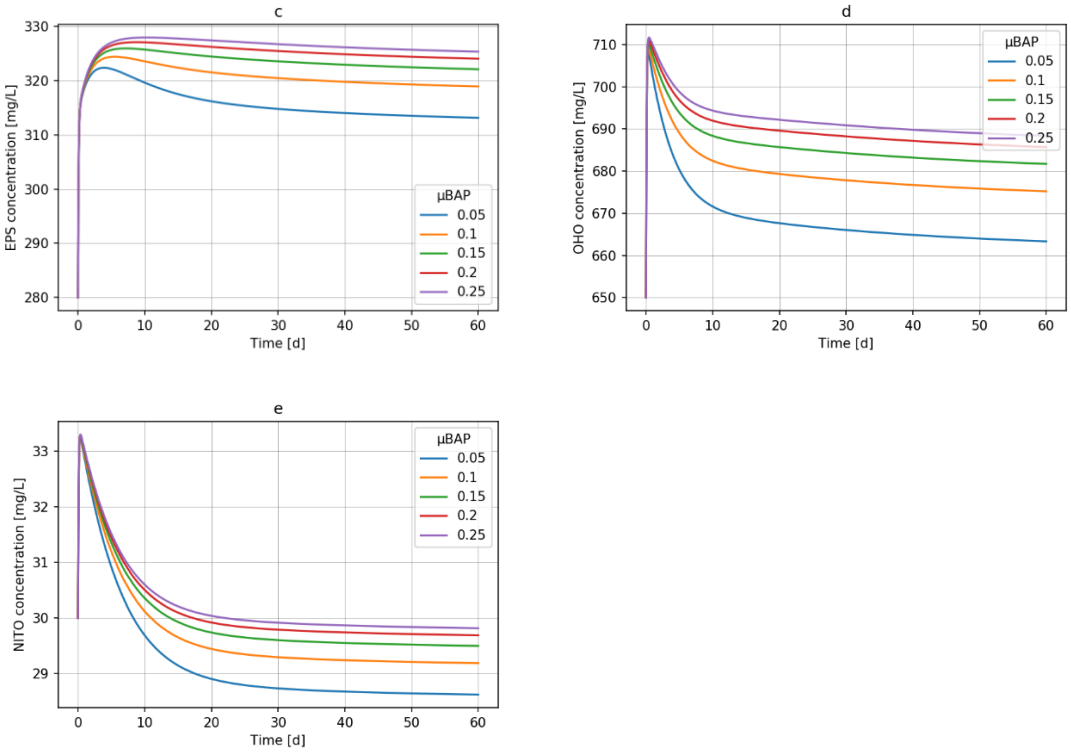

Figure 19. Simulation results with varying μ_{BAP}.

Figure 19a shows that $\mu_{BAP,20}$ has a minimal effect on the S_{UAP} concentration. Figure 19b shows that higher values for $\mu_{BAP,20}$ decrease S_{BAP} concentration. Figure 19c – e shows that increasing $\mu_{BAP,20}$ increase the concentrations of EPS, OHO, and NITO as well.

For the next simulation set, the yield of SMP (Y_{SMP}) was varied between 0.15 and 0.75. The simulation results are presented in Figure 20a – e.

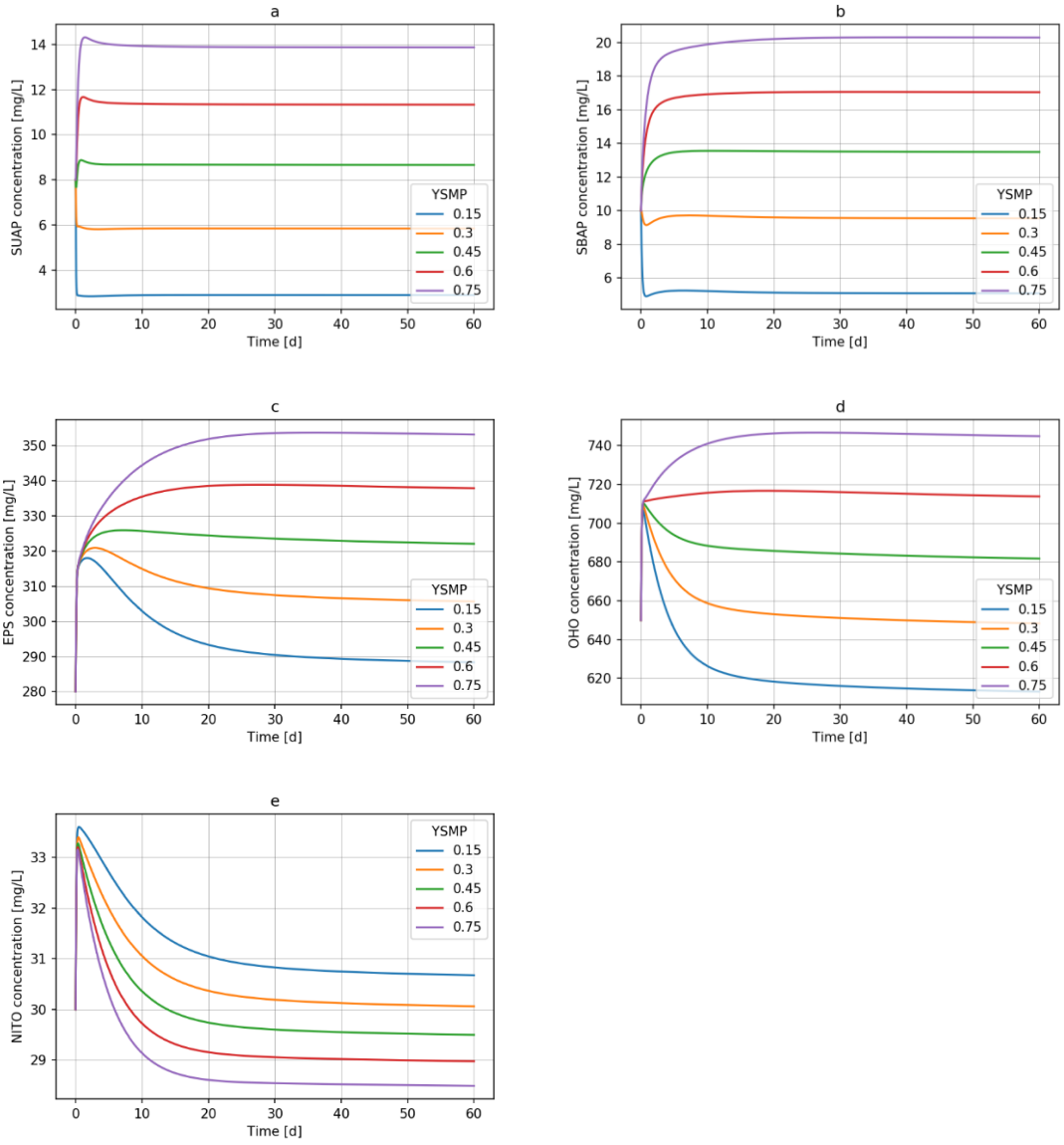

Figure 20. Simulation results with varying Y_{SMP}.

Figure 20a – b shows that higher values for Y_{SMP} increase both S_{UAP} and S_{BAP} concentrations. Figure 20c – d shows that higher Y_{SMP} increases EPS and OHO concentrations. Interestingly, higher values for Y_{SMP} results to lower concentration for NITO.

For the next simulation set, the hydrolysis of EPS ($k_{h,EPS,20}$) was varied between 0.05 and 0.25. The simulation results are presented in Figure 21a – e.

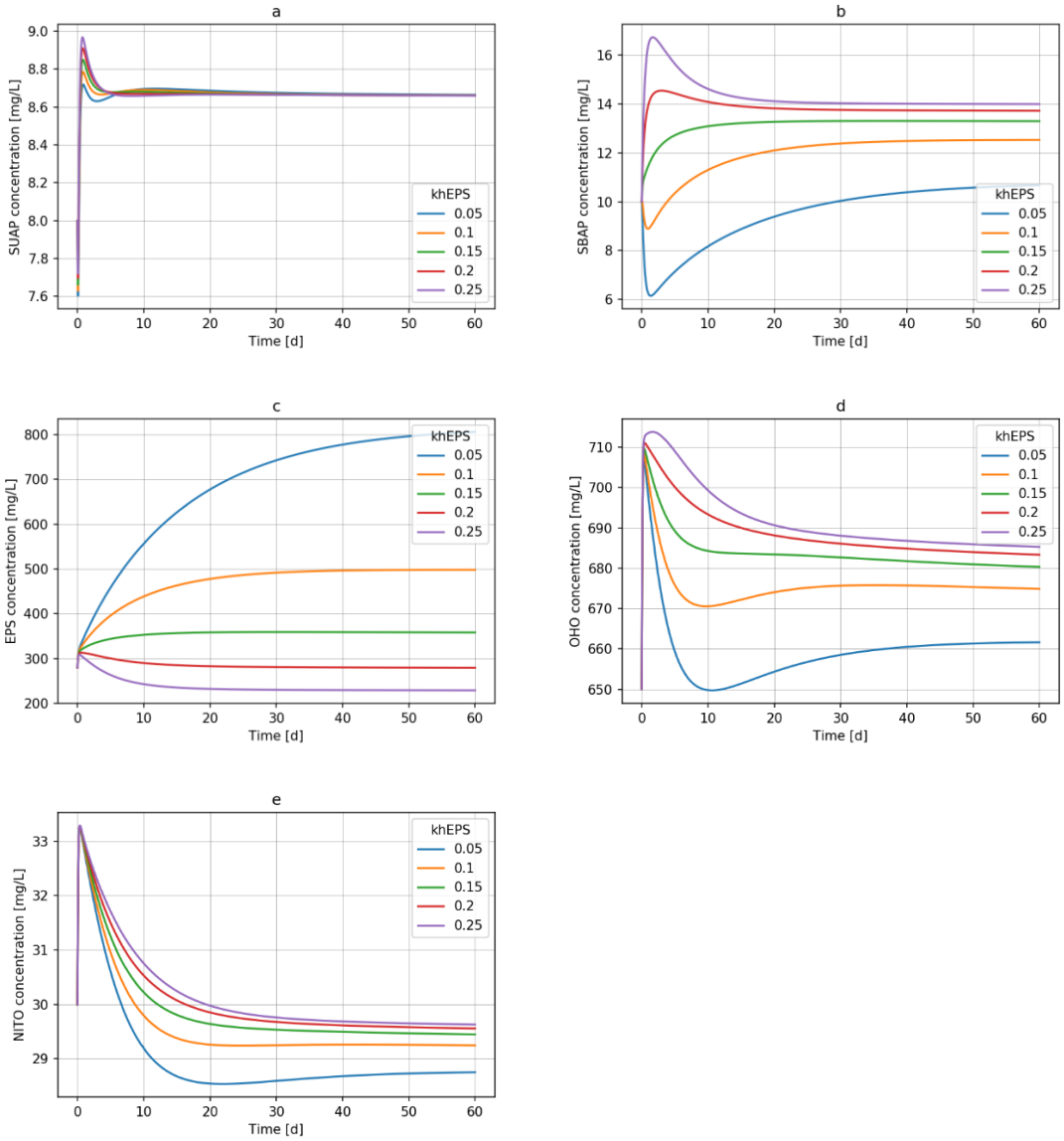

Figure 21. Simulation results with varying $k_{h,EPS}$.

Figure 21 a shows that $k_{h,EPS,20}$ has a minimal effect to S_{UAP} concentration. Figure 21 b shows that higher values for $k_{h,EPS,20}$ increase S_{BAP} concentration. Figure 21 c shows that really low values for $k_{h,EPS,20}$ increase greatly EPS concentration and higher values decrease EPS concentrations. Figure 21 d – e show that higher values for $k_{h,EPS,20}$ increase OHO and NITO concentrations.

Overall, the previously presented simulation results show that extended biokinetic model works and has effect on different components of the model. Also, the model is more sensitive to some kinetic parameters than others. Not all stoichiometric parameters were tested as they

were found to have less effect especially on OHO and NITO concentrations and the purpose was only to see that kinetic parts of the model work correctly.

5.1.3 Mechanistic fouling model

The mechanistic fouling model is created mainly according to Janus (2013). Process unit where the fouling model is implemented is the Completely Stirred Tank Reactor (CSTR) created by Dynamita. Some modifications were added to the CSTR with the fouling calculations and they are described in this chapter.

The original CSTR had only one input (*influent*) and one output (*effluent*) with a changing volume (V). To add membrane filtration and create MBR process unit, one output was modified to three outputs as inflow (Q_{inf}) remained the same, one for permeate (Q_{perm}), one for return and/or excess sludge flow (Q_{sludge}) and one for overflow (Q_{ofl}). Overflow is important as the Q_{perm} is being affected by fouling and pumping intensity and may vary so much that maximum volume of the reactor (V_{max}) may exceed, and model needs an output port for excess liquid flowing from influent. General hydraulics of an MBR unit with corresponding calculations is presented in Figure 22.

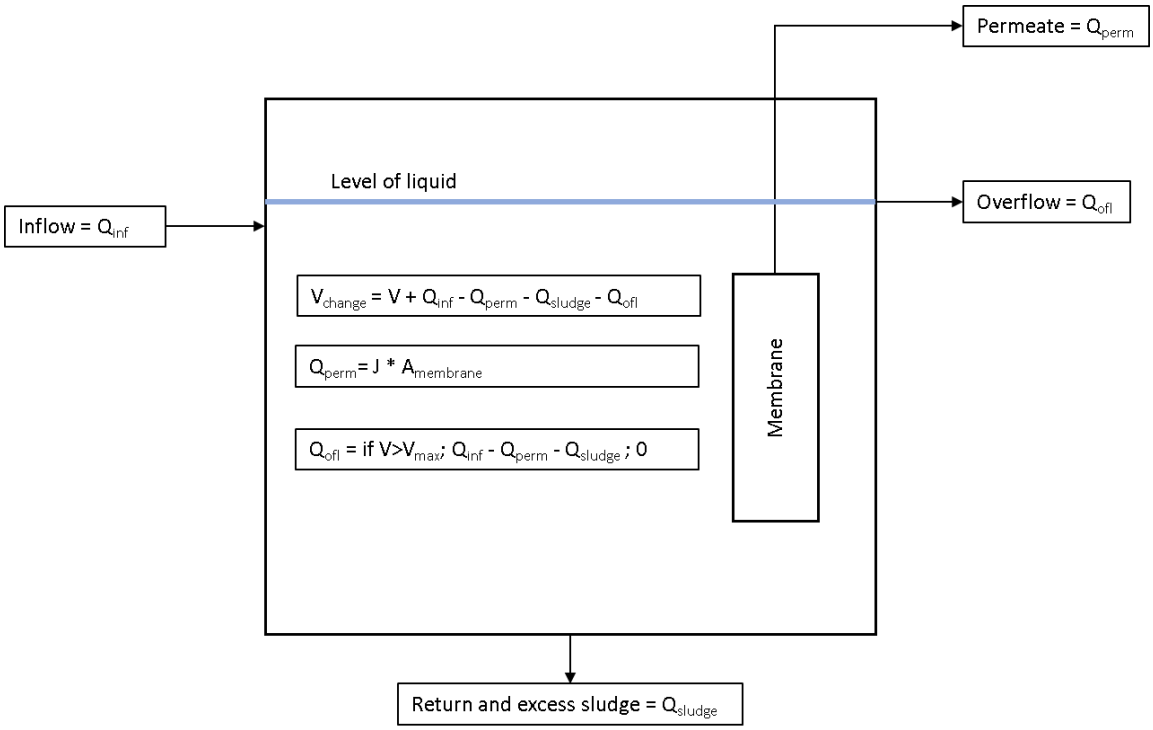

Figure 22. General hydraulics of MBR process unit.

The different components of extended biokinetic model and their calculations are presented in Figure 23. Components in mixed liquor are divided in to three groups, which are soluble (*s*), colloidal (*c*) and particulate (*x*) constituents.

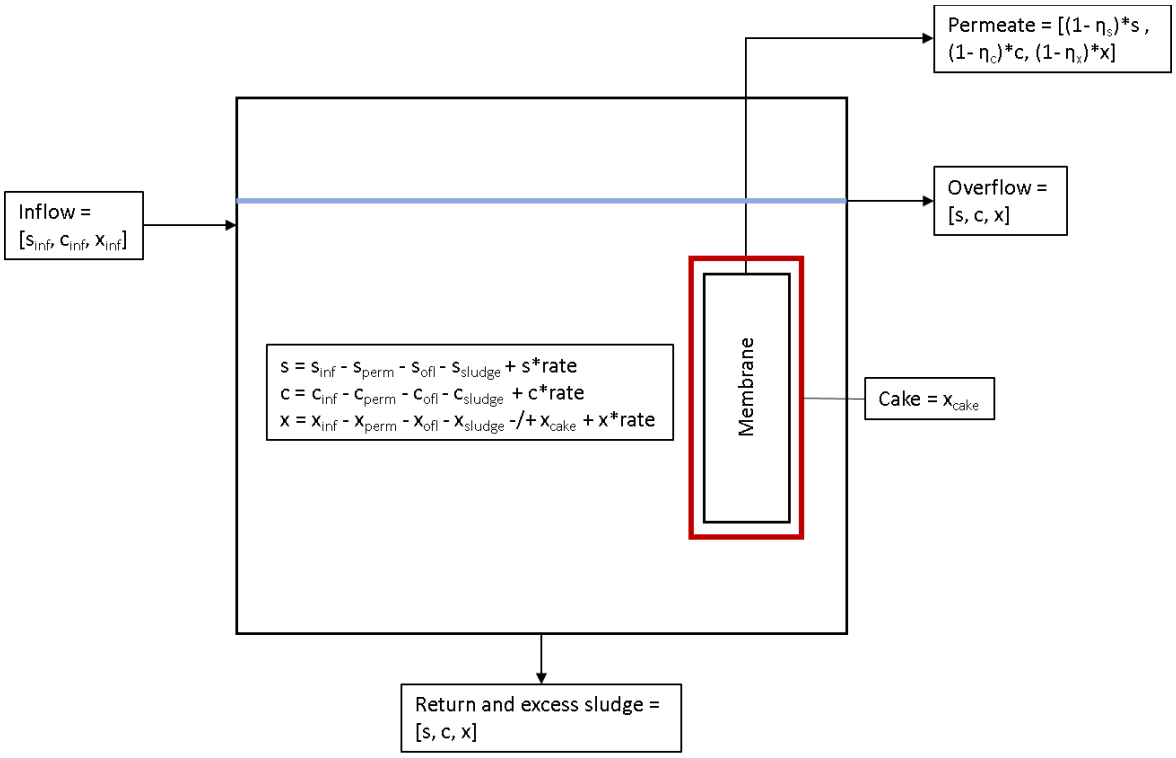

Figure 23. Mass balance of components in MBR process unit.

Figure 23 shows the changes in mass balance inside the MBR process unit. Inflow has a certain concentration of different components expressed as s_{inf}, c_{inf} and x_{inf}. These components react inside the MBR based on extended biokinetic models' reactions. As membrane gets fouled as cake attaching to its surface, the model is created so that only particulate material attaches to it and colloidal and soluble components do not affect the cake mass balance. Q_{ofl} and Q_{sludge} have the same concentration of components as MBR while Q_{perm} contains only the concentration of components, which pass through membrane pores. Rejection coefficients are separate for soluble (η_s), colloidal (η_c) and particulate (η_x) components.

Typically, in MF membranes no particulates are found in permeate. However, in an MBR process unit it is possible to model some situations where some of the particulates pass through membranes. Otherwise, the mass balance includes particles attaching to cake (x_{att}) and particles detaching from cake (x_{det}). The mass balance of cake is presented in more detail in Figure 24.

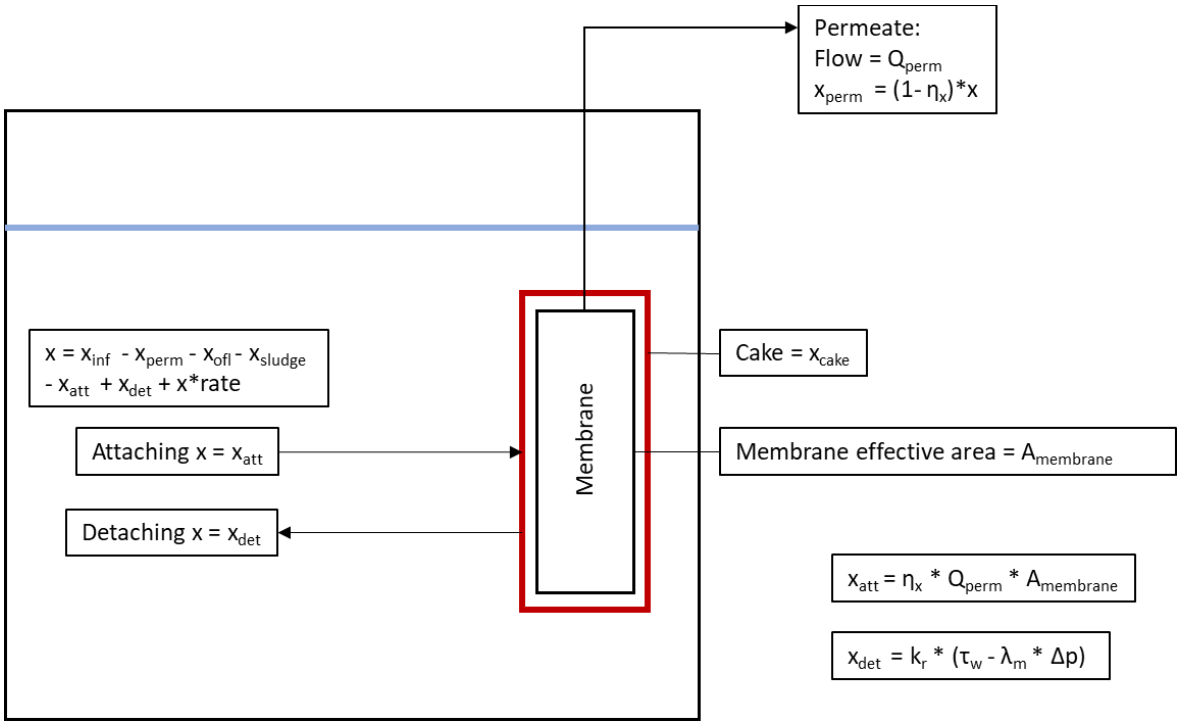

Figure 24. Mass balance of cake.

Attaching cake is directly calculated using the permeate flow with the assumption that particulate material attaches to cake by membrane's rejection coefficient for particulates (η_x) while permeate is sucked through membrane. Detaching cake is calculated by the following equation:

$$x_{det} = k_r * (\tau_w - \lambda_m * \Delta_p) \quad (14)$$

where k_r must be calculated based on calibration data and shear stress caused by air flow (τ_w) is based on scouring air flow (Q_{air}), temperature (T) and mixed liquor suspended solids ($XTSS$) concentration. Static (λ_m) is constant and can be calculated from calibration data or literature values can be used. Δ_p is transmembrane pressure (TMP) and is affected by total resistance and flux.

Calculations for τ_w are same as used by Janus (2013) and are presented in Table 6 with the modification that only some fraction (f_{scour}) of the scouring air flow will flow between the membrane sheets and clean the cake. Area for scouring gas (A_{gas}) is calculated based on the empty bottom space area between the membrane sheets. Static (λ_m) value is estimated to be $2*10^{-6}$ as used by Janus (2013). Δ_p is a simulated value and is affected by both biological and mechanical parameters.

Table 6 Calculations affecting to detaching cake.

Symbol	Expression	Unit
τ_w	$p_1*v_{sg}^3+p_2*v_{sg}^2+p_3*v_{sg}+p_4$	Pa
p_1	$-9.884*10^{-3}-1.106*10^{-4}*XTSS+1.256*10^{-5}*T+1.669*10^{-6}*XTSS^2-3.722*10^{-7}*XTSS*T$	$Pa * s^3 * m^{-3}$
p_2	$4.231*10^{-2}+3.862*10^{-4}*XTSS-9.708*10^{-5}*T+3.378*10^{-6}*XTSS^2+4.288*10^{-6}*XTSS*T$	$Pa * s^2 * m^{-2}$
p_3	$0.2627+6.695*10^{-3}*XTSS-5.703*10^{-4}*T-3.598*10^{-5}*XTSS^2-5.445*10^{-5}*XTSS*T$	$Pa * s * m^{-1}$
p_4	$-0.151-2.212*10^{-3}*XTSS-4.014*10^{-4}*T+1.985*10^{-4}*XTSS^2+8.685*10^{-7}*XTSS*T$	Pa
v_{sg}	$(Q_{air} * f_{scour}) / A_{gas}$	$cm * s^{-1}$
A_{gas}	$n_{cart}*l_{cart}*w_{cart,space}$	cm^{-2}

The membrane case from below with the area for passing gas is illustrated in Figure 25. In calculation presented in Table 6, for A_{gas} it is assumed that all the cartridges are installed horizontally and with the same area between them. The model also assumes that the outer sheet of both outer cartridges is scoured with air.

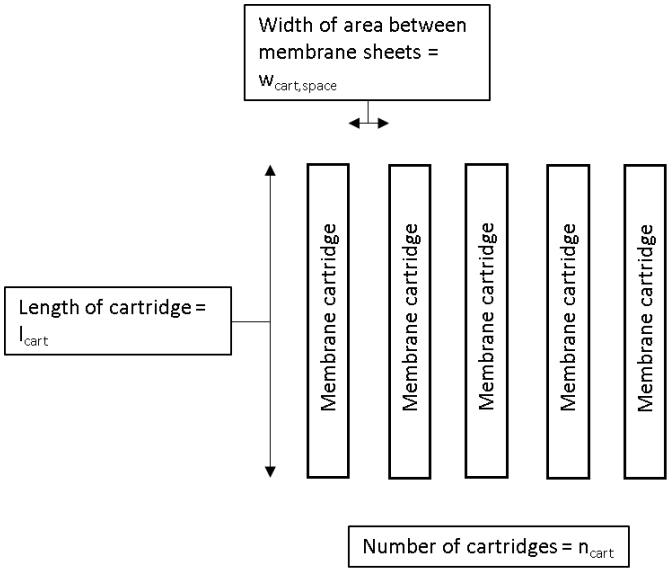

Figure 25. Membrane case from below in MBR process unit.

Membrane fouling can be modeled according to equation for filtration resistance presented in Chapter 2.2. For the resistance in series model, the resistance caused by fouling is divided in two separate resistances as presented in the following equation:

$$R_t = R_m + R_r + R_i \tag{15}$$

where,

R_t = Total membrane resistance

R_m = Clean membrane resistance

R_r = Recoverable resistance

R_i = Irrecoverable resistance

R_m can be calculated from the available filtration data. R_m is membrane and application specific and $R_m = R_t$ in equation 15 when fouling resistances are zero. R_r describes the fouling resistance that can be lowered with air scouring while R_i is the fouling, which accumulates through time and can be only lowered by chemical cleaning.

Reversible fouling resistance is assumed to be caused by cake mass. Change in R_r is calculated using the following equation:

$$\frac{dR_r}{dt} = \alpha_C * (F_{xSVatt} - F_{xSVdet}) \quad (16)$$

where:

α_C = specific cake resistance under field conditions, m/g

F_{xSVatt} = mass flow of particles attaching to cake, g/d

F_{xSVdet} = mass flow of particles detaching from cake, g/d

Cake mass balance is covered in Figure 24 and equation 14. Specific cake resistance under field conditions is calculated using the following equation which relates EPS and VSS concentrations to cake resistance:

$$\alpha_C = \frac{\Delta_p}{\mu_w{}^2} * \left(\frac{\Delta_p}{\Delta_{crit}}\right)^{n_{comp}} * (1057 + 17707 * (1 - e^{\left(118.6 * \frac{XEPS^{40.33}}{XVSS}\right)})) \quad (17)$$

where:

Δ_{crit} = pressure level after compressibility occurs, kPa

μ_w = dynamic water viscosity, Pa * s

n_{comp} = cake compressibility, -

XEPS = EPS concentration in MBR unit, mg/ L

XVSS = VSS concentration in MBR unit, mg/ L

Equation 17 shows that during relaxation time when TMP goes to 0, the specific cake resistance under field conditions goes also to 0. This affects R_r calculations as well with TMP calculations itself. For those purposes, a new constant to be used as specific cake strength (k_s) is introduced in this work and presented in the following equation:

$$\alpha_C = k_s * (1057 + 17707 * (1 - e^{\left(118.6 * \frac{XEPS^{40.33}}{XVSS}\right)})) \quad (18)$$

Dynamic water viscosity is affected by XTSS and temperature (T) according to the following equation:

$$\mu_w = 1.0521 * 10^{-3} * e^{(-1.912 * 10^{-6} * (T-20) * XTSS)} \quad (19)$$

Irreversible resistance (R_i) is assumed to be caused by pore constriction caused by SMP. Change in R_i is calculated using the following equation:

$$\frac{dR_i}{dt} = a * k_i * e^{(b*J)} * J * (S_{UAP} + S_{BAP}) \quad (20)$$

where:

a = fraction of SMP contributing to irreversible fouling, -

b = flux dependency coefficient, m/(m^2 * d)

J = flux, m^3/(m^2 *d)

S_{UAP} = soluble utilization associated products concentration, mg/L

S_{BAP} = soluble biomass associated products concentration, mg/L

5.1.4 Parameter estimations for fouling model in MBR process unit

To estimate fouling related parameters for full plant simulations, some preliminary simulations were run. The following model layout presented in Figure 26 was used for simulations. The layout is simple and includes influent flow (Influent), MBR process unit (MBR), overflow (Effluent2), permeate flow (Effluent) with non-reactive tank (Equalizationbasin) for measuring effluent concentrations, and sludge removal (Sludge).

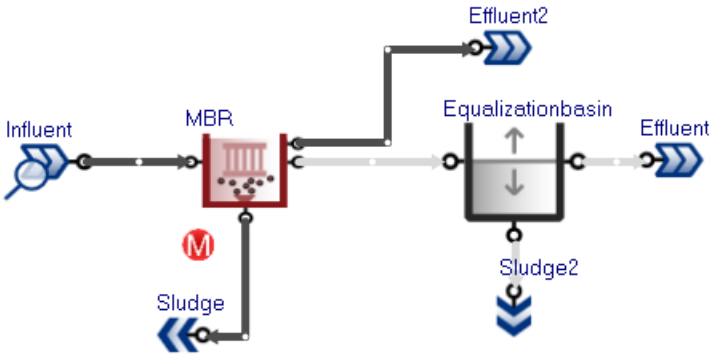

Figure 26. Model layout used in fouling related parameter estimations.

The model for parameter estimations includes extended biokinetic model, but there is no time for proper biological processes to occur as the HRT (around 0.25 days) is so low in the MBR unit. Influent flow is steady and estimated based on simulations in typical MBR plant conditions described in Chapter 5.1.1. A full list of influent variables is presented in Appendix VII. MBR unit's parameters related to fouling behavior with their estimated or default values are presented in Table 7.

Table 7 MBR units' fouling related default parameters.

Symbol	Name	Value	Unit
Q_{air}	Air flow	300	$Nm^3.d^{-1}$
$A_{membrane}$	Area of effective membrane	8	m^2
P_{size}	Membrane pore size	$4 * 10^{-7}$	m
ε_m	Membrane porosity	0.3	-
n_{cart}	Number of cartridges	10	-
$w_{cart,space}$	Space between cartridges	0.033	m
l_{cart}	Length of cartridges	0.512	m
f_{scour}	Factor for gas that passes for scouring	0.6	-
J	Membrane flux	0.336	$m^3.m^{-2}.d^{-1}$
η_S	Rejection ratio of solubles	0	-
η_C	Rejection ratio of colloidals	1	-
η_X	Rejection ratio of particulates	1	-
t_{filt}	Filtration time (no backwash)	9	min
t_{bwash}	Backwash duration	1	min
k_r	Cake detachment rate	200	$kg.m^{-2}.d^{-1}$
k_i	Irreversible fouling strength	$1 * 10^7$	$m.g^{-1}$
k_s	Constant for cake strength	$1 * 10^3$	$m.g^{-1}$
a	Fraction of SMP contributing to irreversible fouling	0.067	-
b	Flux dependency coefficient (irreversible fouling)	0.02	$m^{-1}.m^2.d$
λ_m	Static	$2 * 10^{-6}$	-
R_m	Clean membrane resistance	$8 * 10^7$	m^{-1}
ε_c	Cake porosity	0.6	-
ρ_c	Wet cake density	1150	$kg . m^{-3}$
Δp_{crit}	Pressure level after compressibility occurs	30000	Pa
n_{comp}	Cake compressibility	1	-
$Q_{sludge,target}$	Target sludge flow	5.4	$m^3.d^{-1}$
$R_{i,0}$	Initial irreversible fouling resistance	0	m^{-1}
$R_{r,0}$	Initial reversible fouling resistance	0	m^{-1}
$M_{att,xSV,0}$	Initial state variables mass attached to membrane	0	$g.m^{-2}$

The first set of results is shown in Figure 27a – e. Air flow was varied between 240 - 600 Nm^3/d while keeping the other parameters constant to set the optimal air flow for other parameter estimations. The pilot plant is operated typically with around 310 Nm^3/d aeration to membrane tank.

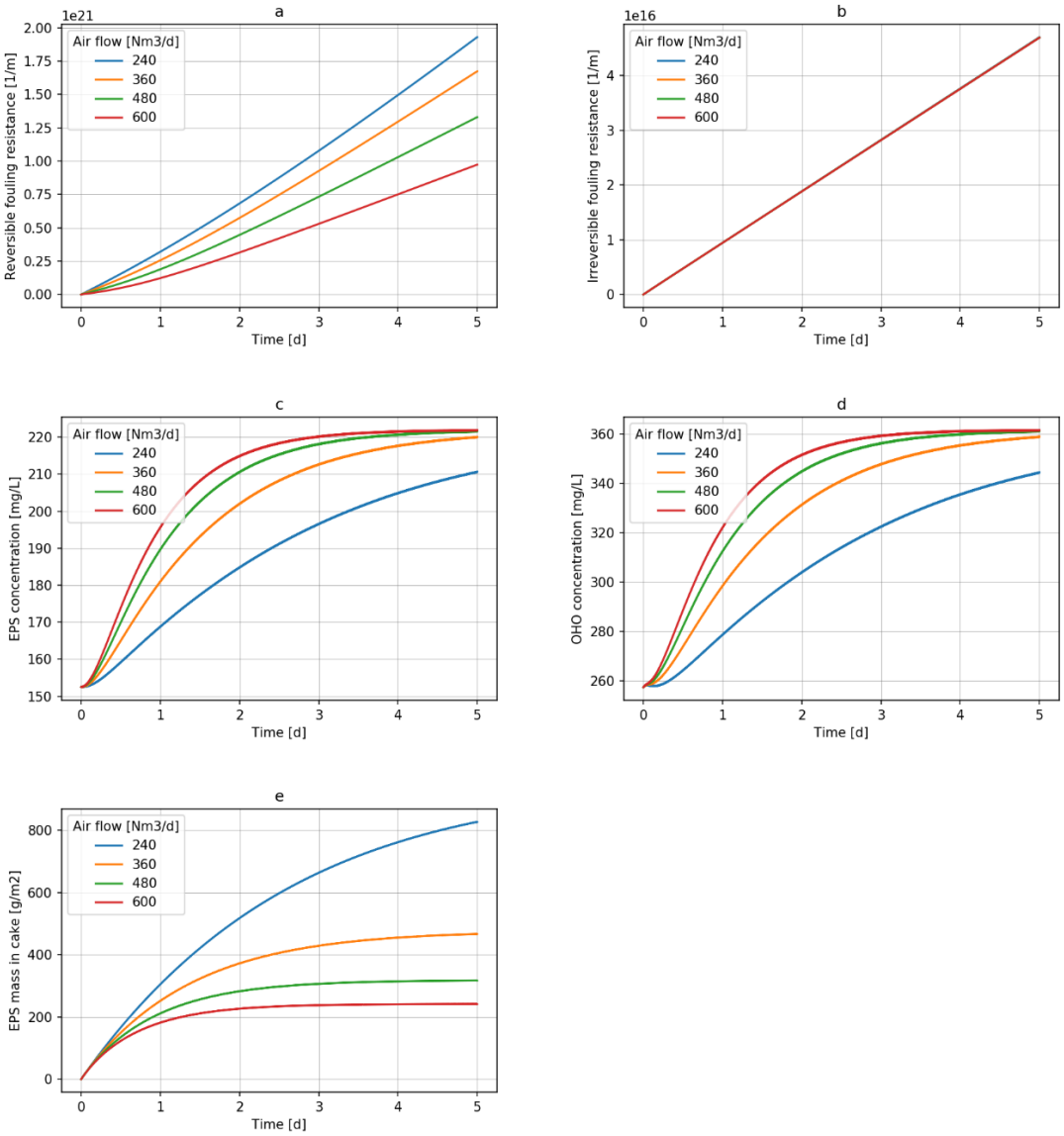

Figure 27. Simulation results with varying air flow.

Air flow of 420 Nm3/d was chosen for estimating the values for k_r as it is a good average as seen in Figure 27. EPS and OHO concentrations inside the unit vary based on the amount of air flow. This is because they will be attached to cake and detached from it based on how intense the scouring air flow is. The values for k_i are only dependent on SMP concentrations so it will not be changed by varying scouring air flow as seen in Figure 27b.

The results for fouling parameter estimations are presented in Figure 28a - d. Values for k_r were varied between 2 – 10 while keeping other parameters constant.

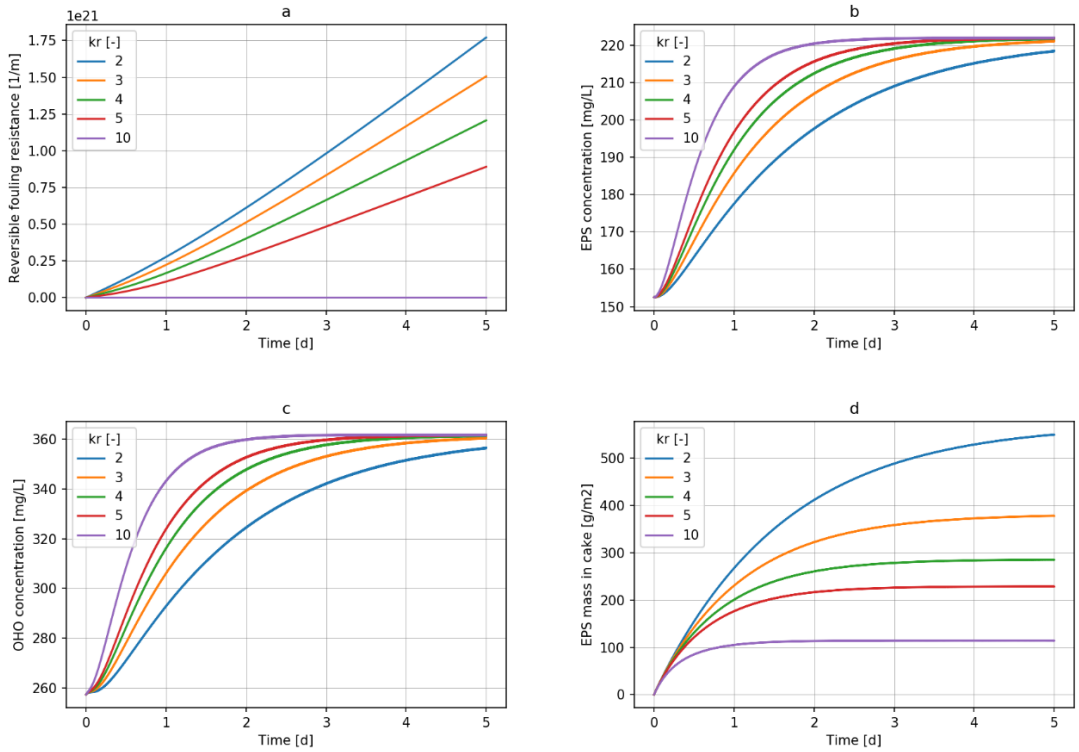

Figure 28. Simulation results with varying parameter for reversible resistance.

Overall, the higher the k_r value, the more cake is detached from the membrane. Determining the correct value for k_r will need a good amount of calibration data. Results show that similarly to varying air flow, different values for k_r will affect the EPS and OHO concentrations inside the tank and in the cake.

5.2 Modeling pilot process

5.2.1 Calibration during stress conditions

At first, a model presented in Figure 29 was created to be used in calibration during stress behaviour. The model includes influent (Influent), completely stirred tank reactor (CSTR), waste sludge control and waste sludge (Side flow divider, Sludge), MBR process unit (MBR), overflow (Effluent), permeate flow (Effluent2), and sludge circulation.

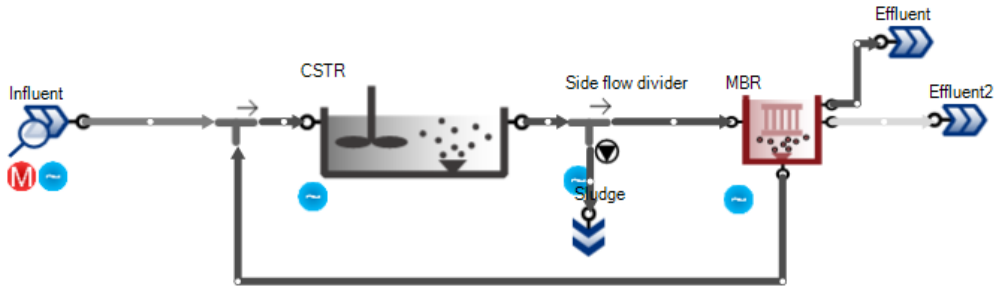

Figure 29. Model used in calibrations.

Data gathered from the pilot between 4th and 21st of December was used for pilot model's calibration. Data included analysis from SMP, EPS, influent flow and analysis, permeate flow, aeration flow, circulation flow, waste sludge amount, TMP, TSS and VSS. During the calibration period pilot was stressed by turning the influent flow off occasionally. Stress test plan with corresponding analysis results is as Appendix IX.

The next step was to calibrate extended biokinetic model. Parameters estimated in Chapter 5.1 were used as a starting point for calibration and the parameters were changed one at a time to get the best fit for measured data. In addition, fouling parameters were checked quickly to ensure that no excess cake was attached to influence the extended biokinetic model calibration. Calibration results are presented in Figure 30 a – b and modified biological parameters are presented in Table 8.

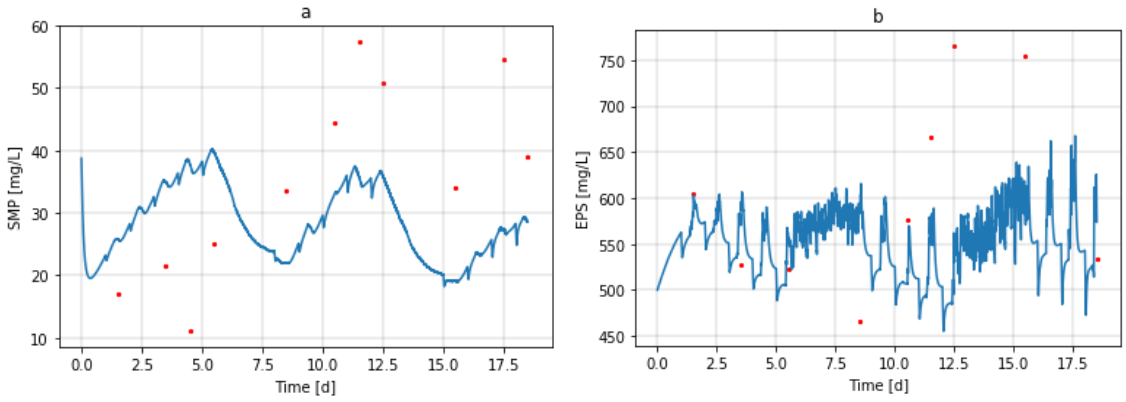

Figure 30. Measured (red dots) and modeled (blue line) SMP and EPS concentrations during the calibration period.

Table 8 Calibrated parameters for extended biokinetic model.

Parameter	Value [-]
K_{UAP}	85
K_{BAP}	85
μ_{UAP_20}	0.45
μ_{BAP_20}	0.1
$k_{h\_EPS\_20}$	0.1
$f_{EPS\_d\_OHO}$	0.45
Y_{SMP}	0.2
f_{BAP}	0.0215
γ_{OHO}	0.0924

Figure 30 a shows the measured and simulated SMP values. It can be seen that the model predicts quite well the measured values. The direction of change is similar in both simulated and measured SMP values. However, the simulated values do not fit perfectly the measured ones, especially in the beginning of the calibration period.

Figure 30b shows the measured EPS values (red dot) and simulated EPS values (blue line). As with SMP, the simulated EPS values fit nicely with measured ones. Especially in the beginning the measured values are very well fitted and the model also mimics the mid-section of the calibration period nicely. However, some values around days 12 - 15 of the calibration period are not very well fitted.

The next step was to calibrate the fouling model. As in extended biokinetic model, parameter estimations from previous chapter were used as a starting point and they were also changed one at a time to get the best fit for measured values. During the calibration steps, it was noted that fouling parameters do not strongly affect the biological behavior of biopolymers. Only the fraction of EPS that attaches to cake affects the mass balance and biological interactions. Calibration results are presented in Figure 31a – c and modified parameters are presented in Table 9.

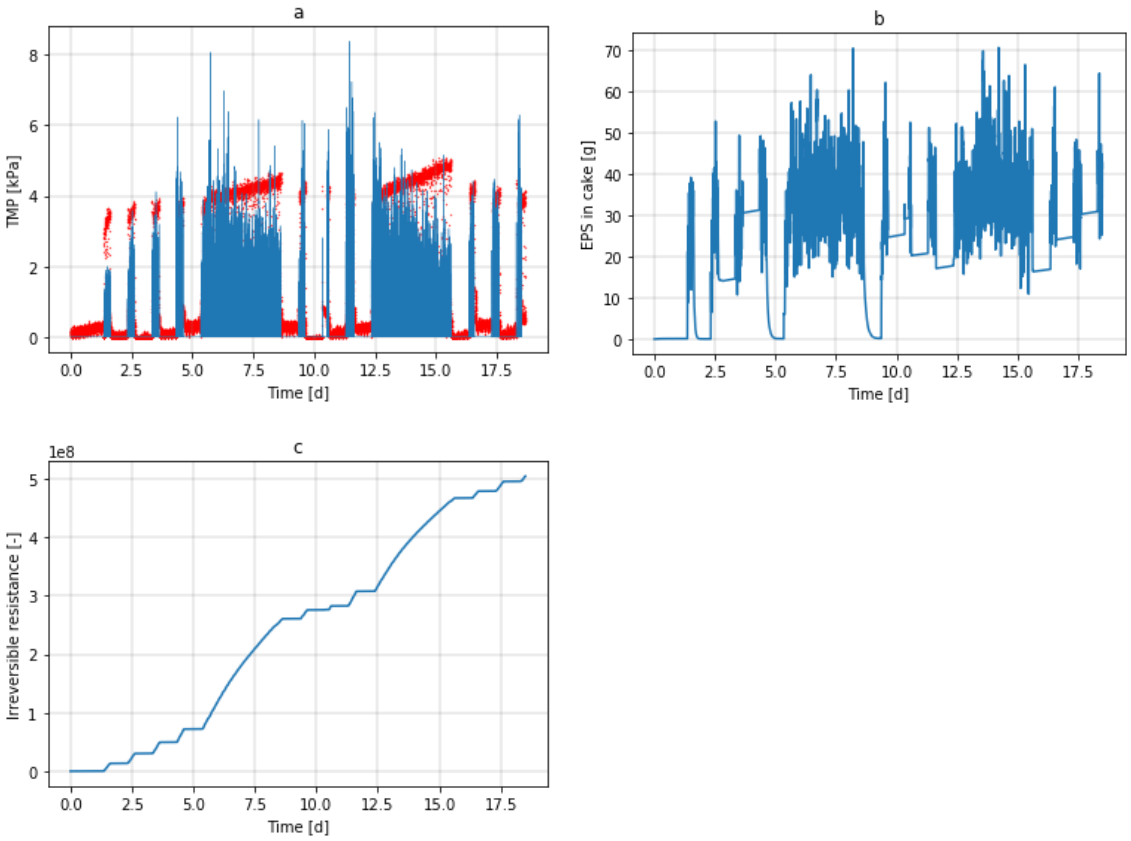

Figure 31. Measured (red dots) and modeled (blue line) values from fouling behavior calibration

Table 9 Calibrated parameters for fouling model.

Parameter	Value [-]
k_r	300
k_i	$1 * 10^8$
f_{scour}	0.8
k_s	$4.8 * 10^8$
constant for dynamic water viscosity and temperature	$6.1 * 10^{-5}$

Figure 31a shows the simulated and measured values for TMP [kPa].Figure 31b shows the simulated values for EPS amount in attached cake [g] and Figure 31c for irreversible fouling resistance, respectively. From the Figure 31a can be seen, that the simulated TMP values (line in blue color) match well the measured TMP values (points in red color). Only some peak values are present in the simulated values and they occur only during short time periods. Also, the irreversible resistance presented in Figure 31c would need a much longer period to impact the overall resistance of membranes.

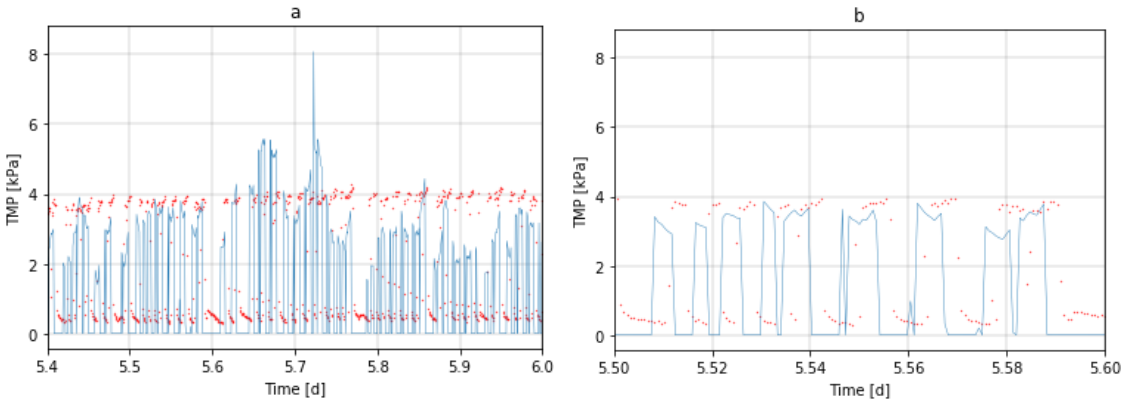

Figure 32. Measured (red dots) and modeled (blue line) values from shorter time period.

Figure 32a - b show the simulated and measured values for TMP [kPa] in a shorter time frame starting from day 5 of the measuring period. Figure 32a shows the half days period of measured (red points) and simulated (blue line) TMP values. Figure 32b shows an even shorter time frame of a bit over one hour from calibration period. The simulated values fit very nicely to the measured data points, there is only some short delay between the measured values and simulation results which might be caused by some offset of the measured data analysis. Also, the measured values are average values of 1 minute period, so they are not exact.

5.2.2 Calibration of irreversible fouling during high TMP

Parameters for irreversible fouling do not stay constant as the pores get constricted and they get narrower, and the gel layer starts to block permeate flow. These behaviors are not included in the fouling model. However, the behaviors can be adjusted by modifying the irreversible parameters and initial values for fouling resistance. Irreversible fouling parameters were fitted for high TMP period from 15th March until 6th April 2017. The simulation results are presented in Figure 33 a-b and fitted parameters in Table 10.

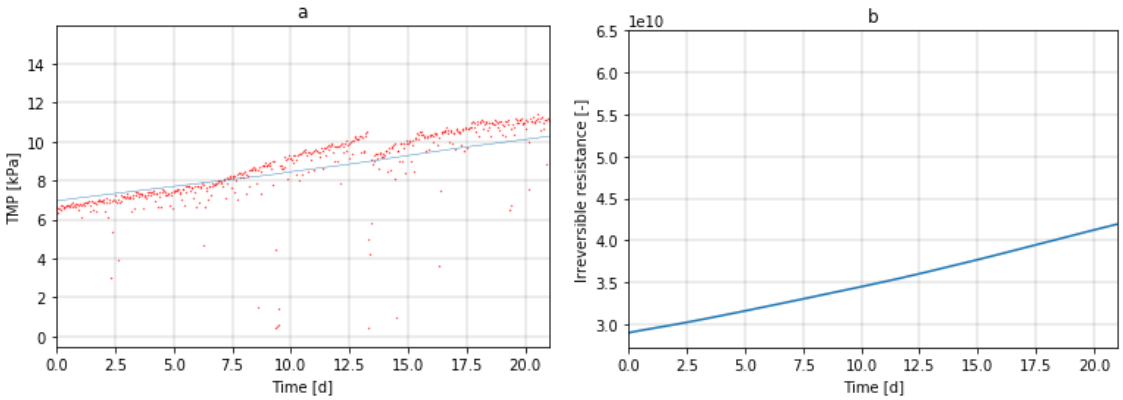

Figure 33. Measured (red dot) and simulated (blue line) values of irreversible fouling during high TMP calibration.

Table 10 Calibrated parameters for high TMP conditions.

Parameter	Value [-]
k_i	$1.2 * 10^9$
Initial fouling resistance	$2.9 * 10^{10}$

6 Modeling Metsä-Sairila new MBR plant

The modeling and simulations in this chapter are done to test the previously created extended biokinetic model and MBR process unit in full scale plant conditions. Different influent compositions and operational process conditions were simulated to get understanding of full plant behavior. Also, some of the results will help to prepare plant operators to those varying conditions. The simulation results in this chapter are not calibrated as there is no data where to compare them.

6.1 Model creation and initialization

Figure 34 shows the layout used in full plant simulations. The full plant model is created with the intention to keep it simple enough to have reasonable simulation time but still complex enough to be usable in simulations and to get reasonable results. Instead of three separate trains, the model includes one train with a volume fixed to match the full plants volume. A total of six reactors (CSTRs) were used with one MBR process unit in the end. The model also includes waste sludge removal for controlling SRT and sludge circulation flow.

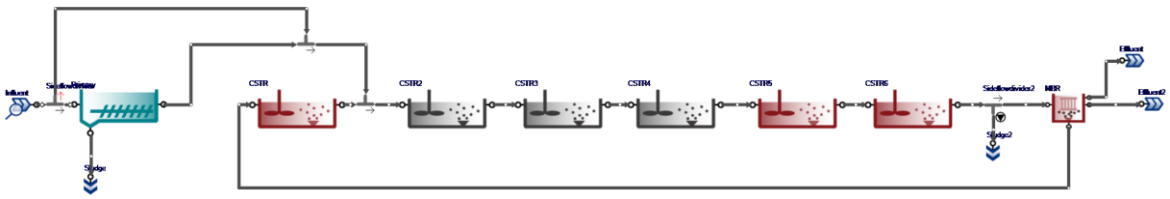

Figure 34. Model used in full plant simulations.

Initial values for calculated variables inside reactors were like those used in calibration simulations and are presented in Appendix VII. Calibrated values for biological parameters were used and they are presented in Table 8. Other parameters used in full plant simulations are presented in Table 11. Some of them were varied in different simulations presented in this chapter to see the behavior of full plant during those simulations.

Table 11 Parameters and units for full plant simulations.

Unit, parameter	Value
CSTR 1, air flow	0 Nm^3/d
CSTR 2, DO set point	0 mg/L
CSTR 3, DO set point	0 mg/L
CSTR 4, DO set point	2 mg/L
CSTR 5, DO set point	2 mg/L
CSTR 6, DO set point	2 mg/L
MBR, aeration	70 000 Nm^3/d
All CSTRs and MBR, volume per unit	1500 m^3
MBR, membrane area	60 000 m^2
Influent, flow	22 300 m^3/d
Influent, temperature	15 °C
Influent, NH_x	48 mg/L
Influent, COD_t	400 mg/L
MBR, filtration time	9 min
MBR, relaxation time	2 min
SRT	37 d
Flux	0.442 $m^3/(m^2*d)$

6.2 Varying air flow in MBR process unit

First simulations were done to simulate situations with varying air flow in MBR unit to see how it will affect the membrane fouling and biological nutrient removal. The results are presented in Figure 35 and Figure 36.

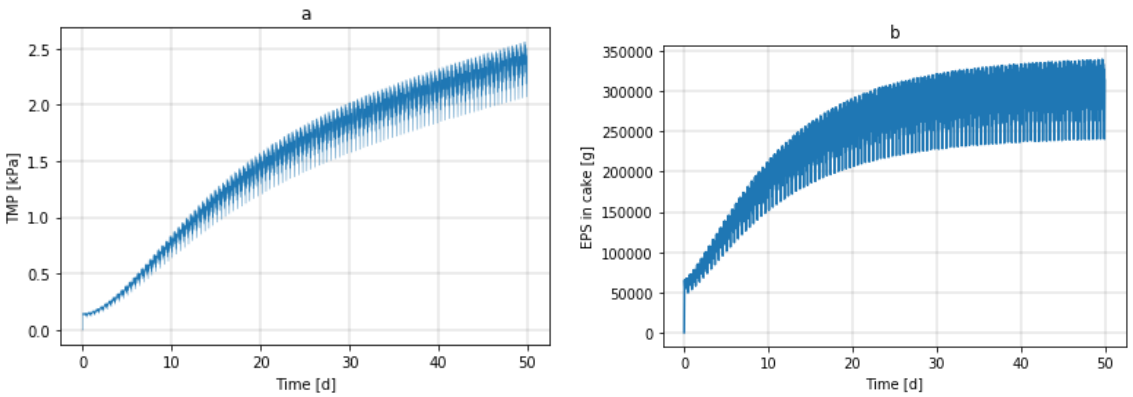

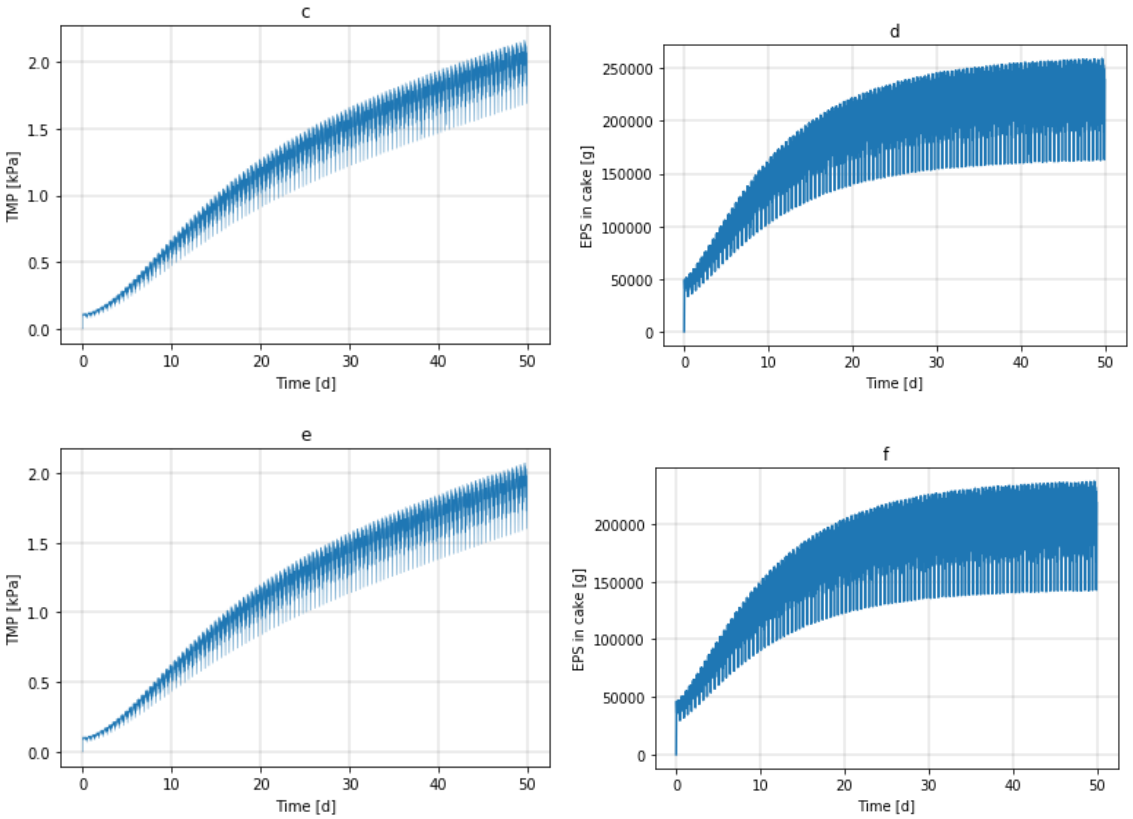

Figure 35. Simulated values for TMP [kPa] and EPS in cake [g] in MBR process unit with air flow 50 000 [Nm3/d] in figures a – b, 70 000 [Nm3/d] in c – d, and 90 000 [Nm3/d] in e – f.

From the Figure 35 it can be seen, that TMP rises more rapidly with the lower scouring air flow reaching the value of around 2.6 kPa. However, there is not that much difference between 70 000 Nm^3/d and 90 000 Nm^3/d air flow with a maximum TMP of around 2.2 kPa. Controversially to TMP, the EPS mass in cake gets lower with a higher air flow. Also, there is no significant difference with higher air flows, but with lower air flow the cake starts to form more rapidly.

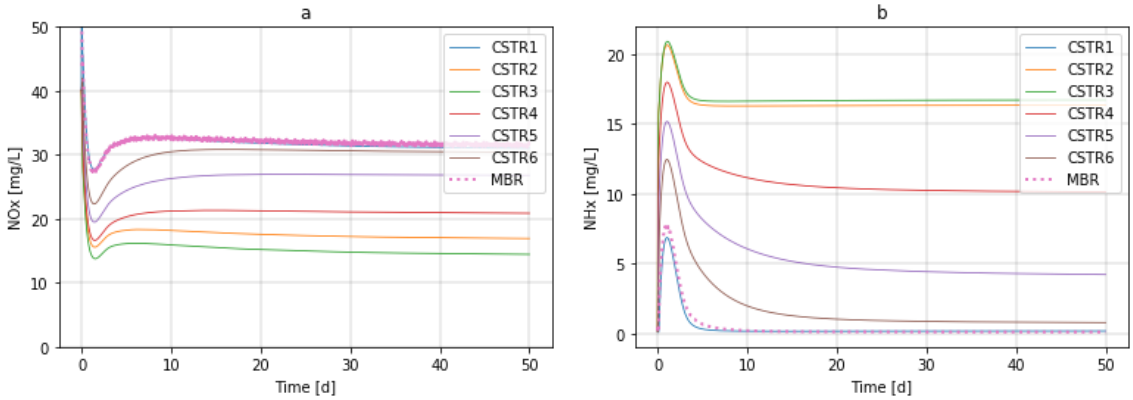

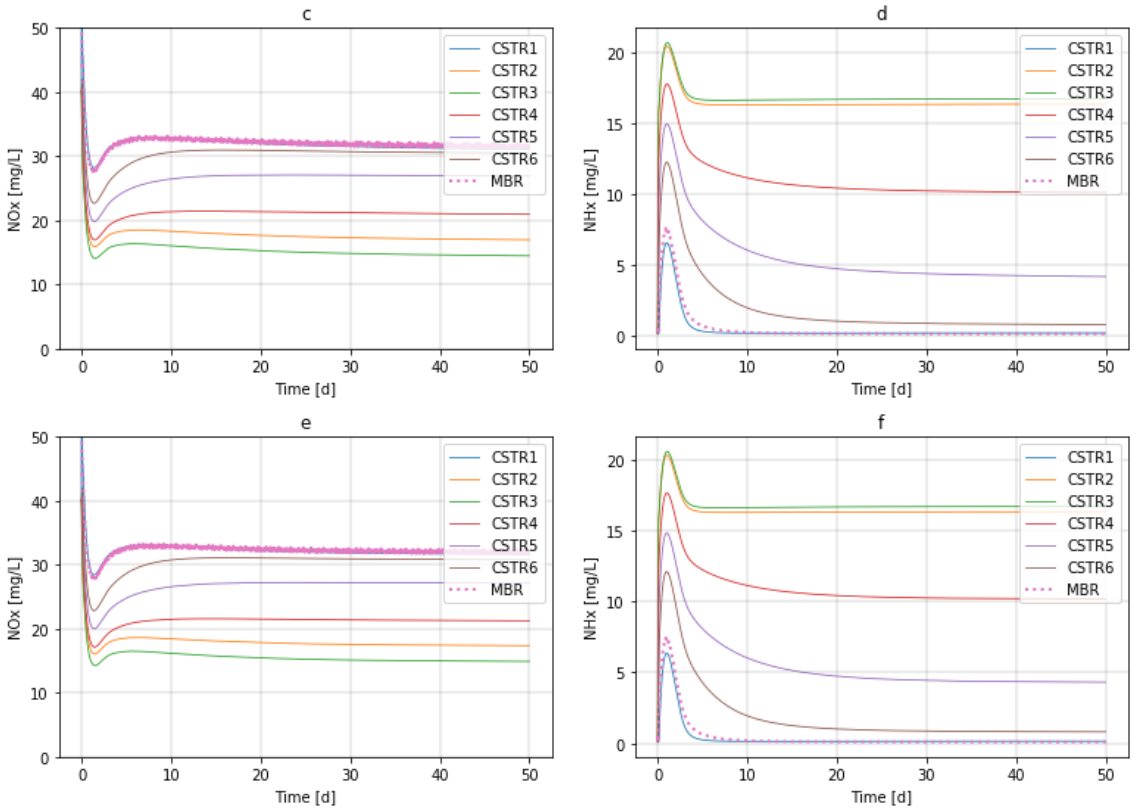

Figure 36. Simulated values for NO_x [mg/L] and NH_x [mg/L] in different tanks with air flow 50 000 [Nm3/d] in figures a – b, 70 000 [Nm3/d] in c – d, and 90 000 [Nm3/d] in e – f.

From Figure 36 can be seen that varying scouring air flow inside the MBR unit has no major effect on nitrification or denitrification of the system. This seems reasonable as the HRT of MBR unit is so low compared to HRT of the whole process. Also, the 50 000 Nm^3/d already has significant impact on DO levels inside the MBR unit and is not restricting nitrification.

6.3 Varying influent COD concentration

In Figure 37, Figure 38, and Figure 39 are presented the effects of different influent COD concentrations on NO_x, NH_x, SMP, and EPS concentrations inside MBR unit as well with TMP and EPS mass in cake to see the fouling behavior.

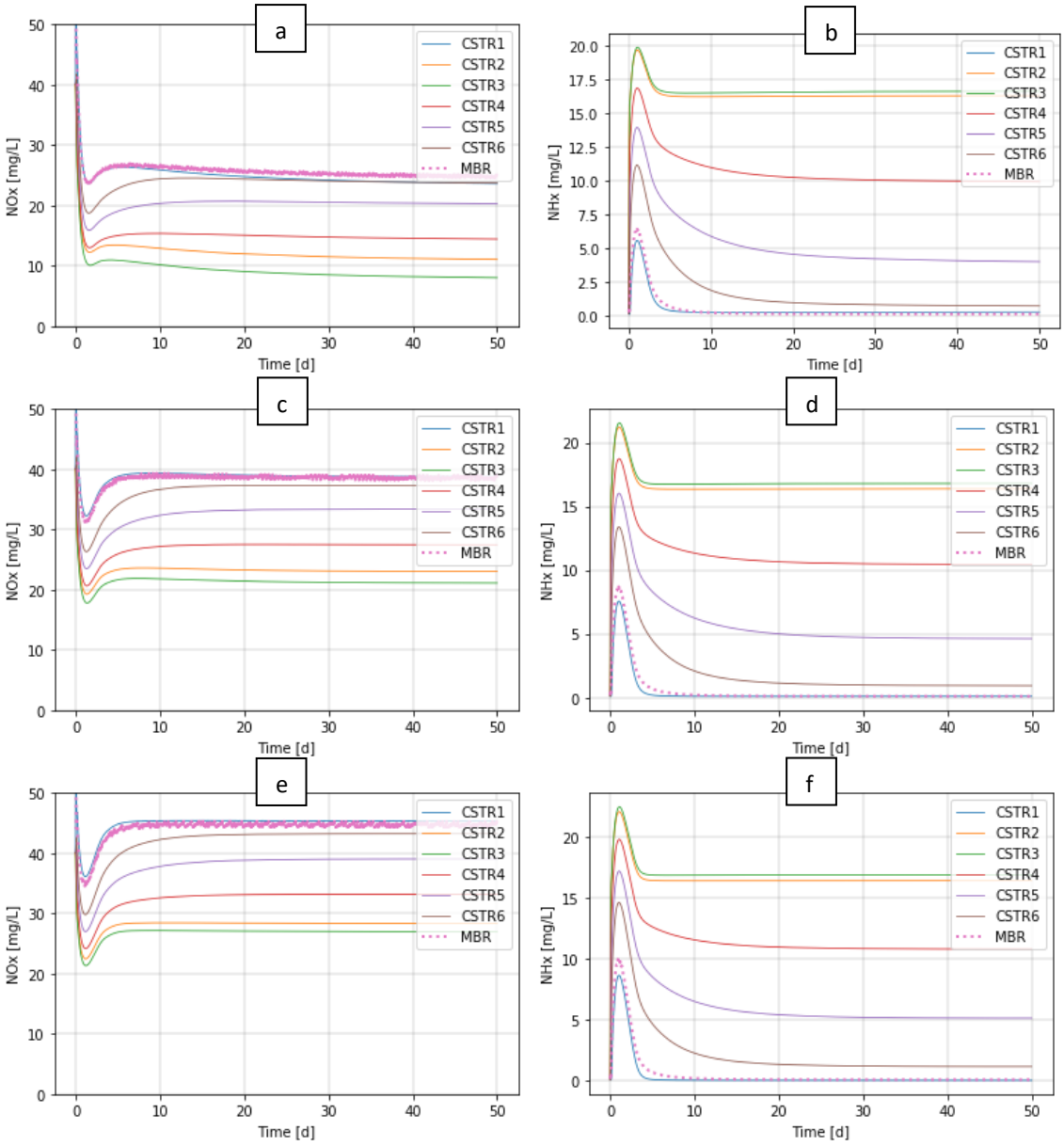

Figure 37. Simulated values for NO_x [mg/L] and NH_x [mg/L] in different tanks with influent COD 500 [mg/L] in figures a – b, 300 [mg/L] in c – d , and 200 [mg/L] in e – f.

From Figure 37 a – b can be seen that even with higher influent COD, the process seems to nitrify as the NH_x levels are close to 0 in the MBR unit and NO_x levels are around 25 mg/L which sums up to around 50 % of nitrogen removal. Figure 37 c – d show that nitrification is complete, as with higher COD load, but nitrogen removal is only around 20%. This might be the cause of overall lower substrates to microbes so that there is not enough carbon source for denitrifying bacteria. Figure 37 e – f show that nitrification is complete, as with the higher COD loads, but nitrogen removal is only around 5%. Also, nitrification starts slower and

during the first days NH_x values are higher inside the MBR unit than in the higher influent COD load simulations.

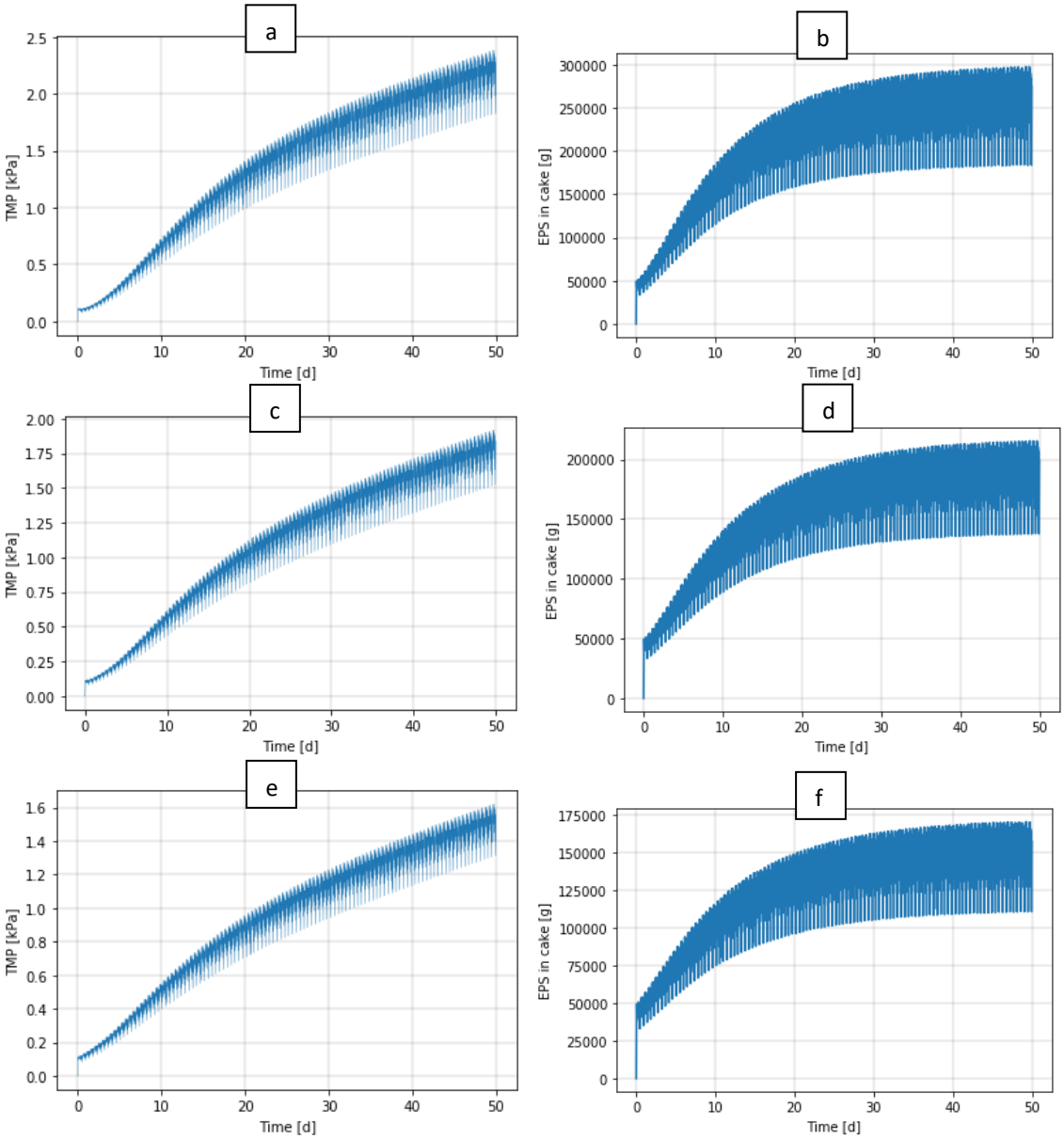

Figure 38. Simulated values for TMP [kPa] and EPS mass in cake [g] in MBR process unit with influent COD 500 [mg/L] in figures a – b, 300 [mg/L] in c – d , and 200 [mg/L] in e – f.

Figure 38 a – b shows that values for TMP and EPS mass in cake are a bit higher with a maximum value of 2.3 kPa for TMP and 300 kg of EPS in cake than the ones presented in Figure 35 c – d, which had similar air flow for scouring but 400 mg/L influent COD. The main reason might be that biomass grows more rapidly and accumulates more soluble matter leading to increasing TSS which develops more fouling. Figure 38 c – d shows that the

conditions for reversible fouling to occur are much lower with 300 mg/L influent COD and cake is detached more effectively than with 500 mg/L influent COD. TMP has a maximum value of around 1.9 kPa and EPS accumulates to around 220 kg in cake. Figure 38 e – f shows that compared to previous conditions, TMP values are much lower with a maximum value of 1.6 kPa and maximum EPS attached to cake is around 170 kg.

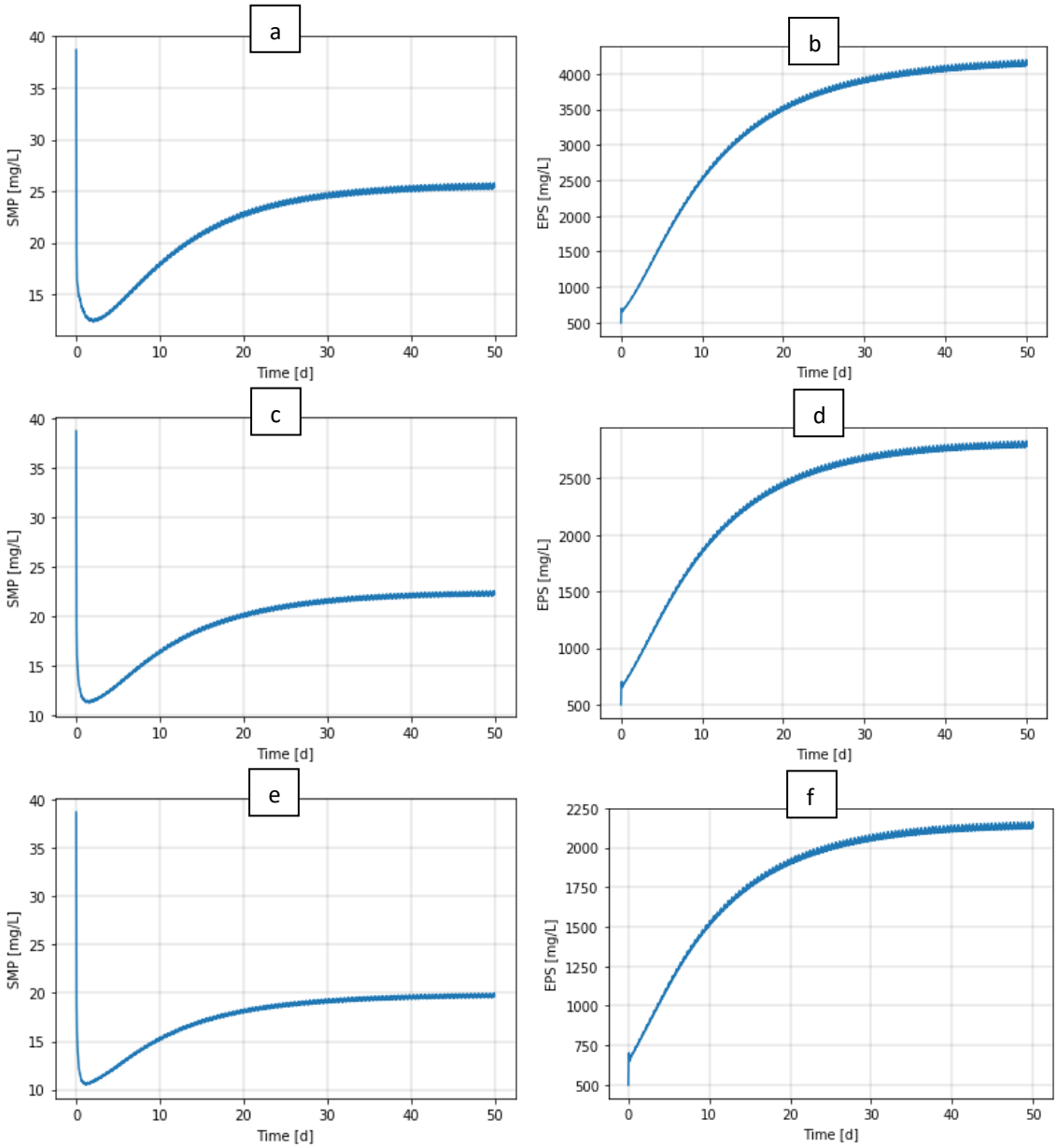

Figure 39. Simulated values for SMP [mg/L] and EPS [mg/L] in MBR process unit with influent COD 500 [mg/L] in figures a – b, 300 [mg/L] in c – d , and 200 [mg/L] in e – f.

Figure 39 a – b show that compared to measured and simulated values in the pilot process, the EPS concentration seems to be high, over 4000 mg/L, and SMP on the other hand a bit

lower, around 25 mg/L, than during the calibration period. This might be the cause of stress conditions and that parameters used in full plant simulations are calibrated to match those stress conditions, which will not occur in full plants conditions. Figure 39 c – d show that the overall values are lower than in the previous simulation with higher influent COD load. Figure 39 e – f show that like TMP and EPS in the cake, the concentrations are lower than with higher influent COD load. Especially, the EPS values are lowering very quickly with lower influent COD load.

6.4 Varying influent NH_x concentration

Figure 40 shows the simulation results of changing the influent NH_x load to a higher value. This was done to see if full plant model can manage to fully nitrify with a higher NH_x load with default values.

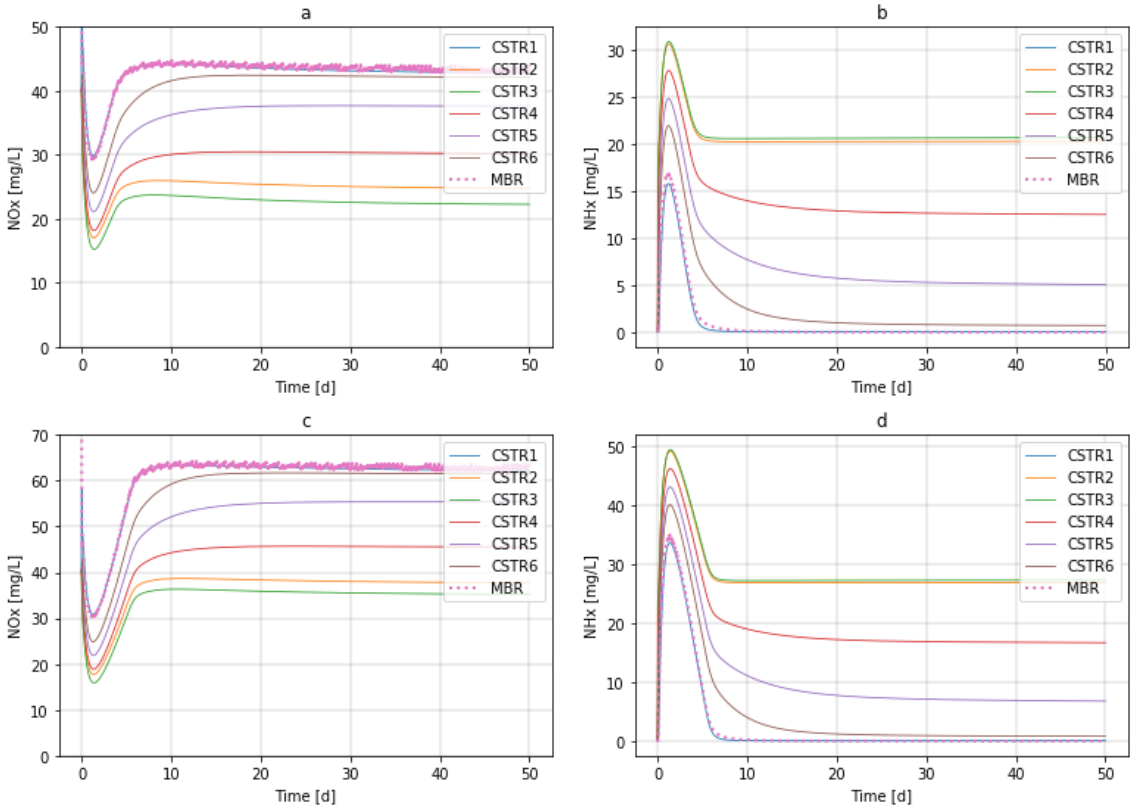

Figure 40 Simulated values for NO_x [mg/L] and NH_x [mg/L] in different tanks with varying influent NH_x to 60 [mg/L] in figures a – b and 80 [mg/L] in c – d.

From Figure 40 can be seen that full plant model can nitrify completely even with a higher NH_x influent load. Comparing Figure 40 b and d, a higher NH_x load of 80 mg/L leads only

to a few days delay to complete nitrification around days 5 – 8 compared to a NH_x load of 60 mg/L. Nitrogen removal is similar in both situation with around 25% removal rate.

6.5 Varying aerated volume

For the next simulation results presented in Figure 41 aerated volume was decreased by turning off from completely stirred tank reactor unit (CSTR 4) to decrease aerated volume from 6000 m^3 to 4500 m^3 and off in fifth CSTR (CSTR 5) to decrease aerated volume to 3000 m^3. These were done to see if decreasing the aeration volume decreases nitrification, affects fouling, or affects nitrogen removal.

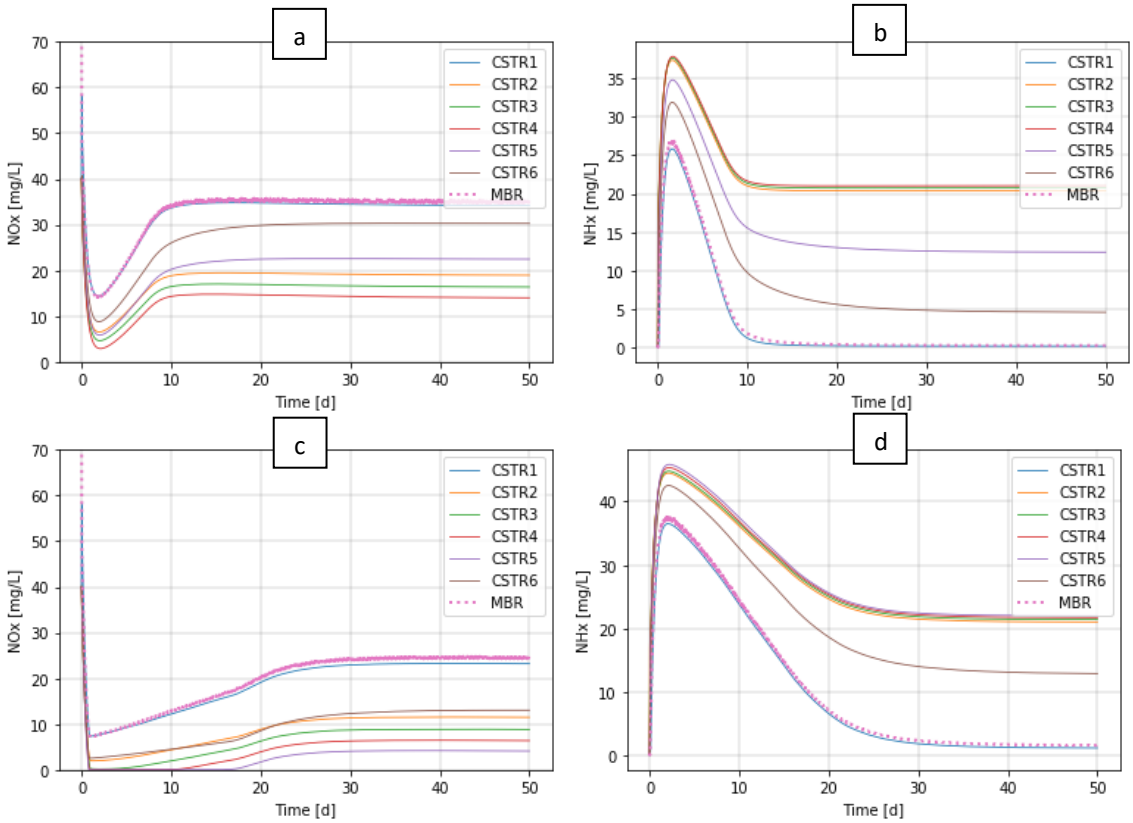

Figure 41. Simulated values for NO_x [mg/L] and NH_x [mg/L] in different tanks with aeration set off in CSTR 4 in figures a – b, and aeration set off in CSTR 4 and 5 in c – d.

Figure 41a – b is show that turning off aeration in one tank has no major effect on overall nitrogen levels. Only a short delay of around 5 days occurs for full nitrification compared to previous simulations. Figure 41 c – d show that turning aeration off in two tanks has some effect on nitrification and denitrification. Nitrification is not complete during 50 days of simulation. However, denitrification is more effective and nitrogen removal is around 60%.

Fouling-related simulation results are in Appendix X. They are like previous results and indicate that turning aeration off from one tank does not have a major effect on fouling. Lowering the aeration volume to 3000 m^3 shows less fouling. The change is not significant, though.

6.6 Varying SRT

For the next simulation results presented in Figure 42, Figure 43, and Figure 44, the SRT was varied between 15 and 20 days. This was done to see how different SRT affects nitrification, denitrification, fouling, and EPS and SMP concentrations.

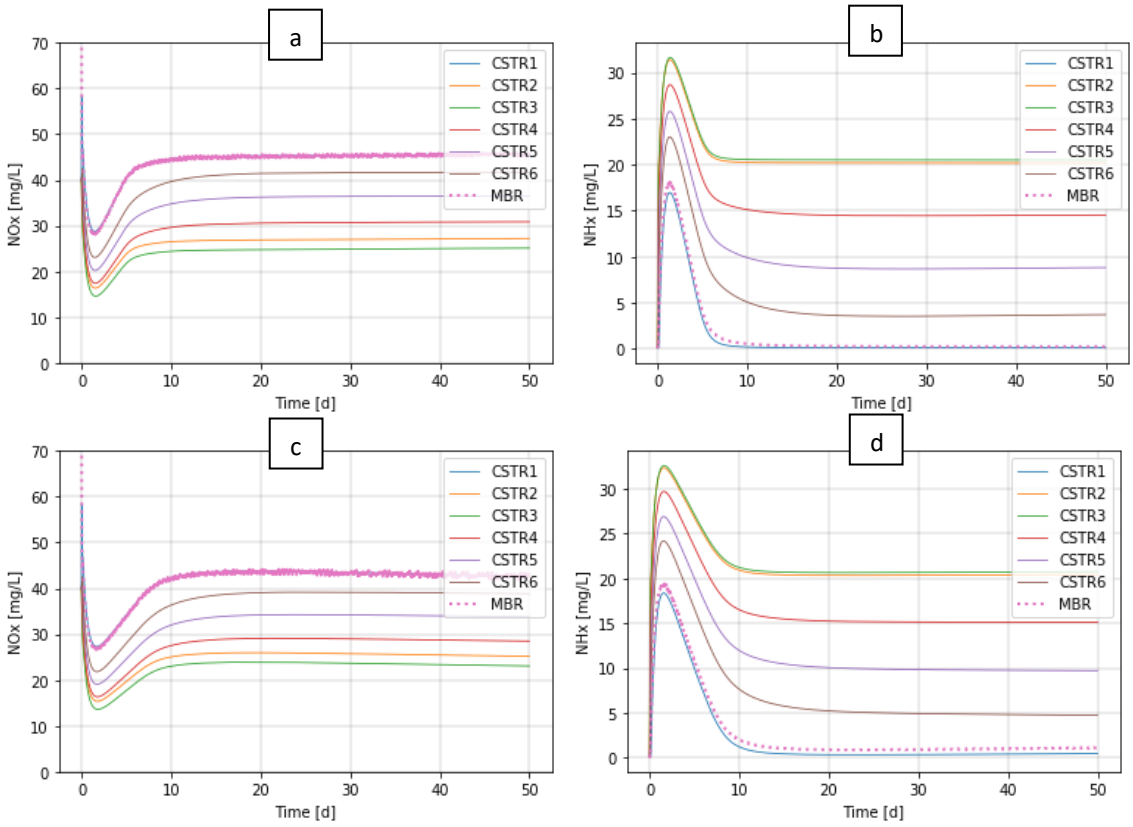

Figure 42. Simulated values for NO_x [mg/L] and NH_x [mg/L] in different tanks with SRT set to 20 d in figures a – b, and 15 d in c – d.

From Figure 42 can be seen that complete nitrification occurs a bit slower with SRT set to 15 days compared to 20 days. However, denitrification is slightly better with SRT set to 15 days with nitrogen removal rate of around 30%.

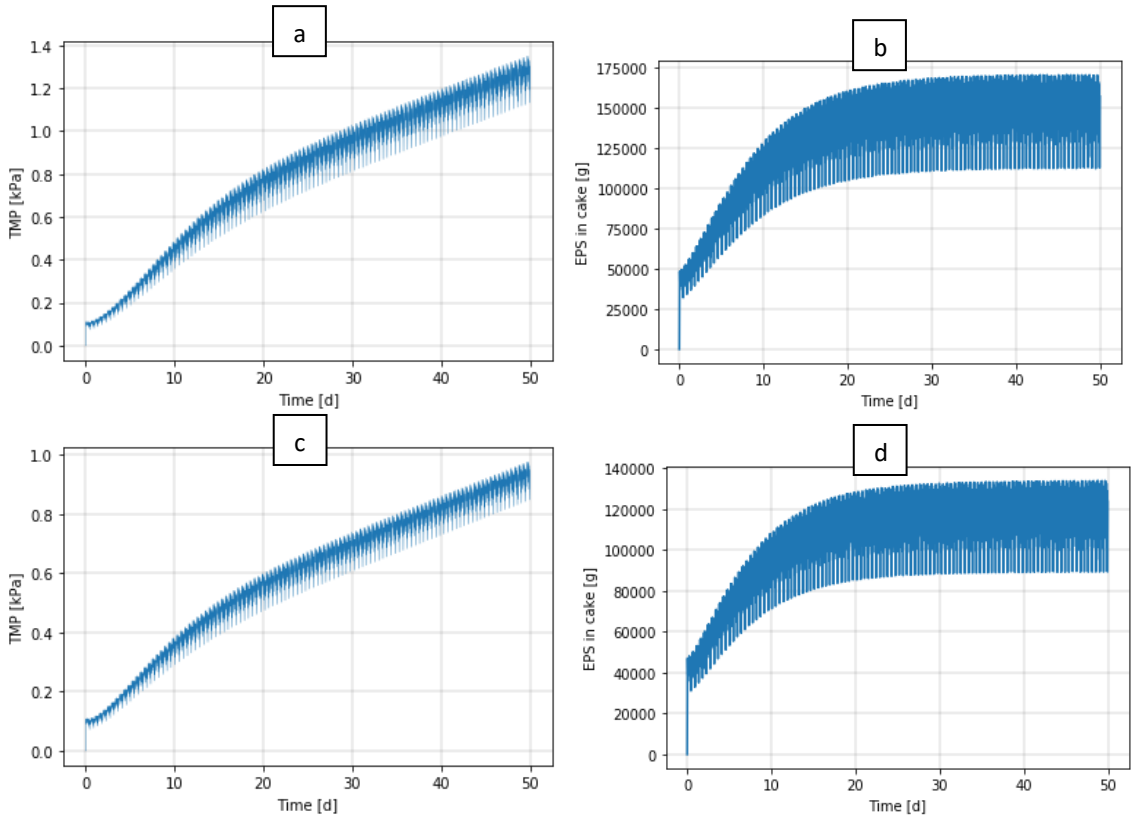

Figure 43. Simulated values for TMP [kPa] and EPS mass in cake [g] in MBR process unit with SRT set to 20 d in figures a – b, and 15 d in c – d.

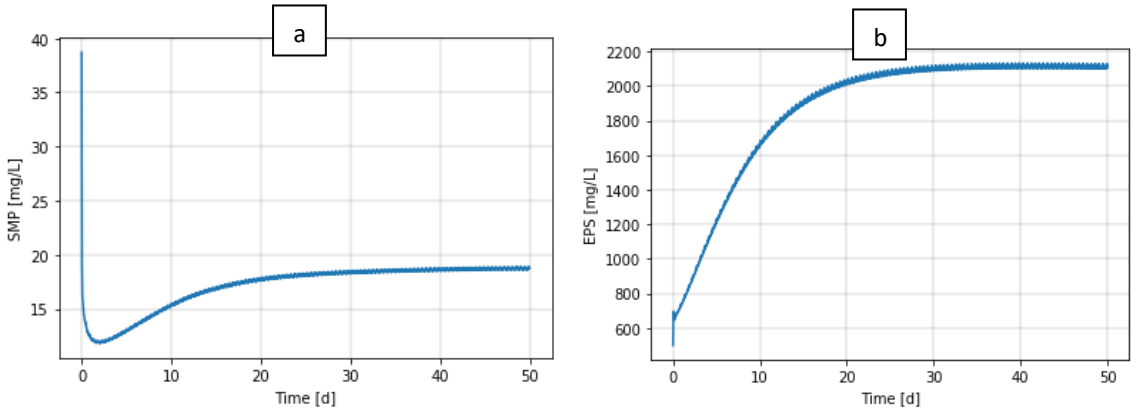

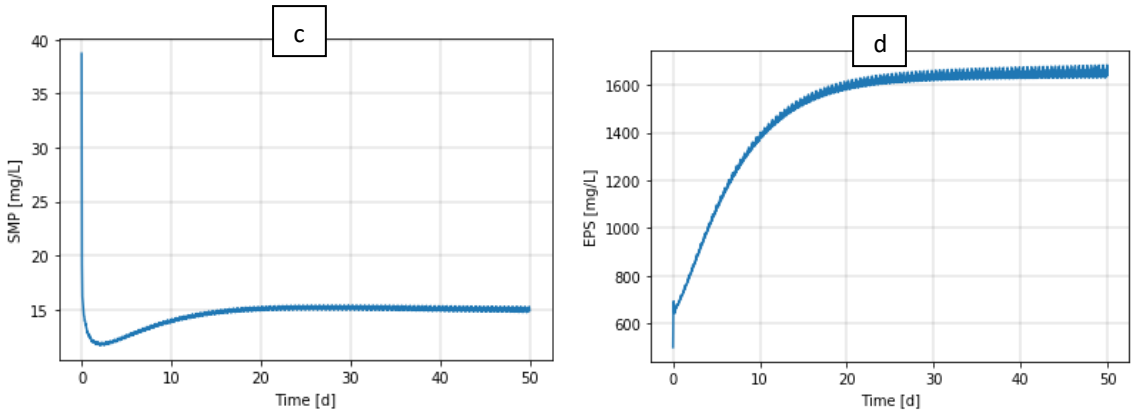

Figure 44. Simulated values for SMP [mg/L] and EPS [mg/L] in MBR process unit with SRT set to 20 d in figures a – b, and 15 d in c – d.

Figure 43 and Figure 44 show that compared to the default SRT set to 37 days, both SRTs, 15 days and 20 days, lead to less fouling. SRT set to 20 days shows the maximum TMP of around 1.3 kPa and SRT set to 15 d shows the maximum TMP of less than 1 kPa. Also, EPS and SMP concentrations are much lower than with an SRT of 37 days.

6.7 Optimizing aerated volume in cold influent conditions

For the next simulation results presented in Figure 45 and Appendix X, the influent temperature was set to 10 °C and SRT was set to 15 days. Aerated volume was also varied to get optimal value for colder influent conditions. These were done to see how the full plant model will work in colder temperatures and whether the temperature affects the nitrification rate or SMP and EPS concentrations.

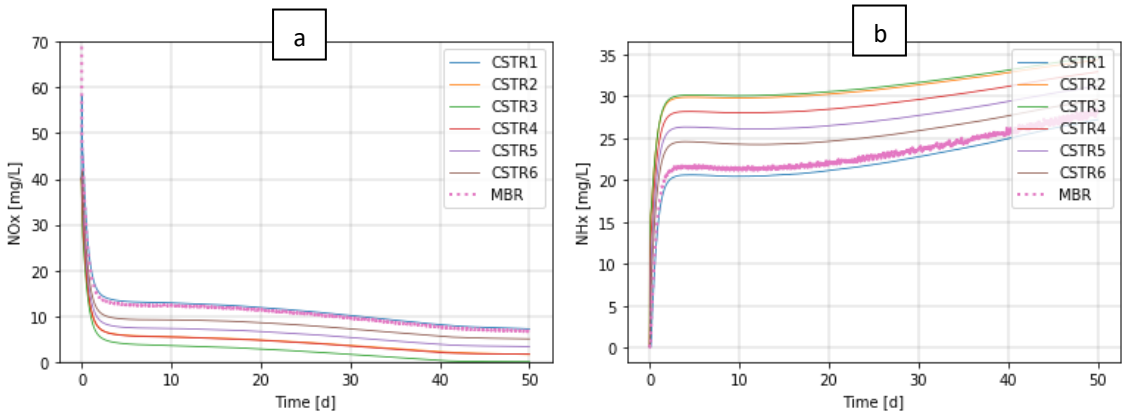

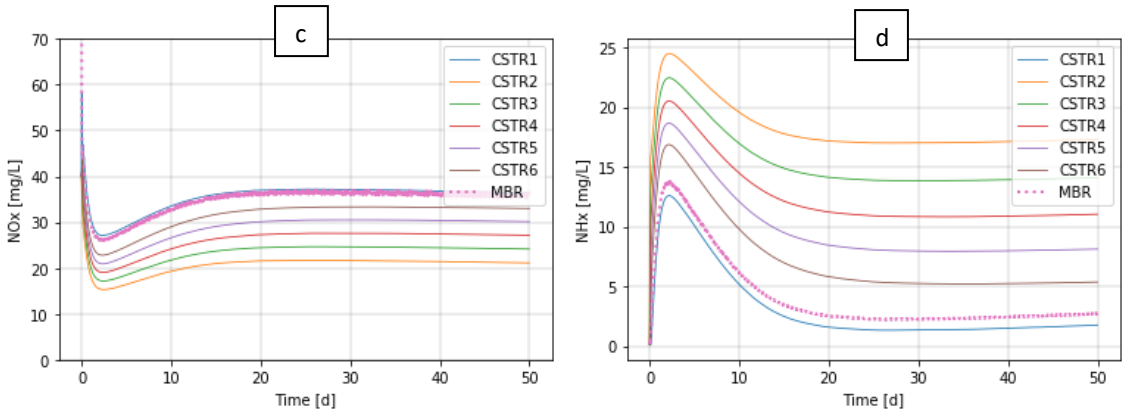

Figure 45. Simulated values for NO_x [mg/L] and NH_x [mg/L] in different tanks with SRT set to 15 d, temperature to 10 °C, and DO set to 0 [mg/L] in CSTR 3 in figures a – b and DO set to 2 [mg/L] d in c – d.

Figure 45 shows that nitrification is low in cold influent conditions and only around 10% of influent NH_x is converted to NO_x. Denitrification does, however, occur, and nitrogen removal is around 30%. Nitrification and denitrification decrease steadily over the 50-day period. Increasing aerated volume increases nitrification and with 6000 m^3 of aerated volume it gets to rather steady rate of around 95%. Also, denitrification occurs with a nitrogen removal rate of around 30%. Nitrification rate will develop slower than in a higher temperature and the 95% rate is achieved in around 20 days.

Fouling related simulation result are presented in Appendix X. Compared to higher temperature, all results except EPS concentration are lower. The possible reason why EPS concentration is higher is that during stress and slow growth period microbes produce more EPS. Increasing aerated volume does not significantly change fouling behavior.

6.8 Varying influent flow

For the next simulation results presented in Figure 46, Figure 47 and Figure 48, the influent flow was varied while keeping the SRT set to 15 days. Also, the flux was changed to meet those flows. These simulations were done to see how the full plant model works during high and low peak flows.

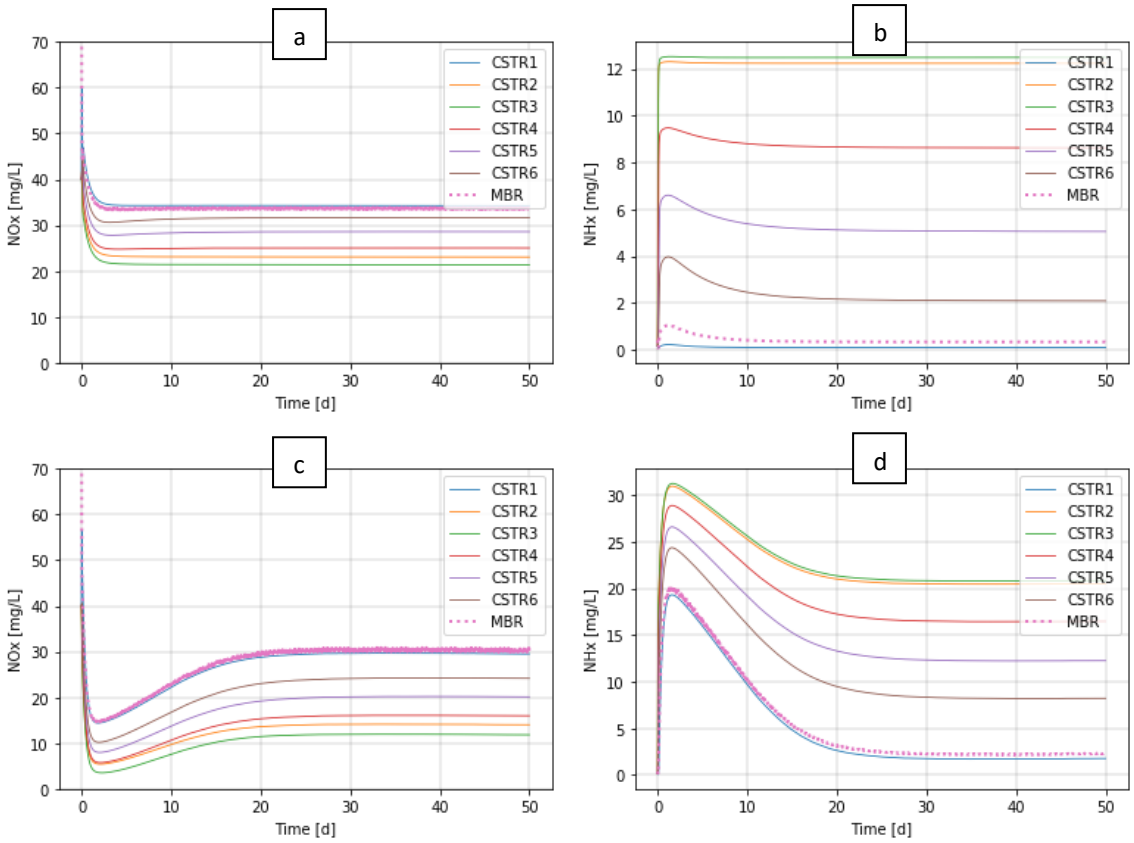

Figure 46. Simulated values for NO_x [mg/L] and NH_x [mg/L] in different tanks with SRT set to 15 d and influent flow to 15 000 [m3/d] in figures a – b and 30 000 [m3/d] in c – d.

From Figure 46 can be seen that nitrification is complete and nitrogen removal rate is around 45% when influent flow is low. During higher influent flow nitrification rate increases slowly and has a maximum value of around 95% after 20 days. Nitrogen removal rate is around 45%, similarly to low influent load.

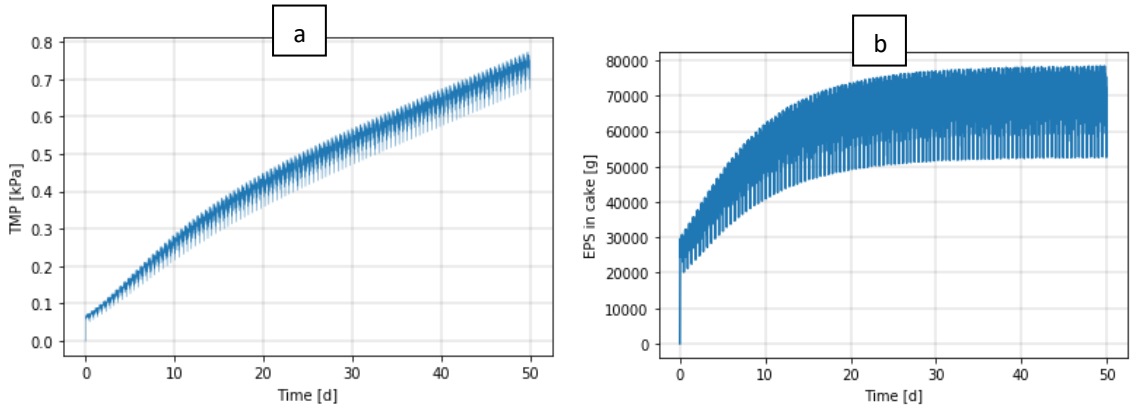

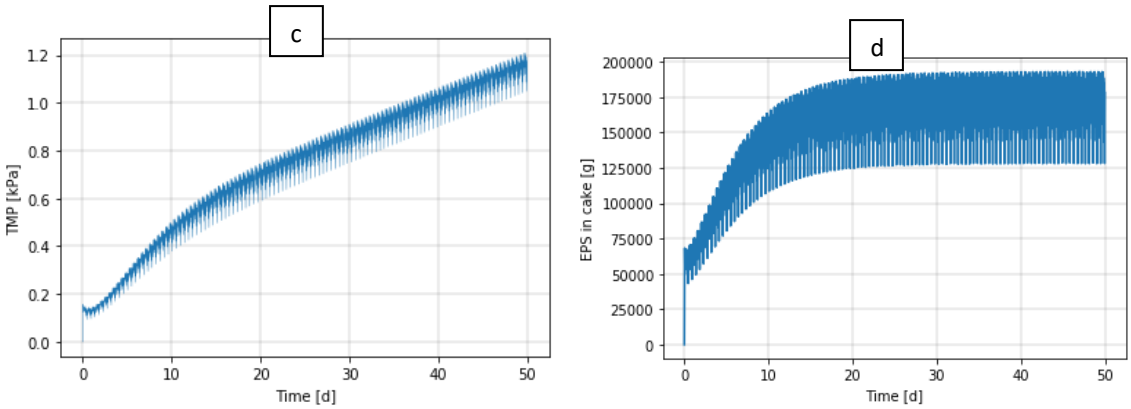

Figure 47. Simulated values for TMP [kPa] and EPS mass in cake [g] in MBR process unit wit with SRT set to 15 d and influent flow to 15 000 [m3/d] in figures a – b and 30 000 [m3/d] in c – d.

From Figure 47 can be seen that during low influent load the maximum TMP is the lowest of all simulation results with a value of around 0.75 kPa. Similarly, the EPS mass in cake is at its lowest with a maximum value of less than 80 kg.

During high influent flow the maximum TMP is around 1.2 kPa and it is much higher than during low influent flow. Similarly, EPS mass in cake is higher with a maximum value of around 190 kg. These results show that a full plant can still work during high influent flow but fouling increases.

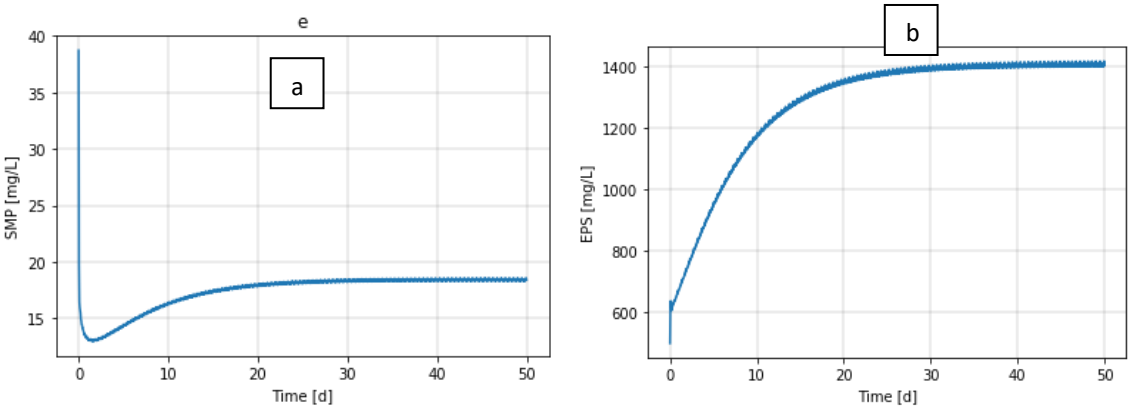

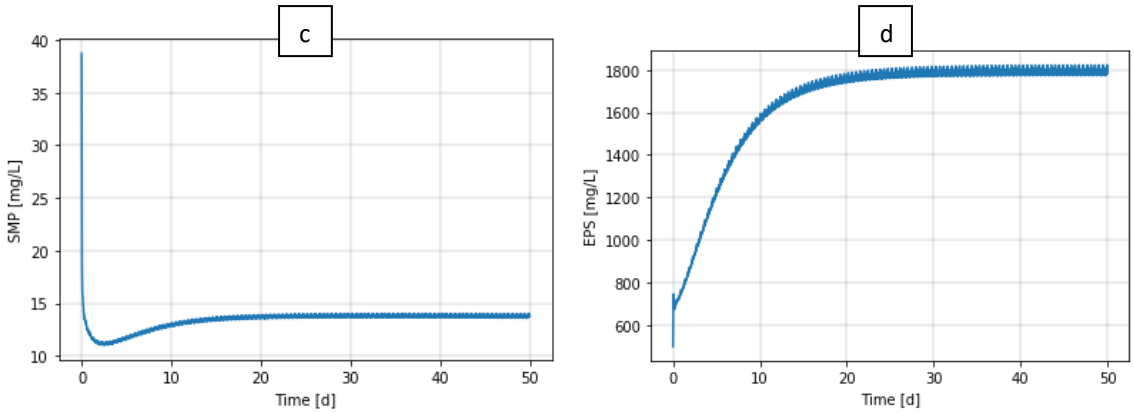

Figure 48. Simulated values for SMP [mg/L] and EPS [mg/L] in MBR process unit with SRT set to 15 d and influent flow to 15 000 [m3/d] in figures a – b and 30 000 [m3/d] in c – d.

From Figure 48 can be seen that SMP concentrations increase a bit from previous simulations and EPS concentrations decrease. During high influent flow The SMP concentration is lower than during low influent flow and the EPS concentration is higher, respectively.

7 IMPLEMENTATION AND ANALYZES OF THE DEVELOPED MODELS

7.1 Model inspection and identification of development targets

The models created, modified and partially calibrated in this work can be used to simulate the pilot process. The extended biokinetic model for biopolymer formation is well fitted during famine stress conditions in pilot process with heavy fouling behaviour. The simulated TMP values correspond reasonably well the measured ones during the calibration period. TMP was mainly fitted by calibrating two different parameters, one for irreversible fouling (irreversible fouling strength k_i) and one for reversible fouling (cake detachment rate k_r).

Liang et al. (2006) fitted irreversible fouling strength (k_i) parameter with a value of 1.48 * 10^{13} [m*kg^{-1}]. This study had two different values which were 1 * 10^{11} [m*kg^{-1}] during stress test with cleaned membranes and 1.2 * 10^{12} [m*kg^{-1}] during high fouling period with heavily clogged membranes, respectively. The values in this study are around 10 - 100 times lower, which seems reasonable as Liang et al. (2006) operated their pilot with TMP values of around 5 to 20 times higher (40 – 60 kPa) compared to pilot plant operated in Mikkeli. However, irreversible fouling develops over long period and it should be calibrated with long period measuring data (Janus 2013). This means that validating irreversible fouling model needs longer calibration period with more intensive measuring than the ones in this study.

Janus (2013) fitted the cake detachment rate (k_r) to 200 [d^{-1}] and Liang et al. (2006) fitted k_r to 3.24 [d^{-1}]. In this study the fitted value for k_r was 300 [kg.m^{-2}.d^{-1}]. The value cannot be directly compared to previous studies as the model in this study has dynamic model for cake strength which varies depending on various parameters and variables. However, the data from pilot plant could be fitted well with the k_r value, which indicates that estimations to cake strength parameters cannot be completely wrong.

The mechanistic fouling model is based mainly on the PhD of Janus (2013) and modifications to completely stirred tank reactor (CSTR) created by Dynamita. The main challenge of the created model is that it includes many parameters that should be estimated, calculated or fitted based on measured values. Parameters influencing cake formation could

not be measured in this work, so the cake mass was estimated to match TMP. Böhm et al. (2013) were able to measure single bubbles and the shear stress [Pa] they create to MBR surface. Wu et al. (2012) measured floc sizes distribution and mass percentage of solids particles and could fit the data to model. They could also relate the air scouring intensity to specific cake resistance. These results show that at least some of the MBR process units' parameters can be measured.

The base for biokinetic model (Sumo1) is created by Dynamita and it includes many unused microbe populations with their corresponding kinetic and stoichiometric components and variables. The extended biokinetic model also includes a wide variety of different processes which are left to default values in this work. However, for future use these variables, components, and processes can be validated with measuring campaigns for different microbe populations. For full plant behaviour, the simulated values for EPS and SMP change based on the operational conditions. S_{UAP} and S_{BAP} were found to act differently in different operational conditions. Jiang et al. (2008) were able to measure S_{UAP} and S_{BAP} separately and model the behaviour of both components. However, their model did not include EPS so the results are not comparable, but the methods for measuring the S_{UAP} and S_{BAP} can be used in the future model calibration.

The extended biokinetic model should be calibrated in different conditions to get corresponding model parameters. After extended biokinetic model matches suitably to measured values, the mechanistic fouling model could be calibrated to match the measured TMP values. After both models are calibrated, they can be used for different simulations.

7.2 Fixing the models

Some modification and components should be added to extended biokinetic model. One interesting addition would be the division of EPS to tightly bound EPS (TB-EPS) and to loosely bound EPS (LB-EPS). The fouling properties and characteristics of LB-EPS and TB-EPS have been studied (Long et al. 2017, Xiao et al. 2017 and Xinying et al. 2018) but no models exist so far for TB-EPS and LB-EPS at least in the knowledge of the author of this thesis.

Model for pore constriction and relation to irreversible fouling's parameters could be added to mechanistic fouling model. Broeckmann et al (2005) modeled the pore blockage and could calibrate the model but were not able to validate it. Wu et al (2012) were able to create calibrated and validated model from pore constriction. These models would help to fit TMP better in longer simulations. However, the need for measuring, calibration, and validation should be planned carefully before model modification

Also, a more correct model for air scouring could be developed with relation to gel layer formation and cake strength. This would give better estimations for aeration demand. However, modelling gel layer formation and its strength may be difficult as it is a complex mixture of particles with different sizes, which form unpredictable patterns as seen in Figure 49.

Figure 49. Gel layer and cake formation on the membrane surface.

7.3 Error checking and the need for further research

Overall, the models introduced in this work can be used for different fouling related simulation purposes. The biological model can be used to mitigate EPS and SMP production in different situations. Fouling model could be used to ensure that chemical cleaning is done frequently enough. One of the most interesting uses for both models is the optimization of aeration. The models could be used to ensure that aeration is sufficient for minimal SMP and EPS production and that air demand for air scouring is optimal.

Influent characterization was done only for the winter period. This gives a good overview of the influent coming to the pilot process during a cold winter season. As the calibration of the current model is done only according to this data, it is only valid for winter. Influent characterization should be done during different seasonal situations.

During calibration it was found that values for maximum growth rate of BAP were much lower than the maximum growth rate on UAP. These should be measured independently during the full plant calibration/validation phase. Overall, the SMP fractions and EPS should have been measured more frequently during different conditions to have better estimations from those different situations and to get correct growth and decay kinetics.

It would have been interesting to test how the model works with complex pH related calculations. Mechanistic fouling model was fast when no dynamic data or complex model set ups were included. However, after applying both, the dynamic data and full plant model, the simulations were quite slow with the fouling model. This should be noted in future simulations and maybe to keep some simulations simple if full plant modeling is not required or only the fouling behavior needs to be simulated.

One of the main concerns was the lack of data of different microbe population concentrations. Population estimations should be measured to get valid data from the plant. Also, data of cake formation, cake strength, cake compressibility and pore constriction are important for fouling model calibration and validation.

8 CONCLUSIONS

In this thesis, dynamic process models for EPS and SMP production and mechanistic membrane fouling were created. The models can be used to predict membrane fouling with current calibrated parameters in pilot plants process set up and during low food conditions. However, the models can also be used to other applications after calibration and validation. Also, membrane scouring coarse bubble aeration inside the MBR unit had insignificant effect on the biological activity of the whole treatment process.

This thesis puts us a step further to better understand the fouling behaviour of MBR, especially in full scale applications as the models are calibrated to pilot plant which treats municipal wastewater. It also raises more questions, which need answering. For example, the gel layer formation and its strength are complex processes to understand and model, but they are important as they directly affect the aeration demand.

Sensitivity analysis or parameter estimations of the created models indicate that the models are sensitive to parameters, input data and operational conditions. However, sensitivity analysis was not made quantitatively to all parameters to see, which of them had the highest impact. In future, it would be interesting to test the models for other applications and do sensitivity analysis to see if different plant set up affects the sensitivity of the model. Also, the most critical parameters and operational conditions to aeration demand should be carefully inspected.

To fully validate the models created in this work, other plant models should be simulated to see ensure they work correctly. Also, long calibration times for irreversible fouling modeling would be important. This would minimize the risks of some model parameters and ensure the overall applicability of the models.

REFERENCES

Ahn, Y. T., Choi, Y., Jeong, H., Chae, S. and Shin, H. 2006. Modeling of extracellular polymeric substances and soluble microbial products production in a submerged membrane bioreactor at various SRTs. Water Science and Technology, Volume 53. Pages 209 – 216.

Aquino, S., Gloria, R., Silva, S. and Chernicharo, C. 2009. Quantification of the Inert Chemical Oxygen Demand of Raw Wastewater and Evaluation of Soluble Microbial Product Production in Demo-Scale Upflow Anaerobic Sludge Blanket Reactors under Different Operational Conditions. Water Environment Research, Volume 81, Issue 6.

Böhm, L. et al. 2013. Bubble induced shear stress in flat sheet membrane systems—Serial examination of single bubble experiments with the electrodiffusion method. Journal of Membrane Science, Volume 437. Pages 131-140.

Capodici, M., Di Bella G., Di Trapani, D. and Torregrossa, M. 2015. Pilot scale experiment with MBR operated in intermittent aeration condition: Analysis of biological performance. Bioresource technology, Volume 177.

Chang, I-S., Le Clech, P., Jefferson, B. and Judd, S. 2002. Membrane Fouling in Membrane Bioreactors for Wastewater Treatment. EBSCO Publishing: Journal of Environmental Engineering. Pages 1018-1029.

Dubois, M., Gilles, K., Hamilton, J., Rebers, P. and Smith, F. 1956. Colorimetric method for determination of sugars and related substances. Anal. Chem. Volume 28. Pages 350-356.

Evenblij, H. 2006. Filtration Characteristics in Membrane Bioreactors. PhD Thesis. Netherlands, Delft: Technische Universiteit Delft. 225 p.

Everette, J., Bryant, Q., Green, A., Abbey, Y., Wangila, G. and Walker, R. 2010. Thorough study of reactivity of various compound classes toward the Folin-Ciocalteu reagent. J. Agric. Food Chem. Volume 58. Pages 8139-8144.

Friedrich, H. Mertsch, V. 2003. Membrane Technology for Waste Water Treatment. Federal Ministry for the Environment, Nature Conservation and Nuclear safety, Berlin. 346 p. ISBN 3-939377-00-7.

Gurung, K. 2014. Feasibility study of submerged membrane bioreactor (MBR) as an alternative to conventional activated sludge process (CASP) for municipal wastewater treatment: a pilot scale study. Master's Thesis. Lappeenranta University of Technology. Lappeenranta.

Hermia, J. 1982. Constant pressure blocking filtration laws - application to power-law non-newtonian fluids. Transactions of the Institution of Chemical Engineers, Volume 60, Issue 3. Pages 183–187.

Hug, T. et al. 2009. Wastewater treatment models in teaching and training: the mismatch between education and requirements for jobs. IWA Publishing: Water Science & Technology Oct 2009. Pages 745-753.

Janus, T. 2013. Modelling and Simulation of Membrane Bioreactors for Wastewater Treatment. PhD Thesis. United Kingdom, Leicester: De Montfort University. 357 p.

Jiang, T. et al. 2008. Modelling the production and degradation of soluble microbial products (SMP) in membrane bioreactors (MBR) Water Research, Volume 42, Issue 20. Pages 4955-4964.

Kunacheva, C. and Stuckey, D. 2014. Analytical methods for soluble microbial products (SMP) and extracellular polymers (ECP) in wastewater treatment systems: A review. Water Research, Volume 61. Pages 1-18.

Laitala, R. 2005. Adequacy of Organic Matter in Finnish Wastewaters to Biological Nutrient Removal. Licentiate's Thesis. Helsinki University of Technology. Helsinki.

Laspidou, C. Rittmann, B. 2001. A unified theory for extracellular polymeric substances, soluble microbial products, and active and inert biomass. Water Research, Volume 36. Pages 2711 – 2720.

Liu, H. and Fang, H. 2002. Extraction of extracellular polymeric substances (EPS) of sludges Journal of Biotechnology, Volume 95, Issue 3. Pages 249-256.

Long, X., Tang, R. et al. 2017. The roles of loosely-bound and tightly-bound extracellular polymer substances in enhanced biological phosphorus removal. Chemosphere, Volume 189. Pages 679-688.

Lowry, O, Rosebrough, N., Farr A. and Randall, R. 1951. Protein measurement with the folin phenol reagent. J. Biol. Chem. Volume 193. Pages 265-275.

Lu, S. G., Imai, T., Ukita, M., Sekine, M., Higuchi, T. and Fukagawa, M. 2001. A model for membrane bioreactor process based on the concept of formation and degradation of soluble microbial products. Water Research, Volume 35. Pages 2038 – 2048.

Melcer, H., Dold, P.L., Jones, R. et al. 2003. Methods for Wastewater Characterization in Activated Sludge Modeling. Water Environment Research Foundation. 575 p. ISBN 1-893664-71-6.

Metzger, U. et al. 2007. Characterisation of polymeric fouling in membrane bioreactors and the effect of different filtration modes. Journal of Membrane Science, Volume 301, Issues 1-2. Pages 180-189.

Miura, T., Okabe, S., Nakahara, Y. and Sano, D. 2015. Removal properties of human enteric viruses in a pilot-scale membrane bioreactor (MBR) process. Water Research, Volume 75. Pages 282-291.

Monod, J. 1949. Recherches sur la croissance des cultures bactériennes. Paris, Hermann & cie.

Nagaoka, N., Yamanishi, S. and Miya, A. 1998. Modeling of biofouling by extracellular polymers in a membrane separation activated sludge system. Water Science and Technology, Volume 38, Issues 4-5. Pages 497–504. ISSN 0273-1223.

Park, H.D., Chang I.S. and Lee K.J. 2015. Principles of Membrane Bioreactors for Wastewater Treatment. IWA Publishing. 429 p. ISBN 978-1-4665-9037-3.

Park, J. K., Wang, J. and Novotny, G. 1997. Wastewater Characterization for Evaluation of Biological Phosphorus Removal. Wisconsin Department of Natural Resources. Research Report 174.

Rieger, L., Gillot, S., Langerberger, G., Ohtsuki, T., et al. 2012. Guidelines for Using. Activated Sludge Models. IWA Publishing. 303 p. ISBN 9781780401164.

Skinner, S. 2017. Interactive map: History of municipal membrane bioreactor installations. [Accessed 22.9.2019] Available at https://www.thembrsite.com/interactive-map-history-of-municipal-mbr-installations/

Tchobanoglous, George. 2003. Wastewater Engineering; Treatment and Reuse. Fourth edition. The McGraw-Hill Companies, New York. 1819 p. ISBN 0-07-041878-0.

Wang, Z., Wu, Z. Tang, S. 2009. Extracellular polymeric substances (EPS) properties and their effects on membrane fouling in a submerged membrane bioreactor. Water Research, Volume 43, Issue 9. Pages 2504-2512. ISSN 0043-1354.

Wentzel, M. C., Mbewe, A. and Ekama G. A. 1995. Batch test for measurement of readily biodegradable COD and active organism concentrations in municipal waste waters. Water SA, Volume 21, Issue 2. Pages 117-124.

Wentzel, M. C., Mbewe, A., Lakay M. T. and Ekama G. A. 1999. Batch test for characterization of the carbonaceous materials in municipal wastewaters. Water SA, Volume 25, Issue 3. Pages 327-335.

Wu, J., He, C. and Zhang, Y. 2012. Modeling membrane fouling in a submerged membrane bioreactor by considering the role of solid, colloidal and soluble components. Journal of Membrane Science. Volume 397-398, Pages 102-111.

Xiao, K., Chen, Y., Jiang, X. and Zhou, Y. 2017. Evaluating filterability of different types of sludge by statistical analysis: The role of key organic compounds in extracellular polymeric substances. Chemosphere, Volume 170, Pages 233-241.

Xinying, S. and Zhigang, Z. 2018. Structural characteristics of extracellular polymeric substances (EPS) in membrane bioreactor and their adsorptive fouling. London. Water Science and Technology, Volume 77, Issue 6. Pages 1537-1546.

Zhang, B., Baosheng, S., Min, J., Taishi, G. and Zhenghong, G. 2007. Extraction and analysis of extracellular polymeric substances in membrane fouling in submerged MBR. Desalination, Volume 227, Issues 1-3. Pages 286-294.

Appendix I, course program for dynamic process modeling

Dynamita SARL
7 Eoupe
Nyons, 26110 France
info@dynamita.com

Course program

Advanced Sumo and dynamic modeling course – 2017

Course duration: 3 days

1. Creating your own biokinetic models in Sumo
    - Introducing the Microsoft Excel workbooks storing Sumo models - model format
    - Model checking macros: how and when to use them, interpreting outputs
    - Creating a new Gujer matrix
    - Mass balance / elemental balance checks on the Gujer matrix
    - Equilibrium code notation used in Sumo models – develop your own pH model
    - State variables, model components, parameters, built-in constants, calculated variables – how to define them
    - Deploying custom models to make them available from the Sumo GUI

2. Creating your own process units in Sumo
    - General structure of Microsoft Excel workbooks storing Sumo process units
    - Process unit attributes, attribute groups
    - Defining process unit parameters
    - Organizing code equations – readable for the developer, readable for the end user
    - Defining custom popups and variable categories
    - Creating custom process unit graphics, connection location, connection attributes

3. SumoSlang principles and fundamentals
    - Writing equations in SumoSlang
    - Variable templating, using the triplet notation, useful shorthands
    - Built-in physical constants, parameters, predefined functions – a quick review
    - How to write your custom SumoSlang functions
    - Codelocations – how to use them to write efficient dynamic models; code blocks, block sections
    - Time event definition, event scheduling

Dynamita SARL
7 Eoupe
Nyons, 26110 France
info@dynamita.com

4. How to debug your custom SumoSlang code
    - Interpreting error messages – Sumo variable name construction rules
    - How to catch the missing variable
    - Sumo model building internals – how to read the generated XML file

5. Special topic: implementing controllers in Sumo
    - Controller principles: P, PI and PID controller basics
    - Using the event handling infrastructure for controller implementation
    - Recursive event scheduling to implement periodic controllers
    - Testing, introducing debug variables as good practice for controller development

6. Special topic: developing a custom membrane bioreactor with fouling processes

7. Special topic: extending Sumo1 model by extracellular polymeric substances and two soluble microbial products to enable membrane fouling estimations

Appendix II, illustration of GMP unified protocol steps and links between them

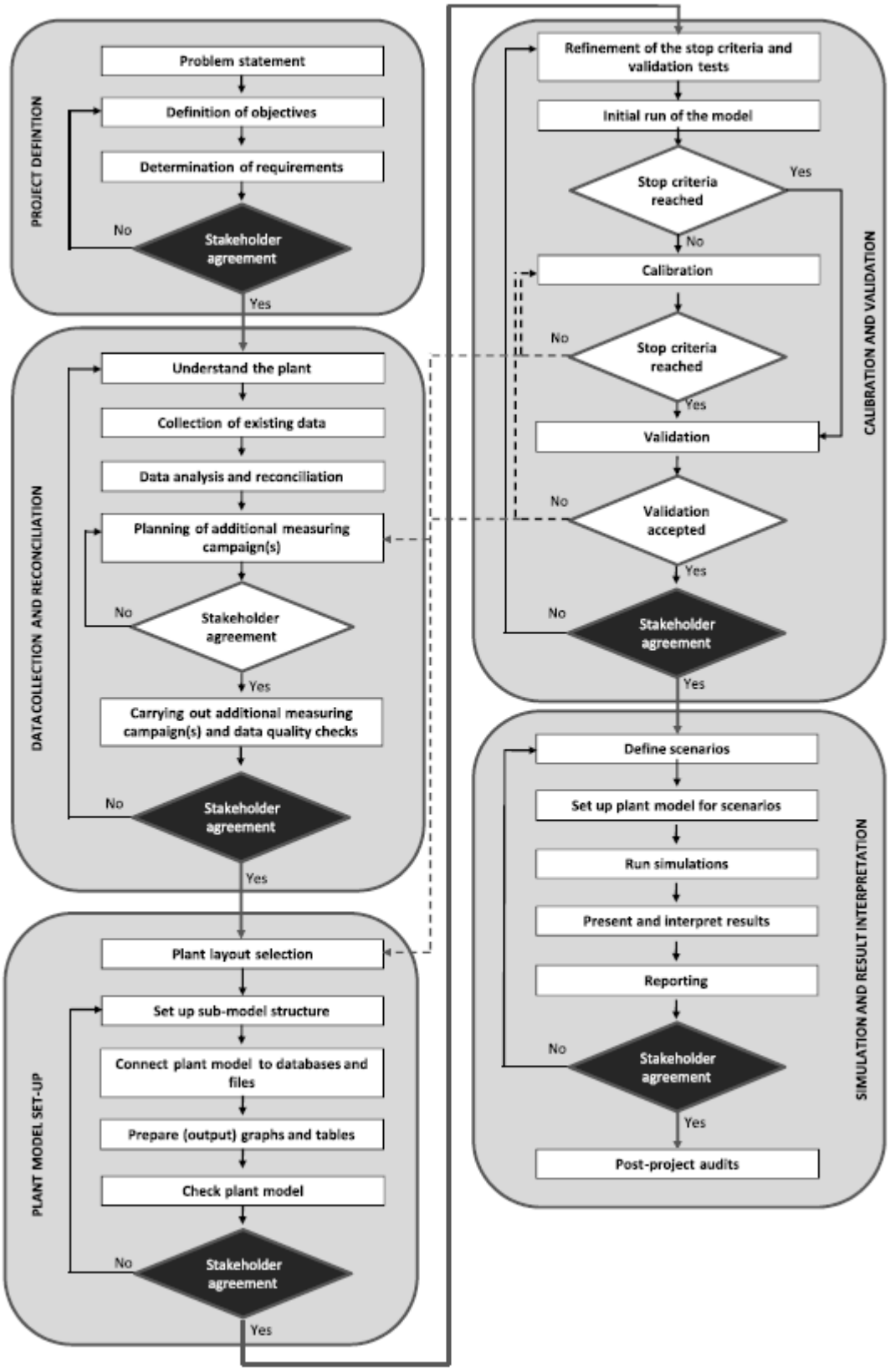

Appendix III, the full analytical sheet from influent wastewater

MBR PILOT, PERMEATE

Analysis	Date	14-15.11.16	22-23.11.16	29-30.11.16	13-14.12.16	20-21.12.16	18-19.1.17	24-25.1.17	31.1-1.2.17	7-8.2.17	14-15.2.17	21-22.2.17	7-8.3.2017	14-15.3.17	21-22.3.17	28-29.3.17	4-5.4.17	10-11.4.17	18-19.4.17	25-26.4.17	3-4.5.17	9-10.5.17	16-17.5.17	6-7.6.17	13-14.6.17	19-20.6.17	27-28.6.17	4-5.7.17
Phosphorus total P (mg/l)		0,47	0,45	0,42	0,54	0,39	0,75	1,22	1,10	0,98	0,69	0,33	0,45	0,43	0,63	0,57	0,62	0,63	0,48	0,60	0,44	0,27	0,24	1,17	0,63	0,52	0,41	0,66
Soluble phosphorus (Iliukoinen kok.fosfori) (mg/		0,48	0,45	0,41	0,53	0,39	0,74	1,25	1,08	0,95	0,66	0,32	0,45	0,44	0,63	0,57	0,62	0,65	0,48	0,60	0,45	0,28	0,24	1,12	0,63	0,52	0,43	0,66
Fe (mg/l)		0,13	0,11	0,13	0,16	0,18	0,14	0,30	0,22	0,23	0,19	0,18	0,17	0,13	0,12	0,11	0,10	0,06	0,03	0,08	0,08	0,09	0,11	0,10	0,11	0,25	0,05	0,07
SS (mg/l)		<1	<1	<1	<1	<1	<1	<1	<1	<1	<1	<1	<1	<1	<1	<1	<1	<1		<1	<1	<1	<1	<1	<1	<1	<1	<1
$COD_{cr}(O_2$,mg/l)		32	29	29		32	35	234	62	88	73	45	28	24	22	35	23	23	23	28	26	21	21	28	19	18		14
NO_3-N (mg/l)		55,8	42,9	41,5	54,0	62,1	52,7	29,0	14,3	17,2	13,4	37,5	50,1	50,2	47,9	42,6		38,7	44,9	41,2	38,3	37,3	43,5	56,2	42,1	38,4	40,7	34,2
NH_4-N (mg/l)		<0,02	0,02	<0,02	0,40	0,02	0,02			15,27	10,49	0,31	0,04	0,02	0,30	0,03	0,02	0,01	0,01	0,01	0,02	0,03	0,02		0,08	0,04	0,01	0,08
N total (mg/l)			48	46			55	70	80	73	67	53	56	53	48	48	49	45	47	45	39	41	44	69	43	29	42	42
Alkalinity (mmol/l)		0,32	0,72	0,71	0,48	0,33	0,87	0,00	3,09	0,52	0,95	0,79	0,50	0,73	0,33	1,19	0,84	1,28	0,70	0,80	0,72	0,66	0,71	0,34	0,17	0,22	0,55	0,88
pH		7,1	7,2	7,3	7,1	7,1	7,5	3,9	8,0	7,1	7,4	7,6	7,4	7,5	6,8	7,7	7,4	7,6		7,5	7,1	7,1	7,4	6,8	6,9	6,7	7,3	7,3

MBR PILOT, INFLUENT

Analysis	Date	14-15.11	22-23.11	29-30.11	13-14.12	20-21.12.16	18-19.1.17	24-25.1.17	31.1-1.2.17	7-8.2.17	14-15.2.17	21-22.2.17	7-8.3.2017	14-15.3.17	21-22.3.17	28-29.3.17	4-5.4.17	10-11.4.17	18-19.4.17	25-26.4.17	3-4.5.17	9-10.5.17	16-17.5.17	6-7.6.17	13-14.6.17	19-20.6.17	27-28.6.17	4-5.7.17
Phosphorus total P (mg/l)		5,29	4,93	5,53	4,92	5,71	4,99	5,46	5,41	5,90	5,96	5,27	7,03	5,71	5,35	4,60	4,74	3,97	4,49	5,75	4,46	4,50	4,26	5,38	5,23	4,59	4,79	4,87
Soluble phosphorus (Iliukoinen kok.fosfori) (mg/l)		22,0	19,7	23,2	27,5	20,8	14,9	17,5	15,3	24,4	20,2	20,6	22,9	19,2	20,0	5,3	0,6	18,9	14,4	11,1	13,8	14,6	19,1	17,9	19,7	17,4	17,9	14,4
Fe (mg/l)		148	109	118	163	157	119	144	146	140	156	152	170	150	124	86	117	91	91	91	92	111	110	162	128	138	119	124
SS (mg/l)		329	236	286		325	305	368	357	346	343	337	414	349	302	239	263	274	327	284	269	297	311	595	354	380	317	297
$COD_{cr}(O_2$,mg/l)																												
NO_3-N (mg/l)		<1	<1	<1	1,36	<1	<1	<1	<1	1,48	<1	<1	<1	<1	<1	<1	<1	1,12	<1	1,5	0,73	<1	<1	<1	<1	<1	<1	<1
NH_4-N (mg/l)			37,7	49,6	47,9	58,3	45,0	54,2	56,2	47,6	60,0	52,8	59,3	53,3	48,1	41,6	34,1	53,9	76,0	65,3	37,8	44,9	45,0	48,3	48,4	48,1	35,8	48,4
N total (mg/l)			51	57			55	73	77	59	85	65	71	66	50	57	42	67	79	72	45	53	56	60	57	64	46	64
Alkalinity (mmol/l)		5,6	4,5	5,0	5,4	5,6	5,0	5,7	6,5	4,8	6,2	5,5	6,0	5,7	5,0	5,2	3,8	3,6	4,2	4,1	4,3	4,9	4,4	5,9	5,3	5,1	4,5	5,2
pH		7,3	7,2	7,3	7,2	7,4	7,3	7,4	7,5	7,3	7,4	7,4	7,4	7,4	7,3	7,5	7,3	7,3		7,4	7,3	7,4	7,2	7,1	7,4	7,4	7,4	7,4

Influent COD fractioning							
	21.11.16	27.11.16	25.01.17	31.01.17	05.02.17	Fractions	Average
CODtot	211	253	385	378	333	1	312
bCOD	125	140	190	190	170	0,52	163
rbCOD	9	23	51	26	14	0,08	25
cbCOD	75,1	78,2	138	107	81	0,31	96
xbCOD	49,9	61,8	52	83	89	0,22	67
suCOD	26,1	16,2	30	30	30	0,08	26
cuCOD + xuCOD	50,9	73,8	114	132	119	0,31	98

Appendix IV, MLSS analyses

Date	MLSS								Permeate	
	total sludge		total SMP		EPS					
					LB-EPS		TB-EPS			
	TSS [mg/L]	VSS [mg/L]	COD [mg/L]	TOC [mg/L]	COD [mg/L]	TOC [mg/L]	COD [mg/L]	TOC [mg/L]	COD [mg/L]	TOC [mg/L]
7.2.2017			219,2	-	83,4	24,14	260	107,84	70,3	-
13.2.2017			157,2	75,485	25,64	18,02	265,6	105,2	60,8	44,74
23.2.2017	6285	1890	48	19,175	66,4	11,885	140,4	44,465	42,8	17,83
28.2.2017	5800	4193	51,6	25,415	59,6	14,145	392,2	154,65	37,32	18,565
9.3.2017	6305	4475	57,8	18,125	48,4	14,29	307,6	113,25	38,24	14,8
21.3.2017	4690	3140	54,64	15,775	65,4	11,585	291	110,7	39,08	20,1325
18.4.2017	3675	3040	48,4	15,775	46,8	9,4235	420	157,6	31	19,42
24.4.2017	5570	3890	37,56	21,95	41,6	14,89	387,2	188,45		17,45
10.5.2017	4135	3295	33,08	15,33	46,8	10,74	472	210,95	29,8	16,06
18.5.2017										
9.6.2017	2725	2565	40,48	20,34	49,8	13,34	345,6	143,85	30,48	20,95
20.6.2017	6450	4510	46,8	20,625	55,8	16,16	468	283,55	12,68	21,7
30.6.2017	5250	3865	32,04	18,755	54	9,74	612	184,4	5,24	16,7
7.7.2017		3405		17,065		8,115		143,15		14,15

Appendix V, description of test for EPS and SMP quantification

SMP

1. Centrifuging 6000 x g for 30 min
2. Supernatant to analyzing
3. Add 2 x the volume of supernatant acetone to supernatant
4. Precipitate 24h in 4 °C

5. Collect precipitate and measure COD = SMP

Total EPS

1. Centrifuging 3200 rpm for 30 min
2. Discard supernatant
3. Wash and suspend pellet with 0,9 w-% NaCl solution
4. Heat treatment 100 °C for 1 h
5. Centrifuging 3200 rpm for 30 min

6. Measure COD from supernatant = total bound EPS

LB-EPS and TB-EPS

1. Centrifuging 3200 rpm for 30 min
2. Discard supernatant
3. Wash and suspend pellet with 0,9 w-% NaCl solution
4. Ultrasonic extraction for 2 min (Ultrasonic cleaner KES-1001, 20 kHz and 330 W/L)
5. Centrifuging 3200 rpm for 30 min

6. Measure COD from supernatant = LB-EPS

7. Wash and suspend pellet with 0,9 w-% NaCl solution
8. Heat treatment 100 °C for 1 h
9. Centrifuging 3200 rpm for 30 min

10. Measure COD from supernatant = TB-EPS

Appendix VI, Gujer matrix for biopolymers

j	Symbol	Name	S_S	X_{EPS}	S_{UAP}	S_{BAP}	X_S	X_{OHO}	S_{NOx}	S_{O2}
3	r3	OHO growth on S_B, O_2	$-1/Y_{OHO,SB,ox}$	$f_{EPS,OHO}$	$\gamma_{OHO}/Y_{OHO,SB,ox}$			$1-f_{EPS,OHO}$	$-i_{N,BIO}-(1-f_{EPS,OHO})-i_{N,EPS}*f_{EPS,OHO}-i_{N,UAP}*(\gamma_{OHO}/Y_{OHO,SB,ox})$	$(Y_{OHO,SB,ox}*\gamma_{OHO}-1)/Y_{OHO,SB,ox}$
4	r4	OHO growth on S_B, NO_3	$-1/Y_{OHO,SB,nitox}$	$f_{EPS,OHO}$	$\gamma_{OHO}/Y_{OHO,SB,nitox}$			$1-f_{EPS,OHO}$	$-i_{N,BIO}*(1-f_{EPS,OHO})-i_{N,EPS}*f_{EPS,OHO}-i_{N,UAP}*(\gamma_{OHO}/Y_{OHO,SB,nitox})$	$(Y_{OHO,SB,nitox}*\gamma_{OHO}-1)/(\gamma_{OHO,SB,nitox}*EEQ_{N2,NO3})$
7	r7	OHO decay	$f_{EPS,d,OHO}$					-1	$-f_E*(i_{N,XE}-i_{N,BIO})$	
18	r18	NITO decay	$f_{EPS,d,OHO}$			f_{BAP}	$1-f_{ig}-f_{BAP}*f_{EPS,d,OHO}$		$-f_E*(i_{N,XE}-i_{N,BIO})$	
50	r50	Aerobic growth on SUAP	$f_{EPS,OHO}$	$-1/Y_{SMP}$				$1-f_{EPS,OHO}$	$i_{N,BIO}*(f_{EPS,OHO}-1)-f_{EPS,OHO}*i_{N,EPS}+1/Y_{SMP}*i_{N,UAP}$	$(Y_{SMP}-1)/Y_{SMP}$
51	r51	Aerobic growth on SBAP	$f_{EPS,OHO}$			$-1/Y_{SMP}$		$1-f_{EPS,OHO}$	$i_{N,BIO}*(f_{EPS,OHO}-1)+1/Y_{SMP}*i_{N,BAP}-f_{EPS,OHO}*i_{N,EPS}$	$(Y_{SMP}-1)/Y_{SMP}$
52	r52	Anoxic growth on SUAP	$f_{EPS,OHO}$	$-1/Y_{SMP}$				$1-f_{EPS,OHO}$	$i_{N,BIO}*(f_{EPS,OHO}-1)-f_{EPS,OHO}*i_{N,EPS}+1/Y_{SMP}*i_{N,UAP}$	$(Y_{SMP}-1)/(Y_{SMP}*EEQ_{N2,NO3})$
53	r53	Anoxic growth on SBAP		$f_{EPS,OHO}$		$-1/Y_{SMP}$		$1-f_{EPS,OHO}$	$i_{N,BIO}*(f_{EPS,OHO}-1)+1/Y_{SMP}*i_{N,BAP}-f_{EPS,OHO}*i_{N,EPS}$	$(Y_{SMP}-1)/(Y_{SMP}*EEQ_{N2,NO3})$
54	r54	Hydrolysis of EPS	$f_{SB,EPS}$	-1		$1-f_{SB,EPS}$				

Appendix VII, default concentrations of different components for simulations

Component	Concentration [mg/L]
S_{VFA}	0.0014
S_B	1.6
S_{MEOL}	0
X_{EPS}	152.5
S_{UAP}	14.9
S_{BAP}	23.8
C_B	0.012
X_B	9.2
S_U	18.1
C_U	0.0078
X_U	3975.5
X_{PHA}	0.014
X_E	1174.7
X_{E_ana}	0.0001
X_{OHO}	257.3
X_{PAO}	569.2
X_{MEOLO}	1.5
X_{NITO}	65.2
X_{AMETO}	0.067
X_{HMETO}	0.015
S_{NHx}	0.41
S_{NOx}	106
S_{N2}	15.8
S_{N_B}	0.37
X_{N_B}	0.53
X_{N_U}	39.8
S_{PO4}	177.4
X_{PP_LO}	399
X_{PP_HI}	70.4
S_{P_B}	0.012
X_{P_B}	0.15
X_{P_U}	8
S_{O2}	1.1
S_{CH4}	0
S_{H2}	0.0002
S_{CO2}	1971.8
X_{INORG}	1543.5
S_{CAT}	174.2
S_{AN}	491.9
S_{Ca}	330.8
S_{Mg}	67.2

S_K	83.7
S_{Fe2}	8.8
X_{HFO_H}	0
X_{HFO_L}	0
X_{HFO_old}	0
$X_{HFO\_H\_P}$	0
$X_{HFO\_L\_P}$	0
$X_{HFO\_H\_P\_old}$	0
$X_{HFO\_L\_P\_old}$	0
X_{CaCO3}	0
X_{ACP}	0
X_{STR}	0
X_{Vivi}	0

Appendix VIII, default values of MBR units parameters

Symbol	Value	Unit
$L.V_{min}$	0.001	m^3
$L.V_0$	1.8	m^3
$L.V_{max}$	2.0	m^3
Q_{air}	300	$Nm^3.d^{-1}$
S_{SOTE}	6	%/m
h_{diff}	4.8	m
T_{air}	20	°C
p_{air}	100000	Pa
α	0.7	-
β	0.95	-
F	0.8	-
h_{sea}	200	m
L_{air}	0.0065	K/m
$t_{R,air}$	10	s
ω	0.0645	-
$A_{membrane}$	8	m^2
P_{size}	0.0000004	m
ε_m	0.3	-
n_{cart}	10	-
$w_{cart,space}$	0.033	m
l_{cart}	0.512	m
f_{scour}	0.6	-
J	0.336	$m^3.m^{-2}.d^{-1}$
η_S	0	-
η_C	1	-
η_X	1	-
t_{filt}	9	min
t_{bwash}	1	min
k_r	3	$kg.m^{-2}.d^{-1}$
k_i	11000000000000000	$m.kg^{-1}$
a	0.067	-
b	0.02	$m^{-1}.m^2.d$
R_m	100000000	m^{-1}
ε_c	0.6	-
ρ_c	1150	$kg\ .\ m^{-3}$
Δp_{crit}	30000	Pa
n_{comp}	1	-
$Q_{sludge,target}$	5.4	$m^3.d^{-1}$

$R_{i,0}$	0	m^{-1}
$R_{r,0}$	0	m^{-1}
$M_{att,xSV,0}$	0	$g.m^{-2}$
ρ_w	1000	$kg . m^{-3}$
ρ_p	1060	$kg . m^{-3}$

Appendix IX, test plan for stress test with corresponding results

ANTICIPATED PLAN FOR STRESSED-NON-STRESSED TEST AT MBR PILOT PLANT -FOR FOULING MODEL VALIDATION															
Day	Date	Test period	Flow regime	Task	Remarks	Influent flow		MBR Sludge			Sludge removal	PERMEATE FLOW	INFLUENT FLOW	AIR FLOW	DO	TMP
						COD	TSS	SMP	totEPS	TSS/VSS						
Monday	4-Dec-17	morning 8:15am afternoon 3.15 pm	on off- afternoon	not stressed test	Sampling during morning- before ON	x	x	x	x	noon	100 L	Online data during the whole period				
Tuesday	5-Dec-17	morning 8:15am afternoon 3.15 pm	on- morning off- afternoon	No test	No sampling						100 L					
Wednesday	6-Dec-17	morning 8:15am afternoon 3.15 pm	on- morning off- afternoon	Stressed test	Sampling during morning- before ON	x	x	x	x	noon	100 L					
Thursday	7-Dec-17	morning 8:15am afternoon 3.15 pm	on- morning off- afternoon	Not stressed test	Sampling during afternoon before OFF	x	x	x	x	noon	100 L					
Friday	8-Dec-17	morning 8:15am	on- morning	Stressed test	Sampling during morning- before ON	x	x	x	x	noon	100 L					
Saturday	9-Dec-17		on													
Sunday	10-Dec-17		on													
Monday	11-Dec-17	morning 8:15am afternoon 3.15 pm	on off	Not stressed test	Sampling during morning- before ON	x	x	x	x	noon	100 L					
Tuesday	12-Dec-17	morning 8:15am afternoon 3.15 pm	on off	No test	No sampling						100 L					
Wednesday	13-Dec-17	morning 8:15am afternoon 3.15 pm	on off	Stressed test	Sampling during morning- before ON	x	x	x	x	noon	100 L					
Thursday	14-Dec-17	morning 8:15am afternoon 3.15 pm	on off	Not stressed test	Sampling during afternoon before OFF	x	x	x	x	noon	100 L					
Friday	15-Dec-17	morning 8:15am afternoon 3.15 pm	on	stressed test	Sampling during morning- before ON	x	x	x	x	noon	100 L					
Saturday	16-Dec-17		on													
Sunday	17-Dec-17		on													
Monday	18-Dec-17	morning 8:15am afternoon 3.15 pm	on off	Not stressed test	Sampling during morning- before ON	x	x	x	x	noon	100 L					
Tuesday	19-Dec-17	morning 8:15am afternoon 3.15 pm	on off	No test	No sampling						100 L					
Wednesday	20-Dec-17	morning 8:15am afternoon 3.15 pm	on off	Stressed test	Sampling during morning- before ON	x	x	x	x	noon	100 L					
Thursday	21-Dec-17	morning 8:15am afternoon 3.15 pm	on	Not stressed test	Sampling during afternoon before OFF	x	x	x	x	noon	100 L					

Appendix IX

Sampling date	Influent (Primary Clarifier of WWTP)				Sludge (Nitrification tank)										Remarks
	TSS	VSS	COD_{cr}	NH4-N	TSS	VSS	SMP	tEPS	NO3-N	VSS/TSS	Carbohydrate (mg/L)		Protein (mg/L)		
	(mg/L)	(mg/L)	(mg O_2 /L)	(mg/L)	(mg/L)	(mg/L)	(mg O_2 /L)	(mg O_2 /L)	(mg/L)		SMP	tEPS	SMP	tEPS	
4-Dec-17	140,00		193,80	67,00	9100,00	6465,00	17,10	604,50	75,00	71,04		9,96	375,67	422,67	Not-stressed
5-Dec-17															
6-Dec-17	150,00		199,40	44,00	9355,00	5305,00	21,50	527,50	64,50	56,71	5,96	7,67	304,00	355,00	Stressed
7-Dec-17	258,00		268,20	48,60	8950,00	6480,00	11,03	574,50	59,50	72,40	5,71	12,26	296,67	491,00	Not-stressed
8-Dec-17	224,80		238,60	45,20	9425,00	5865,00	25,15	523,00	60,00	62,23	10,60	8,11	441,67	368,00	Stressed
9-Dec-17															
10-Dec-17															
11-Dec-17	139,00	100,00	151,60	42,70	8285,00	5355,00	33,60	466,50	45,50	64,63	5,89	8,60	302,00	382,33	Not-stressed
12-Dec-17															
13-Dec-17	120,00	112,00	247,20	34,90	8380,00	4345,00	44,45	576,50	52,00	51,85	9,04	11,36	395,67	464,33	Stressed
14-Dec-17	109,00		319,80	46,00	5625,00	4260,00	57,45	666,00	52,50	75,73	5,87	10,33	301,33	433,67	Not-stressed
15-Dec-17	149,00		305,20	34,20	8325,00	5200,00	50,9	765,50	58,00	62,46	6,38	8,61	316,67	382,67	Stressed
16-Dec-17															
17-Dec-17															
18-Dec-17	116,00		274,40	38,80	7485,00	4215,00	34,00	754,00	59,50	56,31	8,06	9,43	366,33	407,00	Not-stressed
19-Dec-17															
20-Dec-17	128,00		348,00	37,90	7730,00	4635,00	54,60	637,50	51,00						Stressed
21-Dec-17	188,00		349,80	47,00	6685,00	3865,00	38,95	533,00	54,00						Not-stressed

Appendix X, Full plant simulation results

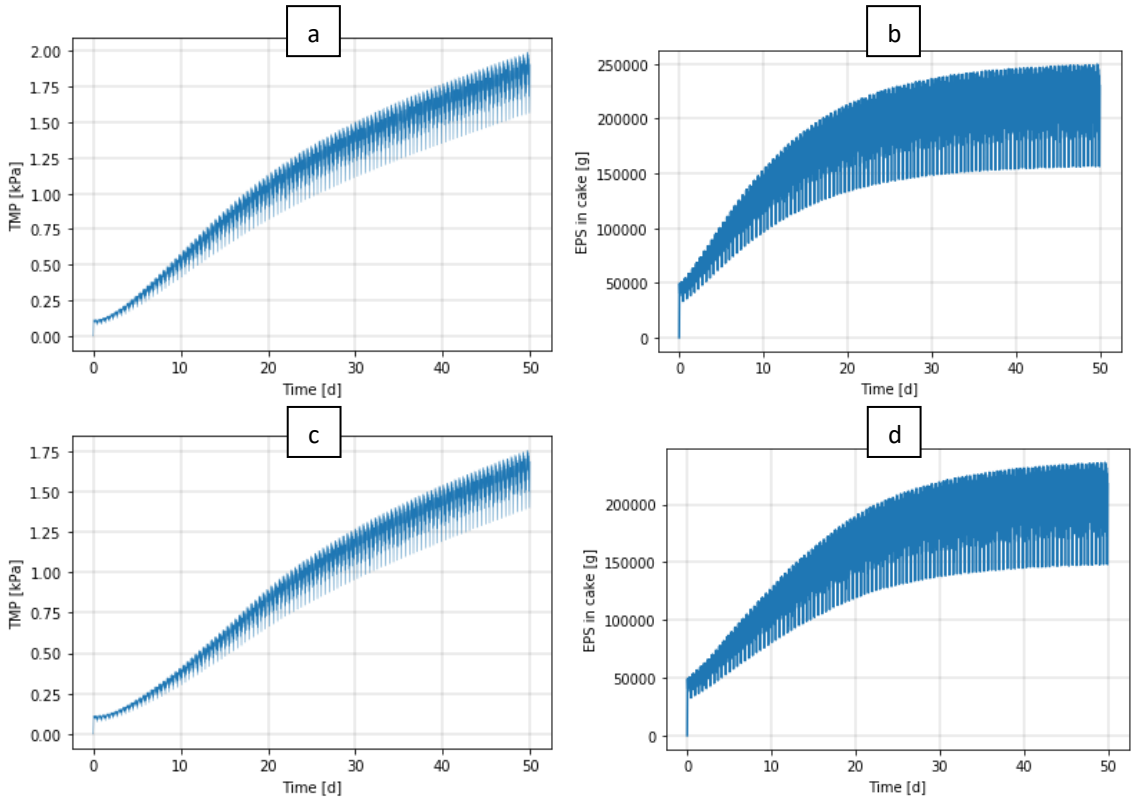

Simulated values for TMP [kPa] and EPS mass in cake [g] in different tanks with aeration set off in CSTR 4 in figures a – b, and aeration set off in CSTR 4 and 5 in c – d.

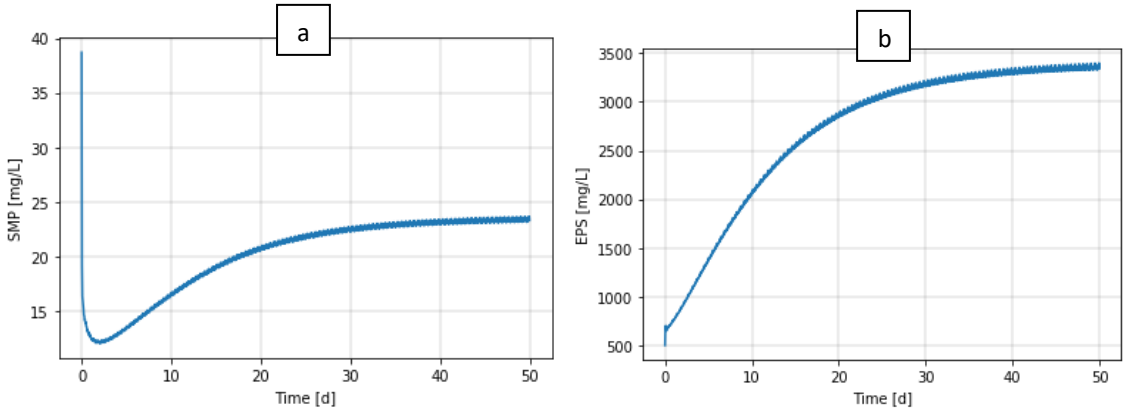

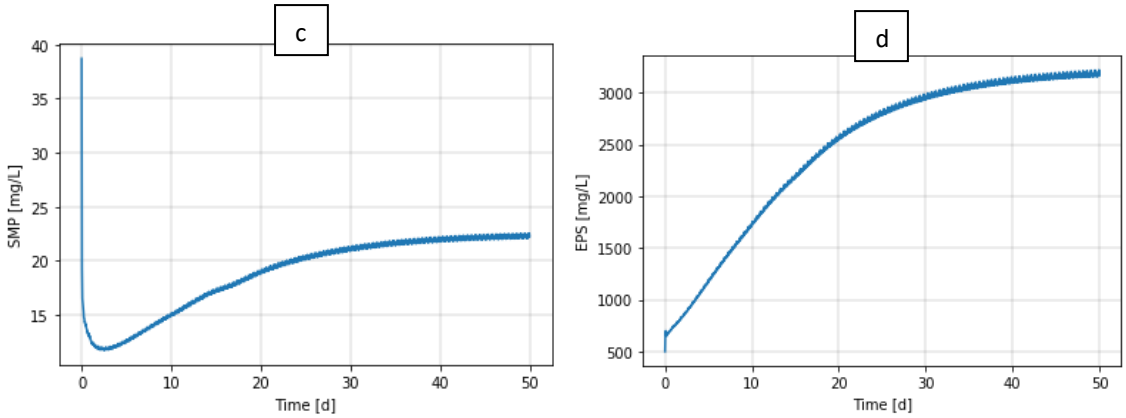

Simulated values for SMP [mg/L] and EPS [mg/L] in MBR process unit with aeration set off in CSTR 4 in figures a – b, and aeration set off in CSTR 4 and 5 in c – d.

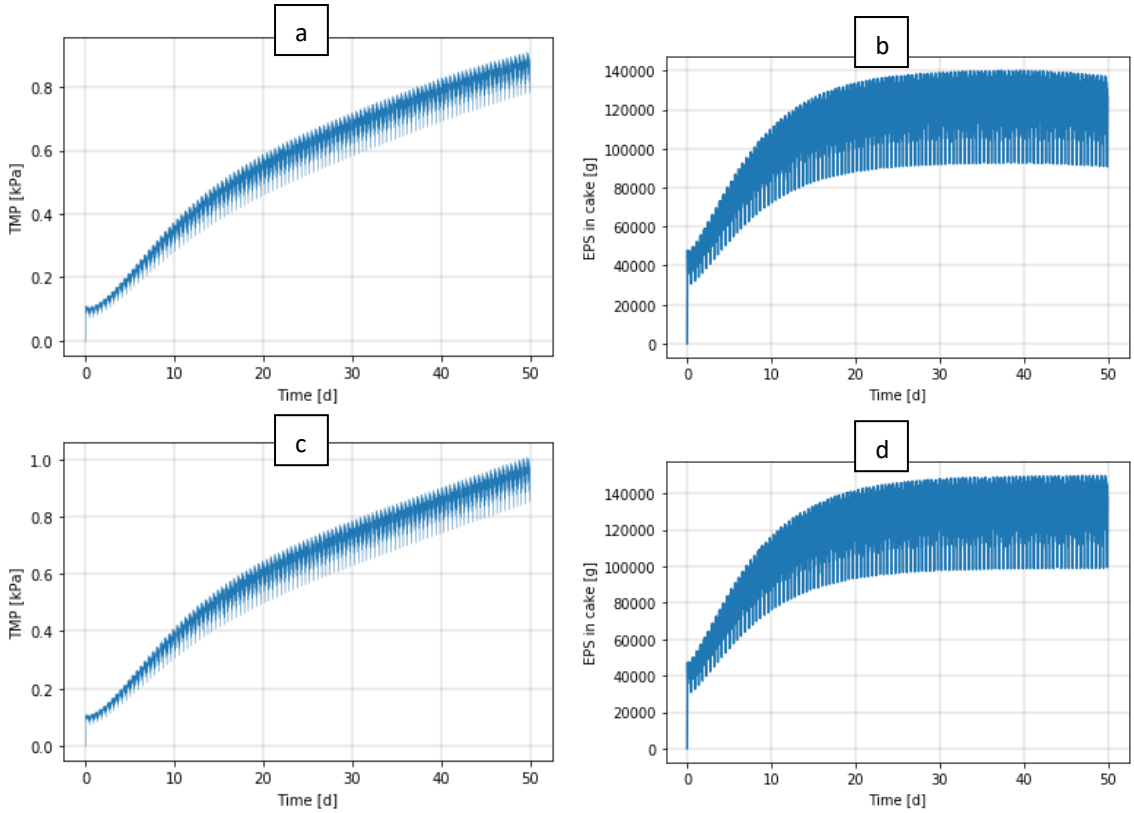

Simulated values for TMP [kPa] and EPS mass in cake [g] in MBR process unit with SRT set to 15 d, temperature to 10 °C, and DO set to 0 [mg/L] in CSTR 3 in figures a – b, and DO set to 2 [mg/L] d in c – d.

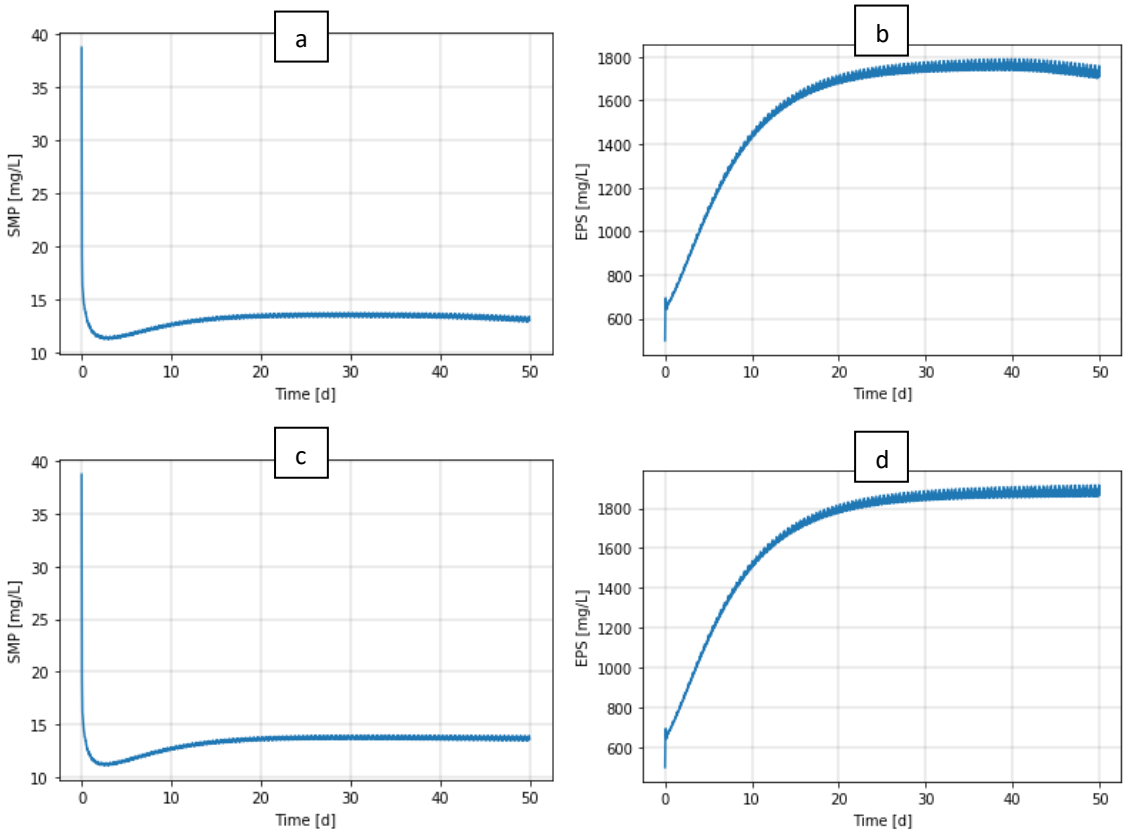

Simulated values for SMP [mg/L] and EPS [mg/L] in MBR process unit with SRT set to 15 d, temperature to 10 °C, and DO set to 0 [mg/L] in CSTR 3 in figures a – b, and DO set to 2 [mg/L] d in c – d.